UNIVERSITY OF CALGARY

DNA damage Signaling in response to Etoposide

by

Marina I. Siponen

A THESIS

SUBMITTED TO THE FACULTY OF GRADUATE STUDIES

IN PARTIAL FULFILMENT OF THE REQUIREMENTS FOR THE

DEGREE OF MASTER OF SCIENCE

DEPARTMENT OF BIOCHEMISTRY AND MOLECULAR BIOLOGY

CALGARY, ALBERTA

February, 2005

FACULTY OF GRADUATE STUDIES

The undersigned certify that they have read, and recommend to the Faculty of Graduate Studies for acceptance, the thesis entitled "DNA damage Signaling in response to Etoposide" submitted by Marina I. Siponen in partial fulfillment of the requirements for the degree of Master of Science.

_____
Supervisor, Dr. S.P. Lees-Miller
Dept. of Biochemistry and Molecular Biology

_____
Dr. G.B. Moorhead
Dept. of Biological Sciences
Division of Biochemistry

_____
Dr. K.T. Riabowol
Dept. of Biochemistry and Molecular Biology

_____
External Examiner, Dr. C.S. Shemanko
Dept. of Biological Sciences
University of Calgary

_____
Date

ABSTRACT

The ataxia-telangectasia mutated (ATM) protein kinase is a major signaling component of the cellular response to DNA double strand breaks (DSBs). Ionizing radiation (IR) induces DSBs which are signaled in a well established, ATM-dependent pathway. Etoposide is a compound in the epidophyllotoxin class of antineoplastic agents. This compound inhibits the topoisomerase II (topo II) enzyme, thereby causing DSBs in treated cells. Although the cellular response to IR-induced DSBs is well established, etoposide-induced DSB signaling is not. This study shows that the ATM kinase is phosphorylated at its autophophorylation site, serine 1981, and has increased protein kinase activity in response to low doses of etoposide (0.8 μM). The activation of ATM results in the phosphorylation of p53 (at serine 15) and NBS1 at (serine 343) within 2 hrs. Treatment of ATM negative lymphoblastoid cells with etoposide, under the same conditions, indicates there is a delay in phosphorylation at these sites, suggesting that ATM plays a role but is not absolutely required for these responses. However, treatment of these cell lines shows that the phosphorylation of the Chk2 protein kinase and SMC-1 require the presence of ATM in response to etoposide. Exposure to etoposide also causes multisite phosphorylation of p53 at serine 6, serine 9, and serine 46 by 4 hrs. Electrophoretic mobility shift assays (EMSA) were performed to show that 0.8 μM etoposide also increases p53 binding ability to its consensus sequence. Phosphorylation of other IR-induced ATM substrates such as histone 2AX (H2AX) and the checkpoint kinase Chk1, did not require ATM in response to etoposide. These results indicate that the DSB-induced pathways are differentially activated in response to etoposide and IR.

ACKNOWLEDGEMENTS

First, I would like to thank Dr. Susan Lees-Miller for providing me with the opportunity to conduct these studies under her supervision. It has proven to be a very valuable learning experience in many aspects. I would also like to thank all the members of the Lees-Miller laboratory for their ongoing support over the course of my stay in the lab. I would like to give special thanks to Mrs. Ruiqiong Ye and Dr. Ebba Kurz for their continuous help in our tissue culture facility.

I would also like to thank the graduate coordinators of the Biochemistry and Molecular biology program, Drs. Jonathan Lytton and Joseph Goren for their help and guidance in this program.

Furthermore, I would like to thank my supervisory committee Drs. Karl Riabowol and Gregory Moorhead, as well as my external examiner Dr. Carrie Shemenko.

Finally, I'd like to thank all my friends and family for the emotional support they provided through the hard times. Special thanks to Arnaud….for your patience!

I dedicate this thesis to my parents,
Mariette and Erik Siponen,

for your continuous support
and
always believing in me.

TABLE OF CONTENTS

LIST OF FIGURES

LISTE OF TABLES

LIST OF ABBREVIATIONS

Abbreviations

a.a.	amino acid
ATLD	A-T like disorder
ATM	ataxia-telangiectasia mutated
ATR	ATM-Rad3 related
ATRIP	ATR-interacting protein
BLM	Bloom's syndrome helicase
Chk1	Checkpoint kinase 1
Chk2	Checkpoint kinase 2
DNA	deoxyribonucleic acid
DNA-PK	DNA-dependent protein kinase
DNA-PKcs	DNA-dependent protein kinase catalytic subunit
ds	double-stranded
DSB	double-strand break
DTT	dithiothreitol
EDTA	ethylenediaminetetraacetic acid
EMSA	electrophoretic mobility shift assays
γ-H2AX	phosphorylation of H2AX on serine 139
H2AX	histone 2A variant X
HRR	homologous recombination repair
IP	immunoprecipitation
IR	ionizing radiation
Ku 70	70 kDa subunit of Ku protein
Ku 80	80 kDa subunit of Ku protein
LSB	low salt buffer
MDC1	mediator of DNA damage checkpoint protein
MRN complex	MRE11/RAD50/NBS1
mRNA	messenger RNA
MW	molecular weight
NBS	Nijmegen Breakage Syndrome
NCS	neocarzinostatin
NET-N	NaCl; EDTA; Tris; Nonidet P-40 lysis buffer
NET-T	NaCl; EDTA; Tris; Triton X-100 lysis buffer
NHEJ	non-homologous end joining
PBS	phosphate buffered saline
PCNA	proliferating cell nuclear antigen
PCV	packed cell volume
PI3-K	phosphatidylinositol 3-kinase
PIKK	PI3-K like kinases
PMSF	phenylmethylsulfonylfluoride
RDS	radiation resistant DNA synthesis
ROS	reactive oxygen species
SCID	severe combined immunodeficiency

SDS-PAGE	sodium dodecyl sulfate-polyacrylamide gel electrophoresis
SMC1	structural maintenance of chromosome 1 protein
ATX/hSMG-1	human nonsense-mediated mRNA decay protein SMG-1
TEMED	tetramethylethylenediamine
topo II	topoisomerase II
TTBS	tris-buffered saline containing Tween
UV	ultraviolet radiation
WCE	whole cell extracts
WRN	Werners syndrome protein
XRCC4	x-ray repair cross complementing defective in Chinese hamster mutant 4

SECTION I : INTRODUCTION

1.1 Introduction

Exposure to ionizing radiation (IR) and several other environmental toxins causes damage to DNA in cells. Furthermore, DNA damage occurs under normal cellular conditions. Not surprisingly, several pathways have evolved to signal the presence, and subsequently repair of, this damage. DNA damage triggers processes that lead either to repair of the DNA damage, or to promote cell death in the event where damage is deemed too extensive for repair. These pathways can be pictured as signal transduction cascades in which the DNA lesion serves as the signal. DNA damage activates a series of signaling proteins, which transmit and amplify the signal to delay progression of the cell cycle through activation of cell cycle checkpoints, modulate repair or trigger programmed cell death/apoptosis. These DNA damage surveillance systems "patrol" the genome on the lookout for DNA damage such as base mismatches, apurinic/apyrimidinic (AP) sites, specific base damage (e.g. deamination, dimer formation, bulky adducts), as well as single and DSBs. The DSB is particularly dangerous in a cellular context. A single unrepaired DSB can induce cell death or lead to chromosomal abnormalities such as mutations or loss of genetic information (Bennett *et al*, 1993).

DSBs can be generated by a variety of factors either intrinsic or extrinsic to the cell. Endogenous factors include: stalled replication forks, site-specific recombination processes in meiosis and immunoglobublin gene rearrangement, and reactive oxygen species (ROS) due to aerobic metabolism. DSBs can be caused by IR, radiomimetic drugs and certain chemotherapeutic agents, for example alkylating agents, anthracyclins, epipodophyllotoxins and platinums. These differ in their mechanism and site of action (Figure 1.1).

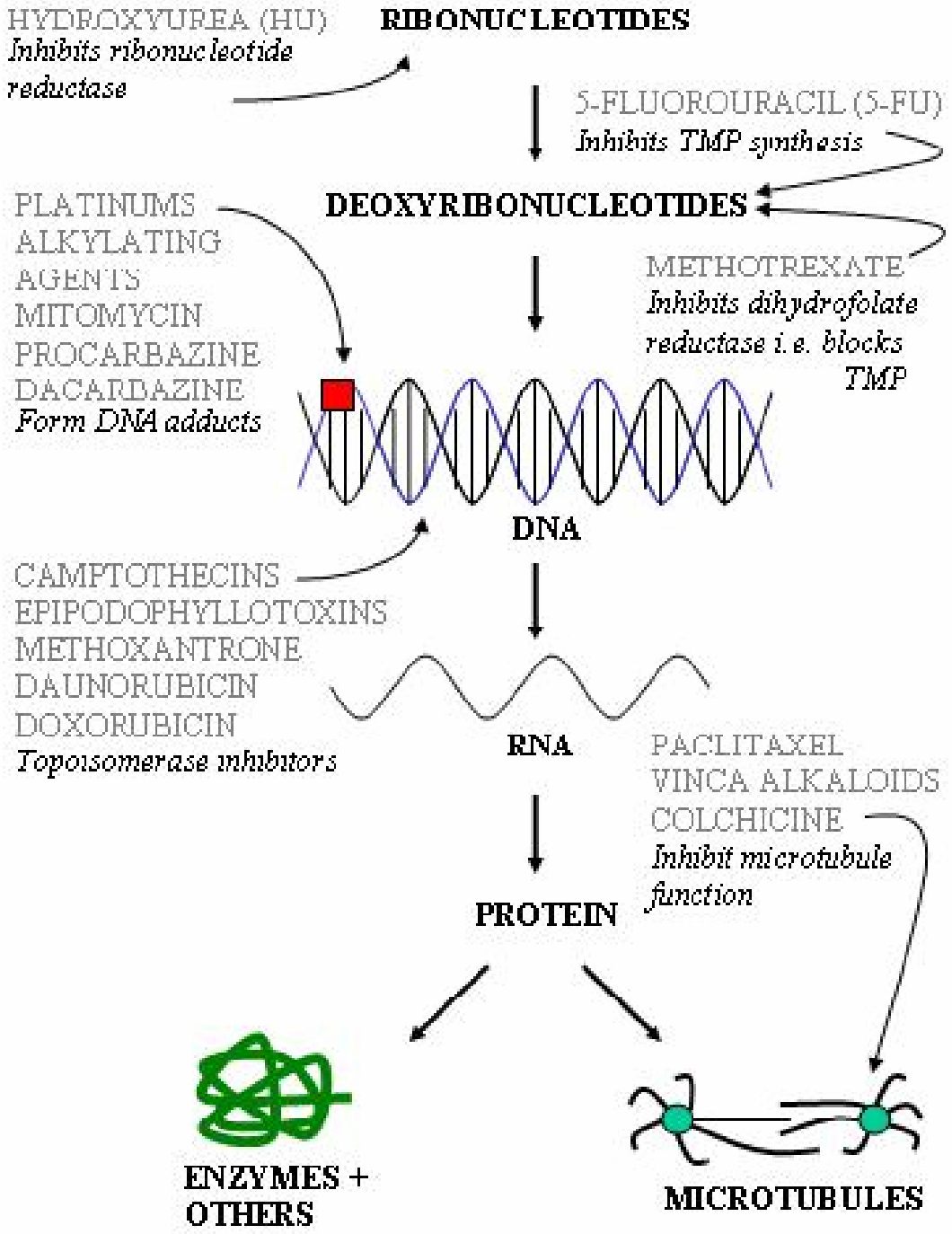

Figure 1.1: Mechanisms and sites of action of chemotherapeutic agents commonly used in cancer treatment. Four classes of chemotherapeutic agents are represented. 1. Agents which inhibit the synthesis of nucleic acids. 2. Agents which cause DNA adducts. 3. Inhibitors of topoisomerase function 4. Inhibitors of microtubule function.

1.2 How are DSBs generated in the cell?

Our genome is constantly challenged both by endogenous and exogenous sources of DNA damage. ROS are constantly being produced in living organisms and are the cause of a significant part of this damage. The presence of excess ROS, due to an inadequate supply of anti-oxidants or an excessive exposure to exogenous sources of ROS, results in oxidative stress to the cell. Cells are exposed to ROS both from endogenous and exogenous sources. Oxidative metabolism is the major source of endogenous ROS. Exogenous sources of ROS include, IR (x-rays and γ-rays), chemotherapeutic and radiomimetic chemicals, all of which are well known as DSB causing agents. IR generates clusters of ROS due to radiation induced dissociation of water molecules.

The different ROS are generated when O_2 accepts an electron to form the superoxide ion ($^{\bullet}O_2^-$), the hydroxyl radical ($^{\bullet}OH$) or hydrogen peroxide (H_2O_2). Each of these ROS possesses a different reactivity towards biological molecules, including DNA. The mitochondrial respiratory pathway is a major source of $^{\bullet}O_2^-$ and this superoxide ion, as such, is not very reactive. However, it can undergo dismution to produce hydroperoxy radical ($HO_2^{\bullet}$), a much more reactive species. H_2O_2 is also quite stable in the cell. It becomes problematic in the presence of transition state metals in which case it can be converted to $^{\bullet}OH$ which is a highly reactive oxidant (Skulachev, 1997). This form of ROS is capable of inducing considerable damage to nuclear and mitochondrial DNA as well as cause lipid peroxidation and protein and carbohydrate oxidation. The $^{\bullet}OH$ is the major form of ROS produced by IR.

Two mechanisms have been proposed for the production of DSBs by ROS (Lieber *et al*, 2003). The first suggests that a ROS may cause damage to one DNA strand while another causes damage to the complementary strand within close proximity (≤12 bps),

thereby resulting in a DSB. Alternatively, the chain-reaction nature of ROS damage can cause damage in a DNA strand resulting in a nick, which causes a reaction by the same ROS with the complementary strand to cause a DSB. DSB can also be generated indirectly by DNA replication across a nick formed by a ROS.

1.3 DSBs caused by topoisomerase II inhibitors and poisons

Linear representations of DNA often ignore the problems caused by its helical nature. The rotational energy required for unwinding long chromosomes, and allowing replication forks to move along the DNA, would be tremendous. Therefore, topoisomerases are a set of ubiquitous enzymes which overcome this problem by altering the topological state of DNA. Their actions include catenation, decatenation and alterations in DNA superhelicity by generating transient breaks in the sugar-phosphate backbone of nucleic acids. The initial characterization of these proteins dates back to the 1970s when the *Escherichia coli* DNA topoisomerase I (topo I) was discovered (Wang, 1971).

These enzymes play a critical role in virtually every aspect of DNA metabolism, including replication, transcription and recombination as well as, chromosome segregation and maintenance of chromosome integrity. During catalysis, type I topoisomerases cleave one strand of DNA, pass single stranded or duplex DNA through the break, and religate the induced break (Lima *et al*, 1994). Type I topoisomerases are classified into two non-homologous subfamilies, type IA and type IB, which differ in the type of DNA adduct they form. Type IA enzymes include prokaryotic topoisomerases I and III, eukaryotic topoisomerase III and archael reverse gyrase, while the type IB class includes eukaryotic topoisomerase I, archael topoisomerase V and the poxvirus type I topoisomerases (reviewed in Berger, 1998a). Type II topoisomerases cleave both strands of DNA, pass an

intact double helix of DNA through the break generated on a separate helix, and relegate the break (Osheroff *et al*. 1991). Type II topoisomerases all have amino acid (a.a.) similarity at the primary sequence level and include: prokaryotic DNA gyrase, eukaryotic topoisomerase II (topo II), prokaryotic topoisomerase IV (topo IV) and archael topoisomerase VI (topo VI) (reviewed in Berger, 1998b).

Beyond their physiological function, topoisomerases are the target of several catalytic inhibitors and poisons which have gained clinical importance as antimicrobial and anticancer chemotherapeutic agents. These drugs are powerful inducers of DSBs and G_2 arrest. They induce cell death by increasing the number, and stability of the topoisomerase-DNA complex, a normal but temporary intermediate in the catalytic cycle of this enzyme. This section will describe the steps in the catalytic cycle of topo II, the classification and mechanisms of topo II inhibitors and poisons, and signaling by the epipodophyllotoxin class of drugs.

1.3.1 ***Topoisomerase II and its catalytic cycle***

Topo II functions as a homodimer with a monomeric molecular mass ranging between 170 and 180 kDa. This discrepancy in size corresponds to the different topo II isoforms. As opposed to lower eukaryotes (*Saccharomyces* and *Drosophila*), which contain a single isoform of topo II, two closely related isoforms, designated α and β have been identified in vertebrates (Drake *et al*, 1987). The two isoforms share extensive a.a. similarity (~70%) (Austin *et al*, 1993). However, they are encoded by different genes and have different monomeric masses of 170 kDa and 180 kDa for the α and β isoforms respectively. The α isoform was the first characterized and is the more extensively studied

form of topo II. However, the enzymological characteristics of both isoforms are similar and therefore, the term topo II will be used to designate both homodimers of α or β subunits.

Each of the topo II monomers can be divided into three distinct domains (Berger 1998b) (illustrated in Figure 1.2). The first 660 amino acids encompass a region with a.a. similarity to the B subunit of DNA gyrase termed the B' domain. This region contains the ATP binding site which will be referred to as the ATPase region. The central domain, which extends between a.a.s 660 to 1200, is analogous to the A subunit of DNA gyrase and is termed the A' domain. This domain contains the active site tyrosine residue which forms a covalent bond with DNA upon scission. The DNA binding/cleavage core of the enzyme is encompassed within these two regions between a.a.s 410 and 1200. The C-terminal domain contains no a.a. similarity to DNA gyrase. This region is highly charged, it contains a nuclear localization sequence (NLS) as well as *in vivo* phosphorylation sites.

Through an ATP-dependent mechanism, all topo II molecules transport a DNA segment (termed the T-segment) through a cleaved DNA 'gate' on a separate DNA duplex (termed the G-segment). To achieve this, the topo II molecular structure is composed of a portal system with a separate "entry" and "exit" port for the T-segment DNA. The original capture of the T-segment DNA at the entry port is preformed by the N-terminal B' domain (also called DNA capture domain) and ATPase domains. Similarly, the G-segment is held in place by the C-terminal region of the B' domain, the A' domain and the variable C region, which also forms the exit gate. The catalytic cycle (illustrated in Figure 1.3) is initiated by the binding of topo II to the G-segment DNA. This interaction is governed by nucleotide sequence and topological structure of DNA (Burden and Osheroff, 1998). In the

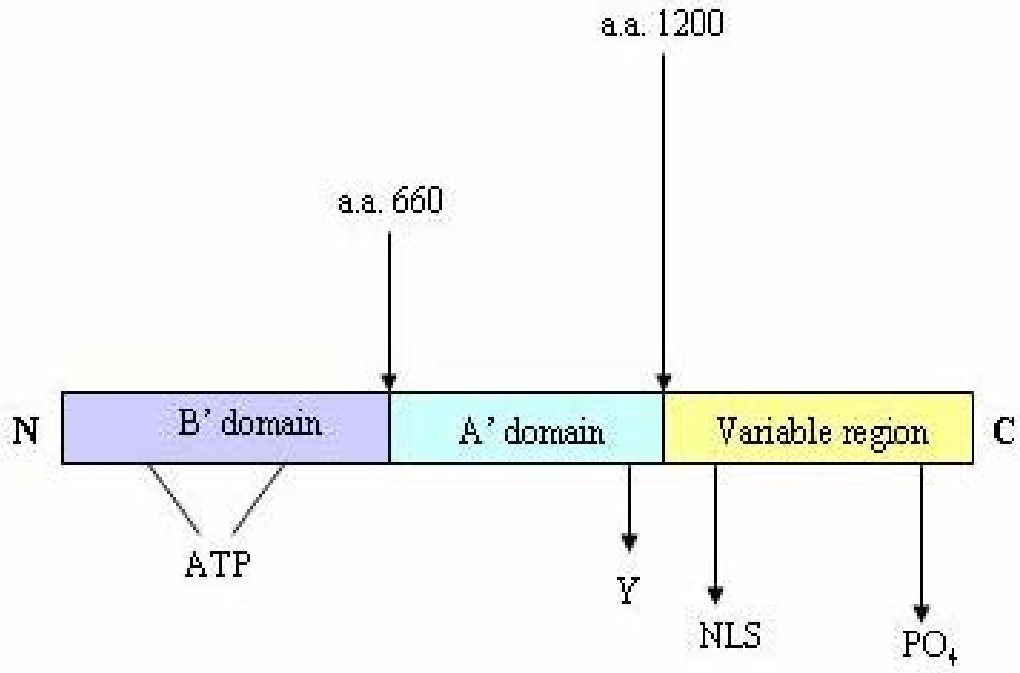

Figure 1.2: Structural organisation of Topoisomerase II. Topo II is composed of three functional domains. 1. The B'domain which contains the ATP binding site. 2. The A' domain which contains the active site tyrosine. 3. The variable region which contains the C-terminal region phosphorylation sites and the nuclear localisation sequence (NLS).

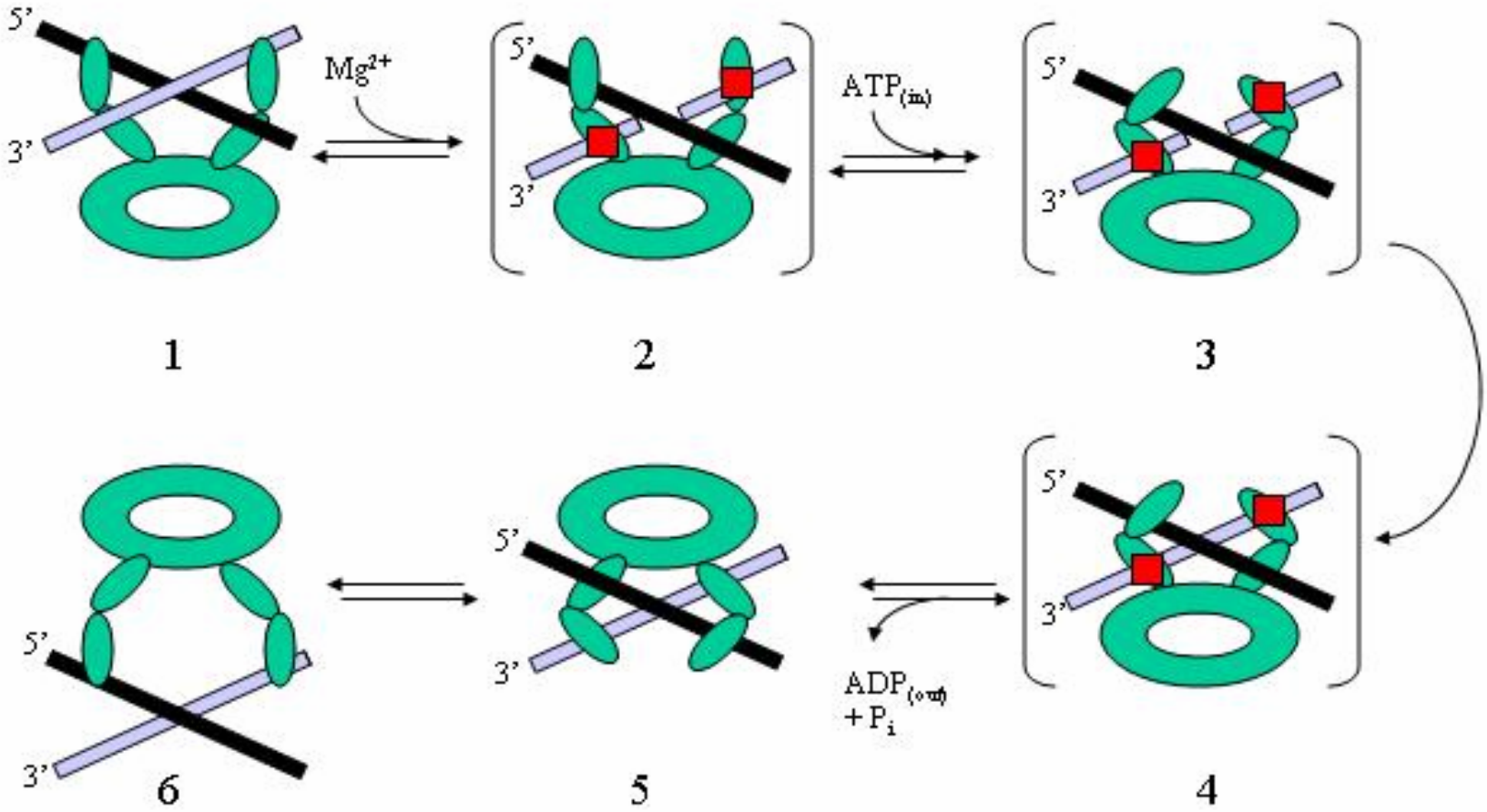

Figure 1.3: Catalytic cycle of DNA topoisomerase II. 1. Topo II binds to DNA. 2. A cleavage equilibrium is established in the presence of Mg^{2+} cofactor, topoII covalently binds DNA and makes two coordinated nicks in the DNA 3. ATP binds inducing a conformational change in topoII triggering DNA strand passage. 4. A religation equilibrium is established 5. ATP hydrolysis changes the topoII conformation. 6. DNA is released and the enzyme recycles

presence of a magnesium divalent cation, a cleavage equilibrium is established, allowing the enzyme to make two coordinated nicks in the DNA double helix. This generates a 4-base pair 5' overhang on each DNA strand (Zechiedrich *et al*, 1989). During scission, topo II drives a transesterification reaction which results in the formation of a covalent bond between its active site tyrosyl residue and the 5'-phosphate of the nicked DNA strands. This results in the enzyme being covalently linked to the 5'-terminus of the cleaved DNA, leaving a free hydroxyl moiety at the 3'-terminus. This intermediate is referred to as the "cleavage complex". The next step involves the binding of ATP. This induces a conformational change in topo II triggering DNA strand passage. After strand passage, topo II reestablishes a religation equilibrium similar to the cleavage equilibrium. In the final step, ATP hydrolysis changes the topoisomerase conformation to allow release of the substrate. Phosphorylation stimulates ATP hydrolysis 2-3 fold suggesting that this is a mechanistic means of enhancing overall catalytic activity of topo II (Corbett *et al*, 1992). Mutation analysis of the C-terminal serine 1106 to alanine was shown to modulate enzymatic activity and increase sensitivity to topo-II targeting drugs (Chikamori *at al*, 2003). Once the T-segment DNA is released, the enzyme can then recycle itself and initiate a new round of catalysis. It appears as though the chemical structure of the DNA product generated by this process is identical to that of the initial substrate molecule.

1.3.2. Classification and mechanisms of topo II inhibitors and poisons

The generation of DSBs by topo II, present in the cleavage and religation equilibrium complexes of its catalytic cycle, has a potentially lethal nature. Several of the widely used anticancer drugs take advantage of this weak point in the catalytic cycle to target topo II. The type II topoisomerases are specific targets of two classes of drugs: the

topo II catalytic inhibitors and the topo II poisons. The catalytic inhibitors are a diverse group of drugs which inhibit the activity of topo II at a stage of its catalytic cycle other than formation of the cleavage/religation complex (for review see Andoh and Ishida, 1998). Several of the topo II catalytic inhibitors are represented in Figure 1.4. Distinct from the topo II catalytic inhibitors are the topo II poisons. These include: the epipodophyllotoxins (etoposide, teniposide), the anthracycline antibiotics (daunorubicin, doxorubicin), an anthracenedione (mitoxantrone) and an aminoacridine (m-AMSA) (Figure 1.5). These drugs can act to significantly increase the half-life of the cleavage/religation complex equilibrium. Although the poisons do not affect the nature of the complex *per se*, they significantly alter its kinetics. Under physiological conditions, the duration of the cleavage/religation equilibrium is in the orders of seconds as compared to minutes, or even hours in the presence of topo II poisons.

Under normal conditions, the level of topo II complexed to DNA is very low. This in confirmed by *in vitro* experiments which estimated that less than 1% of total DNA topo II was complexed with DNA (Fortune *et al*, 2001). A very tight equilibrium exists to control the number of cleavage/religation complexes present in the cell at any given time. When the ability to form this complex is impaired, cells will enter a quiescent state until topo II activity drops below a critical level resulting in death due to mitotic failure (Nitiss, 1998). Inversely, the stabilization of the cleavage/religation complex, resulting in an increased number of complexes, is also cytotoxic (Figure 1.6). This results in the complex acting as a blockage to other enzymes such as DNA polymerases and DNA helicases. Collision with such enzymes can disrupt the complex exposing the DSB, leaving it susceptible to becoming a target of repair or recombination pathways. The later can stimulate sister chromatid exchange, the insertion or deletion of DNA segments,

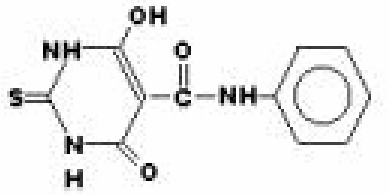

MERBARONE

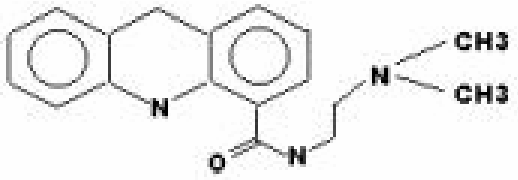

SN22995

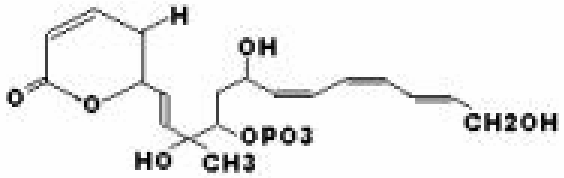

FOSTRIECIN

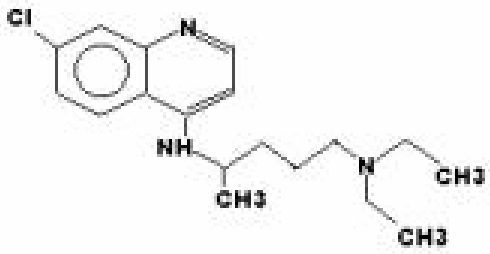

CHLOROROQUINE

Figure 1.4: Structural representation of the topoisomerase II catalytic inhibitors

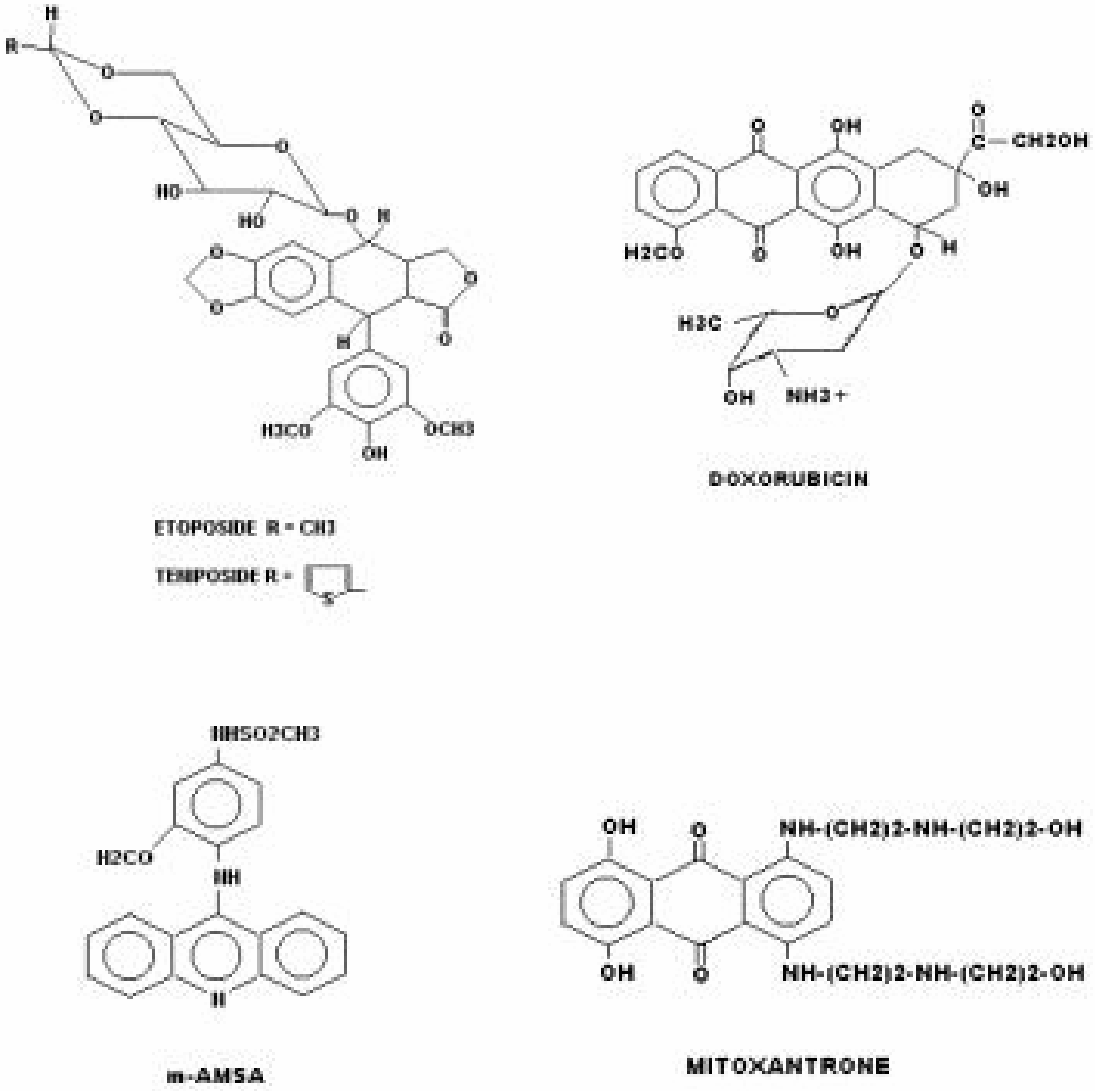

Figure 1.5: Structural representation of the topoisomerase poisons.

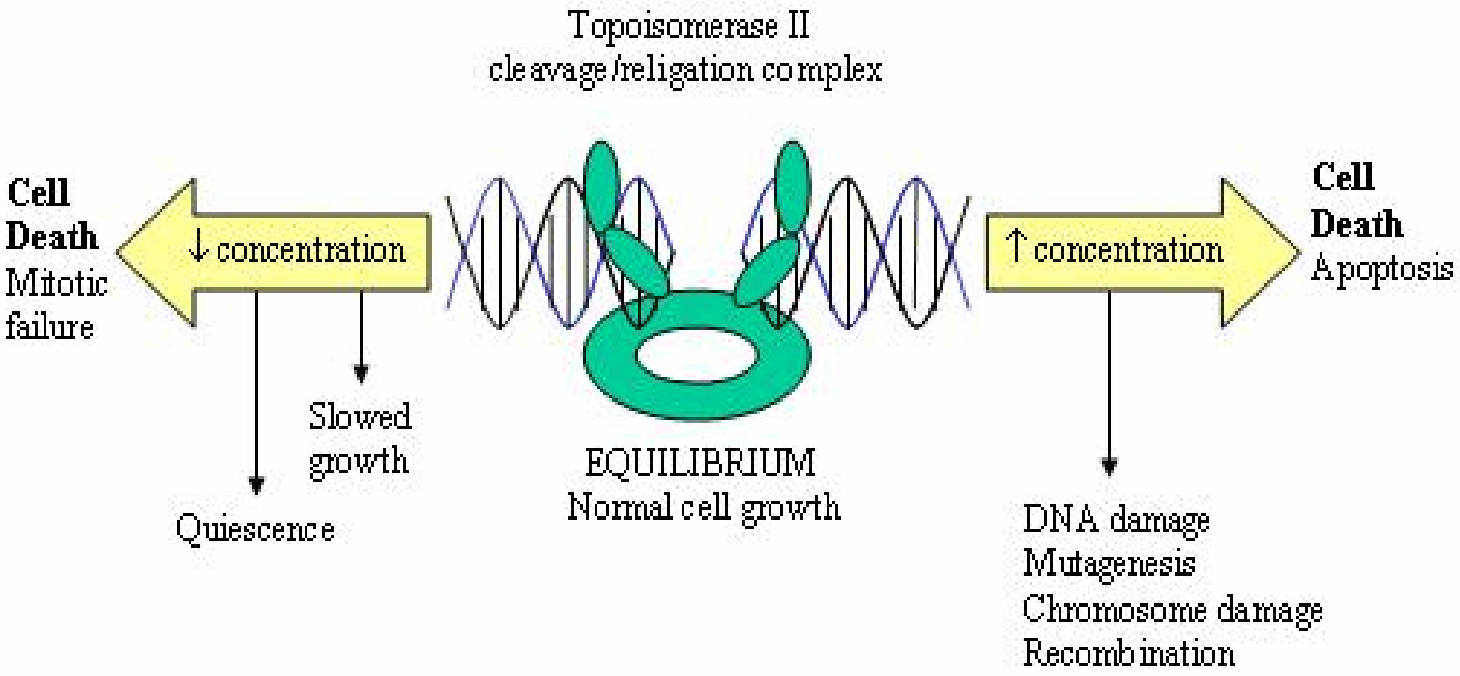

Figure 1.6: Concentration effects of the topo II cleavage/religation complex on the cell. 1. Increased concentration of the topo II cleavage/religation complex results in DNA damage, mutagenesis, chromosome damage, recombination events and culminates in cell death 2. Decreased concentrations of the topo II cleavage/religation complex results in slowed growth, quiescence and eventual cell death

chromosomal translocations and other aberrations (Wilstermann and Osheroff, 2003). In addition, exposure to etoposide and doxorubicin is associated with the generation of the H_2O_2 ROS (Larsen *et al*, 2003). The formation of DNA-topoisomerase cleavage/religation complexes can also be stabilised by H_2O_2.

There exist three possible routes by which a topo II poison can bind to form a topo II-drug-DNA complex (Figure 1.7). The drug can bind: (1) DNA first followed by topo II, (2) the pre-formed topo II-DNA complex or, (3) topo II first followed by DNA. There exists scientific evidence to justify all three routes (Burden and Osheroff, 1998). However, kinetic and binding studies provided the strongest evidence to establish the third route as the predominant one. Interaction characterizations using ellipticine and etoposide indicated that many of the topo II poisons likely form a direct interaction with the enzyme (Burden *et al*, 1996 and Froelich-Ammon *et al*, 1995)

The topo II poisons have been defined as being able to stabilize the topo II-DNA complex. These drugs mediate DNA breakage through one of two mechanisms: inhibition of the enzyme's ability to religate the DNA or, an increase in the forward rate of DNA-topo II complex formation (shown in Figure 1.8). The epipodophyllotoxins and amsacrine have been shown to inhibit the ability to religate DNA (Osheroff, 1989). Three possibilities exist to explain this inhibition of religation. The drug could intercalate at the point of scission and form a physical block to prevent religation. On the other hand, it could interact with the DNA overhang and sterically displace the DNA termini. Alternatively, it could disrupt the non-covalent interactions between topo II and its substrate which are required for correct position of the DNA substrate for religation. The actual mechanism still remains to be elucidated.

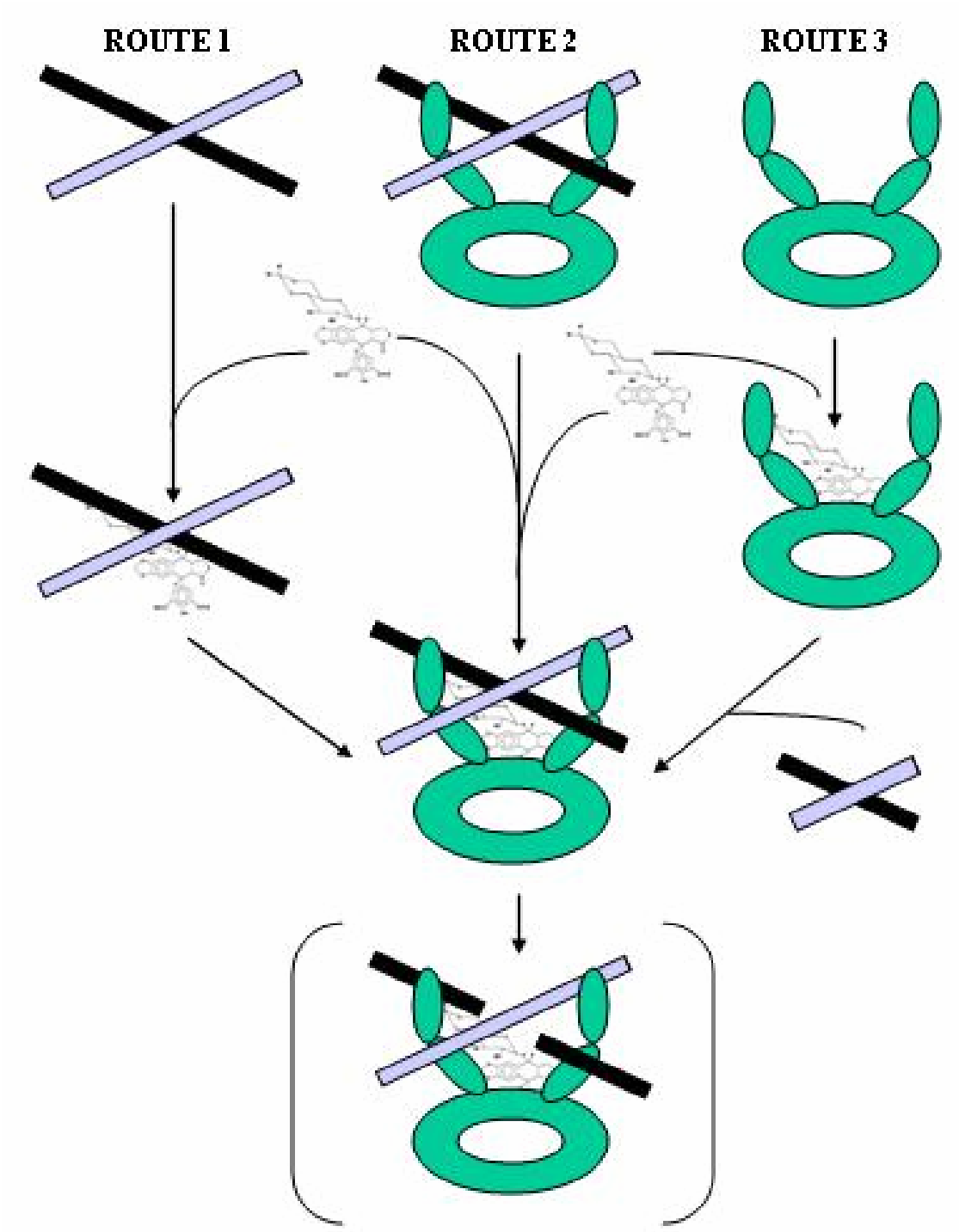

Figure 1.7: Routes of topo II cleavage/religation complex formation. Three routes of complex formation are possible. 1. The DNA binds the drug first. 2. The drug binds the DNA-TopoII complex. 3. The drug binds Topo II first.

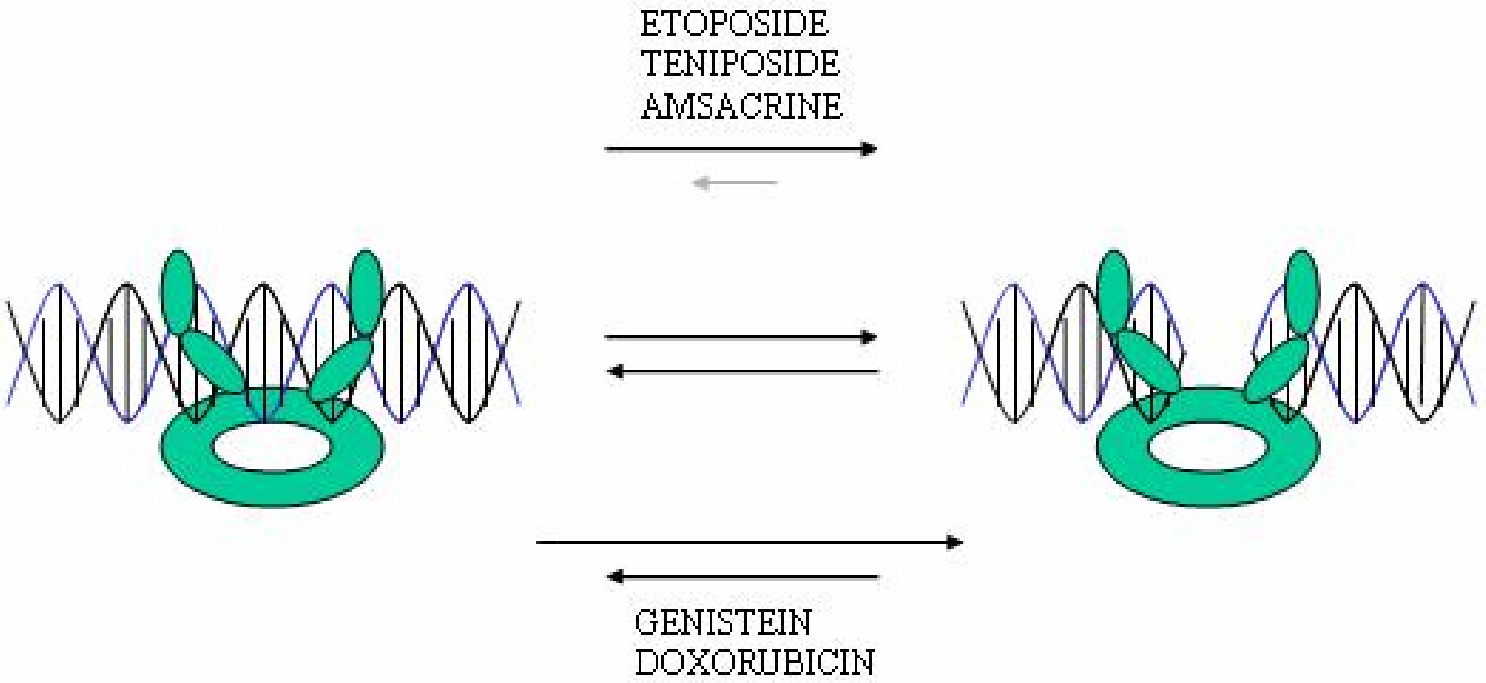

Figure 1.8: Effect of different drugs on the topo II cleavage/religation complex. Two different mechanisms can effect the topoII cleavage/religation complex. 1. The drug can stabilise the formation of the cleavage complex (genistein, doxorubicin). 2. The drug can inhibit religation of the DNA (etoposide, teniposide, amsacrine) (Adapted from: Burden DA and Osheroff N. (1998) Mechanism of action of eukaryotic topoisomerase II and drugs targeted to the enzyme. *Biochim Biophys Acta.* **1400(1-3):** 147).

1.3.3 The epipodophyllotoxins: etoposide (VP-16) and teniposide (VM-26)

Podophyllotoxin is a natural product isolated from the mandrake plant, *Podophyllum peltatum* and *Podophyllum emodi*. They have long been known to possess medicinal properties and were discovered to have antineoplastic properties early on. However, the potency of podophyllotoxin was too great for clinical use. Therefore, investigators tried to synthesize semi-synthetic derivatives of the compound. In the 1960's, two analogues were identified that retained antineoplastic abilities while exhibiting less toxicity, etoposide (VP-16) and teniposide (VM-26). While the podophyllotoxins were inhibitors of mitotic spindle formation, the epipodophyllotoxin did not have this activity but were found later to have activity towards topo II. More specifically, etoposide was also found to cause strand breaks dependent on RNA transcription (Muscarella *et al*, 1998).

1.4 Cellular responses to DNA-double strand breaks

Because of the potential lethal nature of DNA-DSBs, their presence is efficiently detected and transmitted to allow for their repair. The DSB is believed to be one of the most dangerous types of damage to the cell and, if left unrepaired, it is lethal. As such, it is not surprising that eukaryotes have evolved several mechanisms to detect DSBs, repair them and signal their presence to transcriptional, cell cycle and apoptotic systems. This requires very intricate networks of protein kinase cascades. The following section describes the components known to be required from DSB detection through to its repair.

1.4.1 Detection of DSBs

The first step in the DSB response pathway is detection: DSBs must be detected and their presence must be signaled to other cellular components. Typically, the DSB is

initially detected by sensor proteins which promote the recruitment of adaptor and signal transducer proteins. This process culminates in the recruitment of the DSB repair machinery (Figure 1.9). If DNA damage is deemed too extensive and cannot be dealt with during the normal course of the cell cycle, signals are transmitted to delay the cell cycle, to inhibit the transcription of certain genes and promote the recruitment of DNA repair factors. If the damage "overloads" this response, the cell can then initiate cell death pathways to prevent the propagation of severely damaged DNA. These processes are the result of countless post-translation and transcriptional changes which are under very tight control in the cell. This section will describe the factors and pathways responsible for the changes resulting in DSB detection, transduction and repair.

1.4.2 Sensing the DSB: sensor proteins

Several criteria have been suggested to be required by sensor proteins (Petrini and Stracker, 2003). In short, a sensor protein must first be highly sensitive to the presence of DSBs. Due to the potential lethal nature of a single DSB, this is a crucial characteristic of sensor proteins. Furthermore, sensor proteins must be able to transmit the presence of DSBs to trigger a signal amplification cascade. The signal amplification proceeds through the activation of protein kinases and the subsequent phosphorylation of their targets. These important signal transduction pathways are required to either trigger cell cycle delays to allow DNA repair to occur or, alternatively, promote cell death. Based on these characteristics, proteins that bind DNA, could possibly act as sensors. In recent years, ATM and ATR (ataxia-telangectasia and rad3 related protein) have emerged as major players to detect and relay the presence of DSBs. Several studies have started to elucidate the requirements for ATM and ATR activation in response to DNA damage.

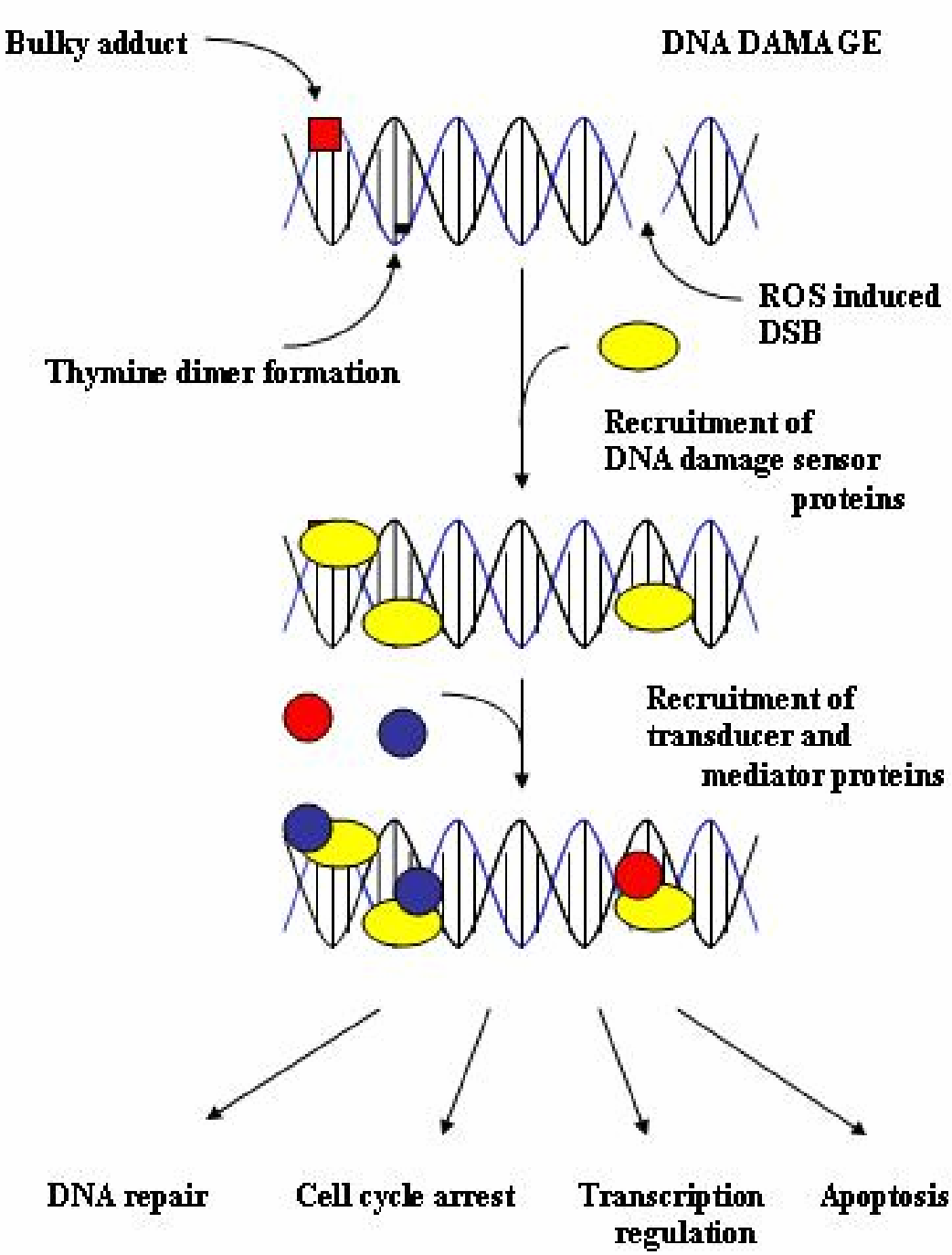

Figure 1.9: Steps involved in double strand break detection and repair. Four categories of proteins are thought to be involved in DNA damage detection and repair. 1. DNA damage sensors detect the damaged DNA. 2. Transducer proteins are recruited 3. Transducers require the assistance of mediators. 4. Effectors of DNA repair, apoptosis etc…are recruited.

However, in light of recent work, other factors have also been identified as potential primary DNA damage sensors.

1.4.2.1 Activation of ATM in response to DNA damage

The rapid induction of ATM protein kinase activity following IR exposure suggests that it plays an important role in the early response to IR-induced DNA damage. The protein kinase activity of immunoprecipitated ATM was shown to increase 2-3 fold after exposure to IR or neocarzinostatin (NCS), a radiomimetic drug (Canman *et al*, 1998; Banin *et al*, 1998). A recent study by Bakkenist and Kastan has provided significant insight into the mechanism by which ATM is activated in response to IR-induced DNA damage. Initial experiments showed that exposure to IR increased phosphate incorporation into ATM while cells containing kinase-dead ATM did not show this increase (Bakkenist and Kastan, 2003). This suggests a model by which ATM undergoes autophosphorylation upon activation. Subsequently, the authors identified serine 1981, an SQ site located in the amino-terminal of the ATM FAT domain (FRAP, ATR, TRRAP domain), as an ATM autophosphorylation site. This site was shown to be crucial for the cellular response to IR. Cells containing a serine to alanine mutation at a.a. 1981 of ATM did not support either p53 phosphorylation or cell cycle arrest. Furthermore, this study showed that *trans*-phosphorylation was occurring to dissociate the dimeric, non-active form of ATM to its monomeric, phosphorylated, active form. This presents a novel mechanism for protein kinase regulation and activation. Although this study provided a mechanism for ATM activation, it did not clarify whether ATM was the primary sensor of DSBs or not. This study has demonstrated that ATM could be activated in response to chromatin changes,

suggesting that changes in local chromatin structure may also be a trigger for sensor proteins.

1.4.2.2 The quest for a primary sensor continues

The experiments done by Bakkenist and Kastan definitely place ATM as an upstream regulator of the DNA damage induced pathways. However, it remains unclear whether ATM detects DNA damage directly or indirectly. The mode by which DSBs are conveyed to, or by, ATM is also unclear. An important characteristic of a DNA damage sensor is the ability to bind to damaged DNA directly. ATM has been shown to bind DNA *in vitro* (Smith *et al*, 1999). However, experiments showing that ATM associates with chromatin or localizes to DNA damage foci (discussed later) do not address whether the interaction with DNA is direct or indirect (Andegeko *et al*, 2001; Bakkenist and Kastan, 2003). Therefore, other primary DNA damage sensors have been suggested.

The MRN complex (MRE11/RAD50/NBS1), of the homology directed recombinational repair (HRR) pathway (described later), has recently be proposed as a good candidate for primary a DNA damage sensor. ATM is not required for MRN to bind sites of DSB immediately after they occur (Mirzoeva and Petrini, 2001). Experiments done in cell lines established from Nijmegen Breakage Syndrome (NBS) patients suggested that the MRN complex may play a role in ATM activation. These cells do not produce full length NBS1, as a result, the phosphorylation of the Fanconi Anemia protein (FANCD2), the checkpoint serine/threonine-protein kinase Chk2 (Chk2) and the structural maintenance of chromosome 1 protein (SMC1) by ATM is defective in these cells (Nakanishi *et al,* 2002; Buscemi *et al*, 2001; Yazdi *et al*, 2002). Furthermore, autophosphorylation of ATM on serine 1981 is defective in both NBS1 and Mre11 deficient cells (Uziel *et aI,* 2003;

Carson *et al*, 2003), promoting the idea that the MRN complex is required for activation of ATM and phosphorylation of several downstream targets.

Several recent studies have placed the MRN complex as an upstream activator of the ATM kinase (Lee and Paull, 2004; Uziel *et al*, 2003; Carson *et al*, 2003). The most recent of these studies demonstrated that the MRN complex directly stimulates the protein kinase activity of ATM. In the presence of the MRN complex, ATM-mediated phosphorylation of Chk2 on threonine 68, and p53 on serine 15, was stimulated up to 15-fold and 12-fold, respectively (Lee and Paull, 2004). Furthermore, it was shown that phosphorylation of NBS1 at serine 343 was essential for the ATM kinase activity towards Chk2 but not p53. A-T like disorder (ATLD) cells (Mre11 deficient) were also shown to have defective ATM phosphorylation of Chk2 while p53 phosphorylation was normal. Binding studies demonstrated that stimulation of ATM by the MRN complex increased its binding to substrates, Chk2 and p53. These experiments suggest an attractive model by which the MRN complex would act as the primary sensor, inducing a change in ATM which increases its affinity towards its substrates.

The NBS1 protein is not just involved in the activation of ATM in response to DNA damage but is also a target of ATM. Therefore, since this is the case, the sensor is also a target of the transducing kinase (ATM). This would appear to change its function making it also a mediator of cell cycle checkpoints (discussed later).

1.4.2.3 Activation of the ATR protein kinase

The mechanism underlying the activation of ATR has until recently remained unclear. Several recent studies have shed some light on its mechanism of activation. After its discovery, ATR was quickly identified as a critical protein kinase required for initiation

of cell cycle checkpoints, in particular the intra-S-phase checkpoint, upon treatment with UV, hydroxyurea, DNA alkylating agents, aphidicolin or DNA polymerase inhibitors (Shechter *et al,* 2004). Therefore, ATR was characterized as a transducer and potential sensor of "bulky lesions", while ATM served to modulate the response to DSBs.

This first line of evidence suggesting a mechanism for ATR activation came with the discovery of the ATR interacting protein (ATRIP). This protein was shown to bind the replication protein A (RPA) as well as single stranded DNA. It also serves to recruit ATR (Zou and Elledge, 2003). Other studies have suggested that the RPA-ssDNA complex specifically activates ATR, suggesting that RPA bound to ssDNA serves as a signaling intermediate to sense DNA damage (Cortez *et al,* 2001). Furthermore, RPA and ATRIP are required for the loading of the Rad9-Hus1-Rad1 (9-1-1) clamp complex onto its DNA template (Zou *et al,* 2003). This complex resembles a PCNA-like clamp which promotes ATR mediated activation of Chk1 in response to genotoxic stress (Parrilla-Castellar *et al*, 2004).

1.4.2.4 The detection of DSBs by the BASC complex

Gel filtration studies have identified both ATM and ATR as members of very high molecular weight, multi-protein, macro-complexes (Shiloh, 2001). Immunoprecipitation studies have recently found ATM to be a component of a very large complex containing BRCA1, MRE11/RAD50/NBS1, the BLM helicase, MSH2, MSH6, MLH1 and RC-F (Wang *et al*, 2000). This large complex was termed the BASC (BRCA1- associated surveillance complex) since all of its components were associated with checkpoint control, DNA repair or chromosomal instability disorders. It has been suggested that BRCA1 may act as an adaptor to bring into close proximity several of the factors required for

management of DSBs (Ting and Lee, 2004). It is likely that the formation of BASC, is a dynamic processes. It is also likely dependent on the type of DNA damage incurred and the time delay post-damage.

1.4.2.5 DNA damage induced foci

Several of the proteins discussed above, as well as others involved in the DNA DSB repair pathways are normally found diffused throughout the nucleus. However, upon DNA damage, they localize to specific nuclear sites. These subnuclear complexes, which can be detected microscopically, are referred to as DNA damage induced foci or IRIF (IR-induced foci) (reviewed in Bradbury and Jackson, 2003). Foci are thought to form at the actual sites of DNA damage (Melo *et al*, 2001). Several factors localize to these sites in response to IR. Mre11 of the MRN complex (D'Amours and Jackson, 2002), ATM (Fernandez-Capetillo *et al*, 2003), ATR (Tibbetts *et al*, 2000), H2AX (Paull *et al*, 2000), DNA-PKcs (Chan *et al*, 2002), p53 binding protein 1 (53BP1) (Anderson *et al*, 2001), BRCA1 (Scully *et al*, 1997), Chk2 (Ward *et* al, 2001) and the mediator of DNA checkpoint 1 (MDC1) (Bradbury and Jackson, 2003) have all been shown to localize to foci.

To date, the most rapidly formed IRIF detected have been the foci formed by phosphorylation of H2AX on serine 139 (designated γ-H2AX, Rogakou *et al*, 1998 and 1999). As such, γ-H2AX has been proposed to recruit several of the protein factors required for DSB "management". These foci have been detected as early as 1-3 minutes following treatment with IR (Paull *et al*, 2000). Several of the DSB repair proteins are found to colocalise at these foci. In H2AX deficient mice, the recruitment of BRCA1, Rad51, NBS1, 53BP1 and MDC1 (DSB recognition and repair proteins) is altered (Stewart *et al*, 2003; Fernandez-Capetillo *et al*, 2002; Celeste *et al*, 2002).

At this time, many of the factors localizing to foci and the biological importance of foci formation are unknown. Foci may serve as a control centers to coordinate the appropriate factors required for the signaling and repair of DNA damage. The formation of IRIF is likely a dynamic process with different proteins being present at a particular time and point. BASC may possibly play a role in the coordination of these factors in a DNA damage specific way. Although the formation of foci has been characterized for IR, different types of damage may also induce foci formation. However, this will require additional investigation. Interestingly, Mre11 forms foci in a time and dose-dependent manner in response to DSB-inducing agents but not UV damage (Maser *et al*, 1997). Several questions remain such as: what are the signals for protein relocation after DNA damage and how are proteins directed into repair foci? It has been suggested that the hierarchy of focus formation may provide an approach to determine the order of molecular events which result in DSB detection and repair (Petrini and Stracker, 2003)

1.4.3 Amplification of the signal: transducer proteins

The ATM and ATR protein kinases have been described as primary activators of the cellular response to DNA DSBs. These protein kinases sense the type of damage and transmit the information by activating a "chain reaction", resulting in the phosphorylation of several key players in various branches of the DNA damage signaling pathways (Shiloh, 2003; Kurz and Lees-Miller, 2004). Most recently, a third protein, the human nonsense-mediated mRNA decay protein SMG-1 (ATX/hSMG-1) has also been identified as being involved in the genotoxic stress response pathway (Brumbaugh *et al*, 2004). Early stages of characterization determined these protein kinases had the ability to phosphorylate the p53 tumour suppressor on serine 15 (Nakagawa *et al*, 1999; Tibbetts *et al*, 1999), thereby

activating a stress response. However, although the p53 protein plays a fundamental role as the nodal point in the cellular response to DSBs, a plethora of other substrates are also phosphorylated in response to DNA damage, several of which appear to be involved in DNA repair and checkpoint signaling (Kastan and Lim, 2000, Kurz and Lees-Miller, 2004) (Figure 1.10).

The checkpoint protein kinases Chk1 and Chk2 are phosphorylated as part of the signal transduction cascade to indicate damage to p53. ATM phosphorylates Chk2 on threonine 68 in response to DNA damage which activates Chk2 to phosphorylate both p53 and Cdc25C (McGowan, 2002). Although Chk1 was for long believed to be primarily an ATR substrate, ATM has recently been shown to phosphorylate it on serines 317 and 345 (Gatei *et al*, 2003; Sapkota *et al*, 2002), supplying evidence for an overlap in these two pathways. hMDM2 (human homolog mouse double minute chromosome 2), the negative regulator of p53, is an ATM substrate (Maya *et al,* 2001). Phosphorylation of MDM2 on serine 395 by ATM inhibits its interaction with p53. ATM phosphorylation of BRCA1 on serine 1524 is also critical for cellular recovery after IR induced damage (Cortez *et al*, 1999). The phosphorylation of H2AX on serine 139 by ATM (Rogakou *et al*, 1998), in response to IR, is thought to play a role in the changes of chromatin structure induced in the vicinity of DNA DSBs (Burma et al, 2001). ATM has been shown to phosphorylate the NBS1 of the homologous recombination MRN complex (Gatei et al, 2000). Other substrates of ATM include: the Bloom's syndrome helicase (BLM), LKB1, CtIP, TopBP1, RPA32, E2F1, c-Abl FANCD1, TRF1, PHAS-I, Rad17, Rad9 and MDC1, 53BP1 and SMC1 (reviewed in Kurz and Lees-Miller, 2004 and Goodarzi *et al*, 2003). ATM is also indirectly involved in the phosphorylation of IKK and c-jun (Li *et al*, 2001 and Foray *et al*, 2003). These DNA damage sensing mechanisms trigger cascades of phosphorylation

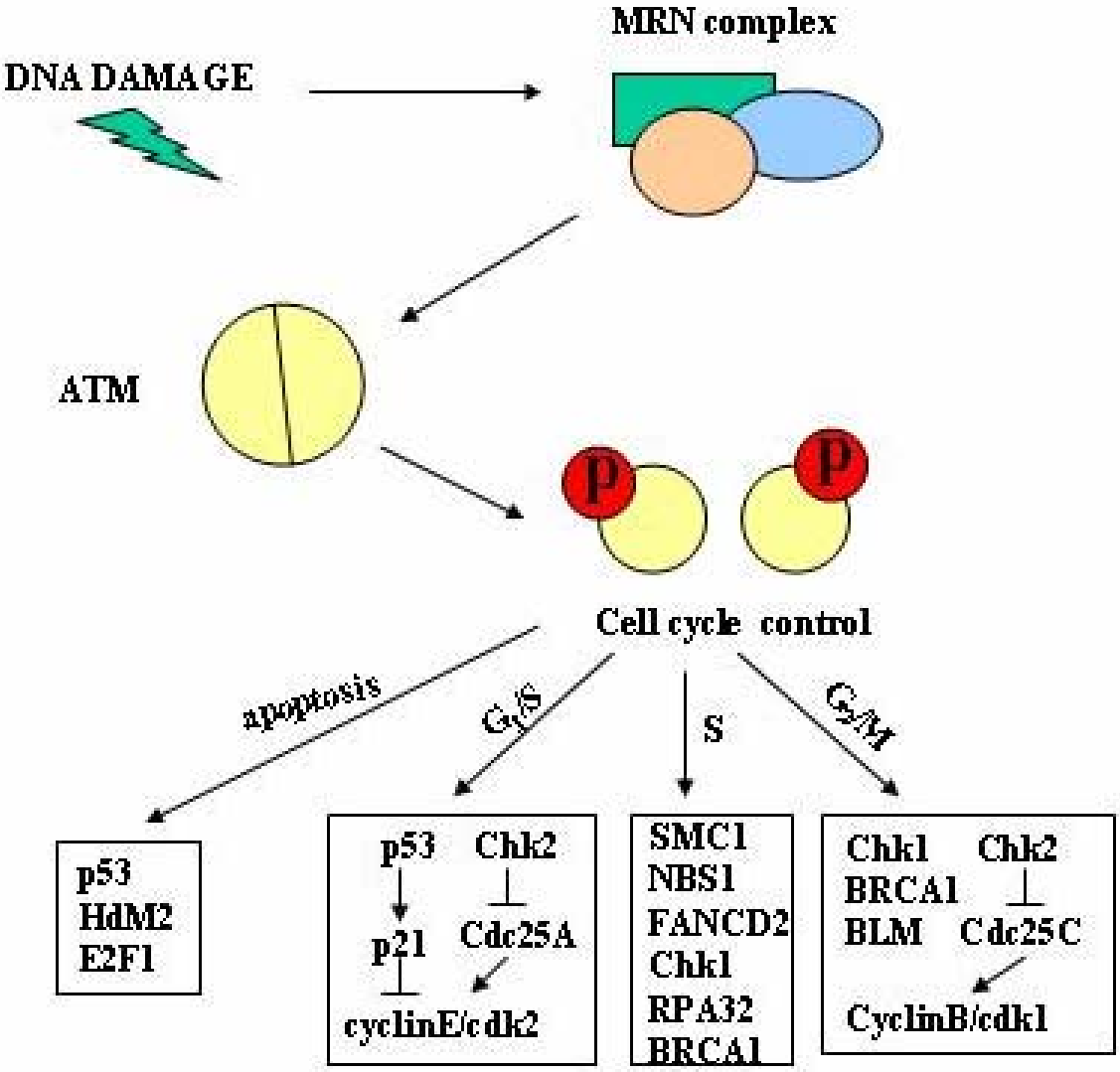

Figure 1.10: A model for ATM activation and signaling in response to DNA damage. DSBs are detected by the MRN complex which leads to the activation of ATM by autophosphorylation on serine 1981. This phosphorylation event causes the dissociation of ATM from a dimeric to a monomeric state. Once ATM is activated, it can phosphorylate several downstream effectors involved in apoptosis and cell cycle control.

events. This results in either, delays in cell cycle progression to allow repair, or if the damage is too extensive, the decision to die through induced cell death pathways.

1.4.3.1 Structural and biochemical properties of the PIKK family of protein kinases

ATM and ATR, the DNA dependent protein kinase catalytic subunit (DNA-PKcs) as well as ATX/hSMG-1 belong to a family of serine-threonine kinases whose catalytic domains have a clear evolutionary relationship to the yeast and mammalian phosphoinositide 3,4-kinase (PI3K). The presence of this signature catalytic domain in the C-terminal region, has defined kinases containing it as being part of the phosphoinositide 3-kinase related kinase family (PIKK) (Hartley *et al,* 1995; Abraham, 2001). In addition to this signature catalytic domain, all family members share several features, including a similar structural organisation (with the exception of hSMG1) (Figure 1.11). They are very large protein kinases, between 300 to 500 kDa in size. All PIKK family members contain a FAT domain, a C-terminal FAT domain (FAT-C) and a PI3K domain. The N-terminal variable region of this family of proteins was recently discovered to contain several HEAT repeats (Huntingtin, elongation factor 3, A subunit of phosphatase 2A and mTOR1) (Perry and Kleckner, 2003). Low resolution molecular structures of ATM and DNA-PKcs have been obtained (Llorca *et al*, 2003; Leuther *et al*, 1999). These structures have provided a model by which these protein kinases can wrap around the DNA with a protruding arm-like region. This model is similar to that of other DNA binding repair proteins such as the human APE1 endonuclease and the *E.coli* Vsr endonuclease (Tsutakawa *et al*, 1999).

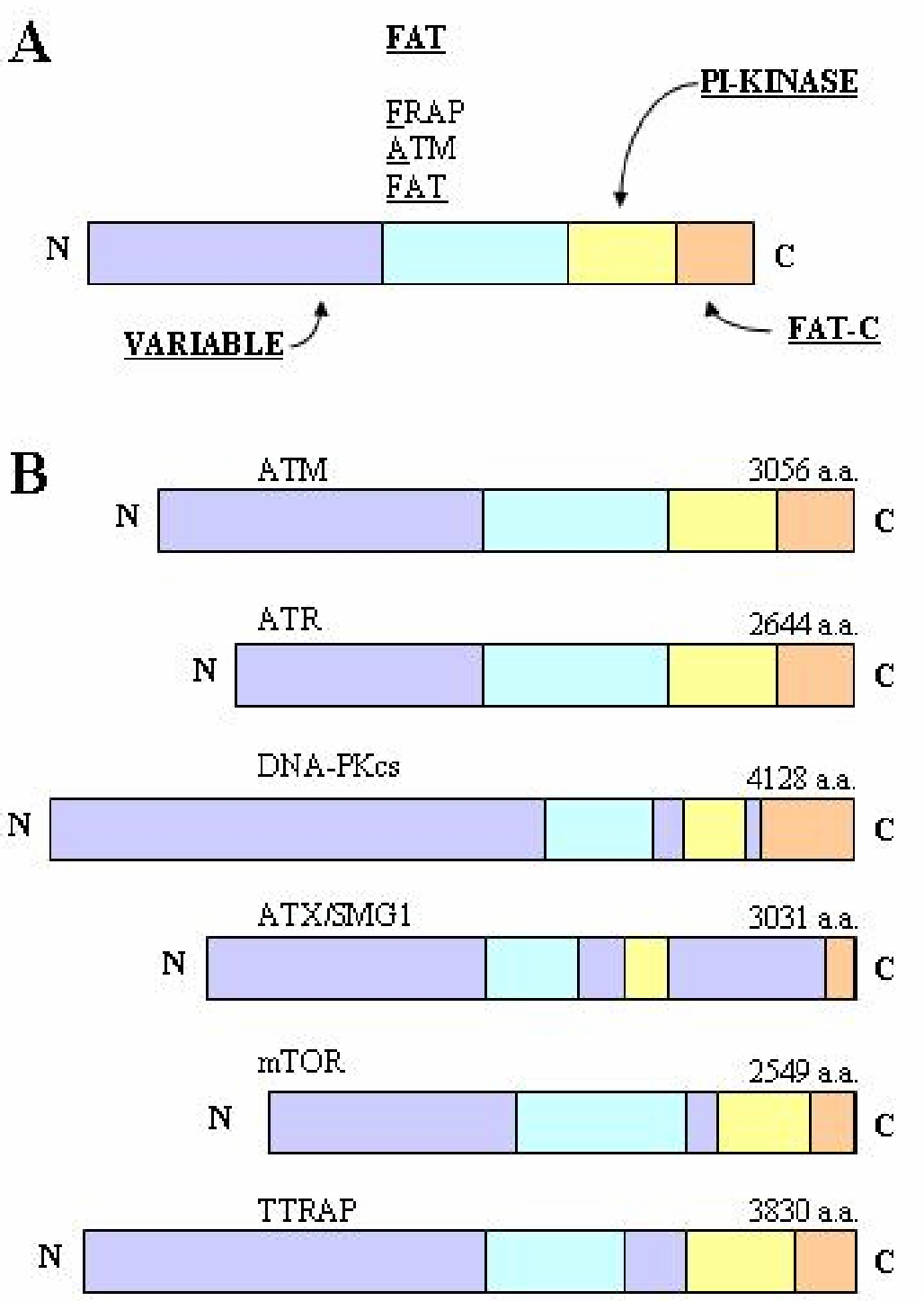

Figure 1.11: Comparison of structural organisation in PIKK family members. A. General structural organisation of PIKK family members. B. PIKK family members

Although they show a.a. sequence similarity with the phosphoinositide kinases, which phosphorylate lipid substrate, the PIKKs appear to phosphorylate protein and peptide substrates exclusively. Along with ATM, ATR and ATX/hSMG-1, which are involved in early signal transduction through cell cycle checkpoints, and DNA-PKcs involved in DNA DSB repair, this family also includes other subfamilies of protein kinases such as FRAP/mTOR (FKBP and rapamycin-associated protein/mammalian target of rapamycin) and TRRAP (Transformation/transcription domain-associated protein) (Figure 1.11). FRAP/mTOR, the mammalian ortholog of the *Saccharomyces cerevisiae* target of rapamycin genes (TOR1 and TOR2), is the target of the antifungal and immunosuppressive compound rapamycin. It has been shown to coordinate G_1 progression with the available supply of nutrients and growth factors (Gingras *et al,* 2001). TRRAP is required for the assembly of a functional histone acetyltransferase (HAT) complex (Park *et al*, 2001). It is also noteworthy to mention that ATX/hSMG1 is also involved in the regulation of nonsense-mediated mRNA decay (NMD) (Yamashita *et al*, 2001), providing a link between genome and transcriptome integrity.

Homologs of ATM and ATR are present in all eukaryotic cells examined to date, including *Saccharomyces cerevisiae* and *Schizosaccharomyces pombe* (Abraham, 2001). Although, ATX/hSMG-1 was named for its sequence homology to the *Caenorhabditis elegans* protein CeSMG-1, it does not have a clear homologue in yeast species. It has been suggested that the need for this factor in NMD appears to have evolved in metazoan species (Abraham, 2004). As previously mentioned, the PIKKs are serine/threonine kinases known to recognise a common motif in their substrates Ser/Thr-Gln-Glu (Lees-Miller *et al*, 1992, Kim *et al*, 1999; O'Neill *et al*, 2000, Brumbaugh *et al*, 2004). This consensus is present at serine 15 of p53. Although there appears to be significant overlap between the

ATM, ATR and ATX/hSMG-1 consensus sequences, selection of substrates phosphorylated by one versus another is likely to depend on the selected genotoxic stress. Activation of ATM and ATR appears to be lesion specific, with ATM being specific to damage which induces DSBs (for example as induced by IR and radiomimetic drugs), while ATR deals with the bulkier type of adducts, often the result of UV damage (Tibbetts *et al*, 1999). The DNA damage specificity of ATX/hSMG-1 remains to be determined. Studies using cells overexpressing a kinase inactive form of ATR (ATR^{KI}) show that phosphorylation of ser15 on p53, a known target of both ATM and ATR, was not sustained after an extended period of time post IR treatment. The same study also showed that p53 serine 15 phosphorylation in response to UV was reduced by overexpressing ATR^{KI} (Tibbetts *et al*, 1999). This evidence suggests that ATR serves as a "backup" kinase for maintaining the ATM response to IR while it plays the primary role in the UV response.

1.4.3.2 Cell-cycle checkpoint functions of ATM and ATR

DNA repair plays a crucial role in the maintenance of genome integrity whether or not cells are proliferating. However, while cells are proliferating added precautions are needed. Since incomplete repair before chromosomal replication or segregation can lead to the propagation of mutations, mechanisms exist to delay cell cycle progression until DNA damaged is fixed. These mechanisms termed "checkpoints" can lead to cell cycle delay in the G_1, S or G_2 phase. It is well documented that ATM-deficient cells display significant defects in the G_1, S and G_2 checkpoints. Due to the inviability of ATR-deficient cells, other means have been used to determine its role in cell cycle checkpoints. Although there seems to be an overlap in ATM and ATR substrates, it also appears as though they have some distinct checkpoint signaling functions.

1.4.3.2.1 *The G_1 checkpoint*

The G_1 checkpoint is thought to prevent the cell from replicating its DNA until it can ensure that the DNA is intact. Therefore, in the event of DNA damage, cell cycle progression is arrested before the cell completes G_1. Arrest in G_1 is primarily controlled by the p53 tumour suppressor protein. Activation of p53 to its transcriptionally active form, results in arrest of the cell cycle in G_1 and a halt in DNA synthesis. Activation of p53 involves several post-translational modifications (described later), protein stabilisation and its translocation to the nucleus (Appella and Anderson, 2001, Prives and Manley, 2001). As a result, p53 can activate the transcription of $p21^{WAF1}$, an inhibitor of the cyclin dependent kinases (cdks), thereby stalling entry into S-phase (Figure 1.12). Although p53 plays an important role in all checkpoint controls of the mammalian cell cycle, only the G_1 checkpoint is completely abrogated when p53 function is lost (Ko and Prives, 1996).

1.4.3.2.2 *The S-phase checkpoint*

This checkpoint occurs within S phase and is characterised by a decreased rate of DNA synthesis after genotoxic stress. The same components involved in the G_1/S transition have been identified as key components for the intra-S-phase checkpoint (Falck *et al*, 2002). Therefore, the ATM/ATR-Chk2/Chk1-Cdc25A-Cdc45 axis plays a role in signaling within S-phase. Defects in any of these components results in a radioresistant DNA synthesis (RDS) phenotype, a condition of persistant DNA synthesis after radiation-induced DNA damage (Falck *et al*, 2002). In order to establish a replication delay at this checkpoint, ATM/ATR phosphorylates Chk2/Chk1 which in turn phosphorylate the Cdc25A phosphatase targeting it for degradation by the proteosome-ubiquitin mediated

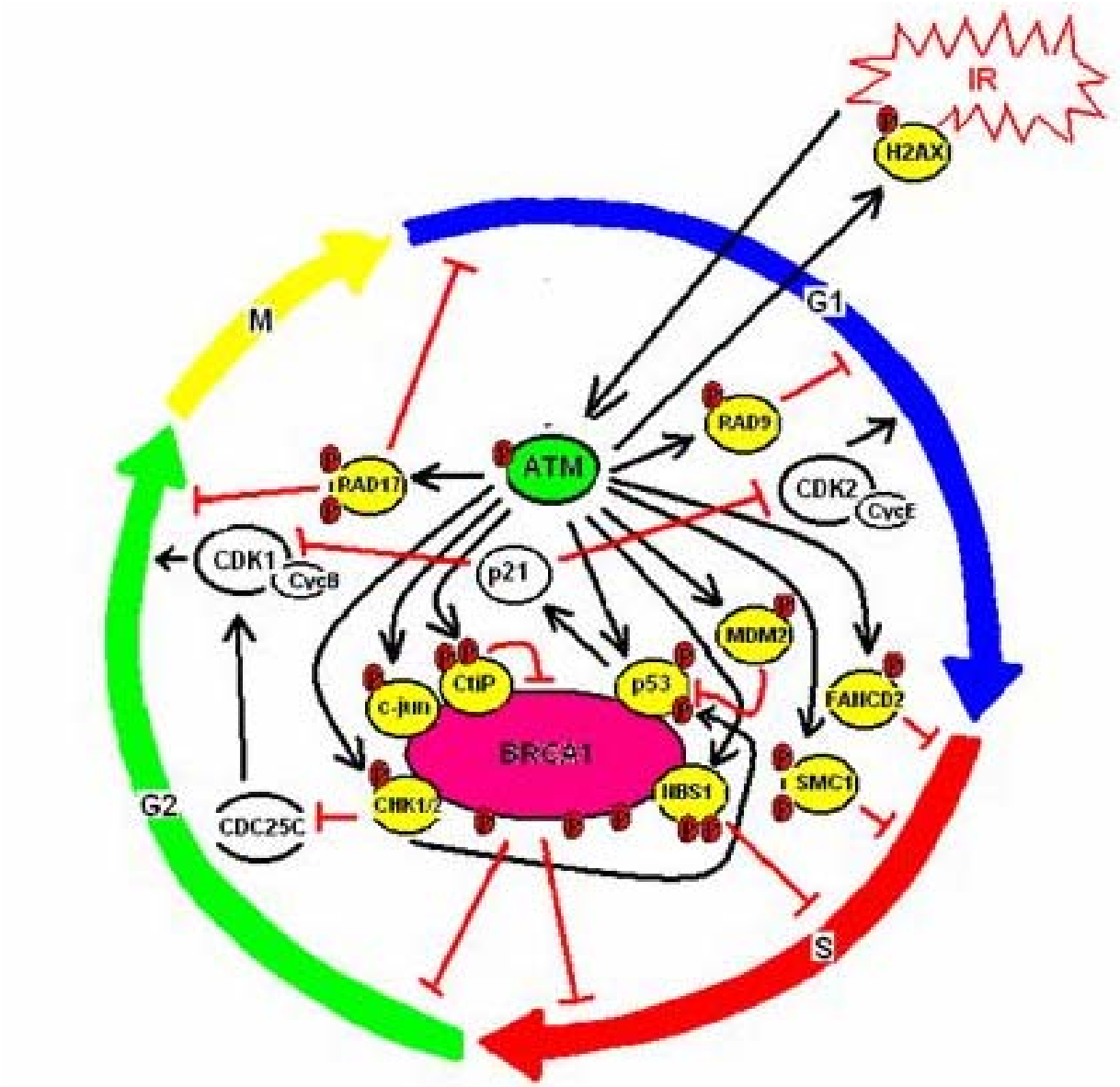

Figure 1.12: ATM (ATR)-dependent cell cycle signaling functions. ATM (or ATR) signaling results in cell cycle arrest in G_1, S or G_2. Solid lines with bars indicate inhibition while arrowheads indicate phosphorylation events.

pathway. Removal of the Cdc25A phosphatase maintains the phosphorylation of Cdk2 on threonine 14 and tyrosine 15 preventing it from loading Cdc45 required for early and late firing at origins of replication (Xu *et al*, 2001). ATM is required to phosphorylate NBS1, a member of the MRN complex, on serine 343 as part of this checkpoint (Zhao *et al*, 2000). Furthermore, NBS1 deficient cells display the RDS phenotype (Xu *et al*, 2001). The same study examined BRCA1 deficient cells, they found that these cells were also deficient in the intra-S-phase checkpoint and displayed a RDS phenotype. Moreover, reintroducing BRCA1 containing a serine 1387 to alanine mutation in BRCA1 deficient cells did not rescue the RDS phenotype (Xu *et al*, 2002), suggesting that this ATM phosphorylation site is important for the intra-S-phase checkpoint. The presence of FANCD2 is also required for this checkpoint (Taniguchi *et al,* 2002).

***1.4.3.2**.3 The G_2 checkpoint*

The control of the G_2/M transition ensures duplication of the centrosome, correct formation of the mitotic spindle and DNA integrity. This checkpoint is ultimately controlled by preventing the dephosphorylation and subsequent activation of the cyclin B1/Cdk1 complex. In response to DNA damage, ATM and ATR phosphorylate Chk2 and Chk1. Both of these kinases can then phosphorylate the mitosis-promoting dual specificity protein phosphatase Cdc25C, sequestering it away from the nucleus through an interaction with the 14-3-3α protein. This prevents the dephosphorylation of Cdc2 kinase on tyrosine 15, which is required for the activation the Cdc2/CyclinB1 complex, allowing entry into mitosis (Lopez-Girona *et al*, 1999).

1.4.4 DNA damage response mediators

MDC1 has also emerged as an important member of the DNA damage response. MDC1 has been shown to interact with the MRN complex independently of DNA damage. Furthermore, MDC1 is required for MRN dependent ATM activation in response to high doses or IR (Mochan *et al*, 2003).

Immunoprecipitation of Rad50 results in the depletion of MDC1, suggesting that MDC1 may be a member of the MRN complex (Goldberg *et al*, 2003). Reduced expression of MDC1, by siRNA, resulted in intra-S and G_2/M checkpoint defects. It is noteworthy to mention that, this is the same effect as observed when deficiencies in the MRN complex members are present. Depletion of MDC1 results in checkpoint defects.

γ-H2AX and 53BP1 may also qualify as DNA damage mediators since their focus formation is affected in the absence of ATM. However, deficiencies in γ-H2AX and 53BP1 only result in mild checkpoint insufficiency. 53BP1 has been shown to be required for the MRN-dependent activation of ATM in response to low doses of IR (Mochan *et al*, 2003)

BRCA1 is required for the ATM-dependent phosphorylation of p53, NBS1, Chk2 and c-jun (Foray *et al*, 2003). BRCA1 is also required for the phosphorylation of SMC1 (Kim *et al*, 2002) and Chk1 (Yarden *et al*, 2001). Thus, BRCA1 may act as a scaffold to bring several other DNA damage response mediators in close proximity with the DSB

1.5 Additional modes of regulation

Protein phosphorylation and dephosphorylation plays an important role in the DNA damage response, including cell cycle progression and arrest. Most efforts have been concentrated on identifying the protein kinases involved in these processes. However, researchers have rarely addressed, for example, how cells reenter the cell cycle after arrest.

It is logical to speculate that if protein kinases initiate a response, protein phosphatases can turn it off. Thus far, it remains unclear whether cells recover from the DNA damage response by dephosphorylation or through other mechanisms such as protein degradation or relocalisation. However, recent reports have revealed that protein phosphatases are involved in the DNA damage response.

Three different protein phosphatases have been identified as modulators of different DNA damage transducer and mediator proteins. Protein phosphatase 5 (PP5) has been identified as playing a role in regulating the activity of both ATM and DNA-PKcs (Ali *et al*, 2004; Wechsler *et al*, 2004). Both studies found PP5 was required to dephosphorylate major phosphorylation sites in these two proteins, serine 1981 on ATM and threonine 2609 on DNA-PK. The *S. pombe* protein phosphatase type 1 (PP1) Dis2 is required for the dephosphorylation of Chk1 and consequently the normal recovery from the G_2 checkpoint (den Elzen and O'Connell, 2004). The human protein phosphatase 1α (PP1α) has also been shown to interact with and dephosphorylate BRCA1 (Liu *et al*, 2002). Protein phosphatases have also been identified as modulators of the phosphorylation on different sites of the p53 tumour suppressor. *In vitro* evidence suggests that PP1 can dephosphorylate serine 15 on p53 (Haneda *et al*, 2004). Furthermore, protein phosphatase 2A (PP2A) was shown to dephosphorylate p53 serine 37 suggesting a role in the transcriptional regulation of p53 in response to DNA damage (Dohoney *et al*, 2004).

1.6 Double strand break repair pathways

There are two primary pathways for DNA DSB repair: HRR and non-homologous end joining (NHEJ). Both pathways are conserved in eukaryotes. The two pathways differ in their requirement for a homologous DNA template and in the fidelity of their respective

repair reactions. While HRR uses an intact sister chromatid as a template for repair, HHEJ simply religates broken DNA ends. Therefore, HRR occurs with high fidelity while NHEJ may result in mutation or deletion due to lost nucleic acid sequence. Although they are not mutually exclusive, the relative importance of each pathway appears to be cell cycle dependent. The contribution of NHEJ is greater in the G_0 and G_1 phases of the cell cycle, while HRR dominates in the S and G_2 phase (Takata *et al*, 1998). This section will describe the two DSB repair pathways.

1.6.1 Homology directed recombinational repair (HRR)

The budding yeast *Saccharomyces cerevisiae* repairs most of its DSBs using HHR (Haber, 1995). As such, the mechanisms and protein components of HRR were originally identified through genetic analysis of this organism. Products of the genes *RAD50, RAD51, RAD52, RAD54, RAD55, RAD 57, RAD59, MRE11,* and *XRS2* were all identified as key players in the HRR process. Mammalian homologues of these gene products have been identified. Figure 1.13 depicts the steps involved in HRR.

The first step of HRR involves homologous pairing and strand exchange. The process is initiated by the Rad50/Mre11/Xrs2 complex (Xrs2 is replaced by NBS1 in humans), which provides the nuclease activity needed for the resection of the DSB in the 5' $\rightarrow$ 3' direction. This creates the ssDNA tail needed for Rad51 to instigate strand exchange. This strand exchange process is facilitated by the DNA end binding Rad52 and by Rad54 (Van Dyck *et al*, 1999). Rad52 was shown to play a dual role in this reaction. First, it stimulates strand invasion by directly interacting with Rad51 (Shen *et al*, 1996) and RPA, a ssDNA binding protein (Park *et al*, 1996). Second, it was shown to promote single-strand

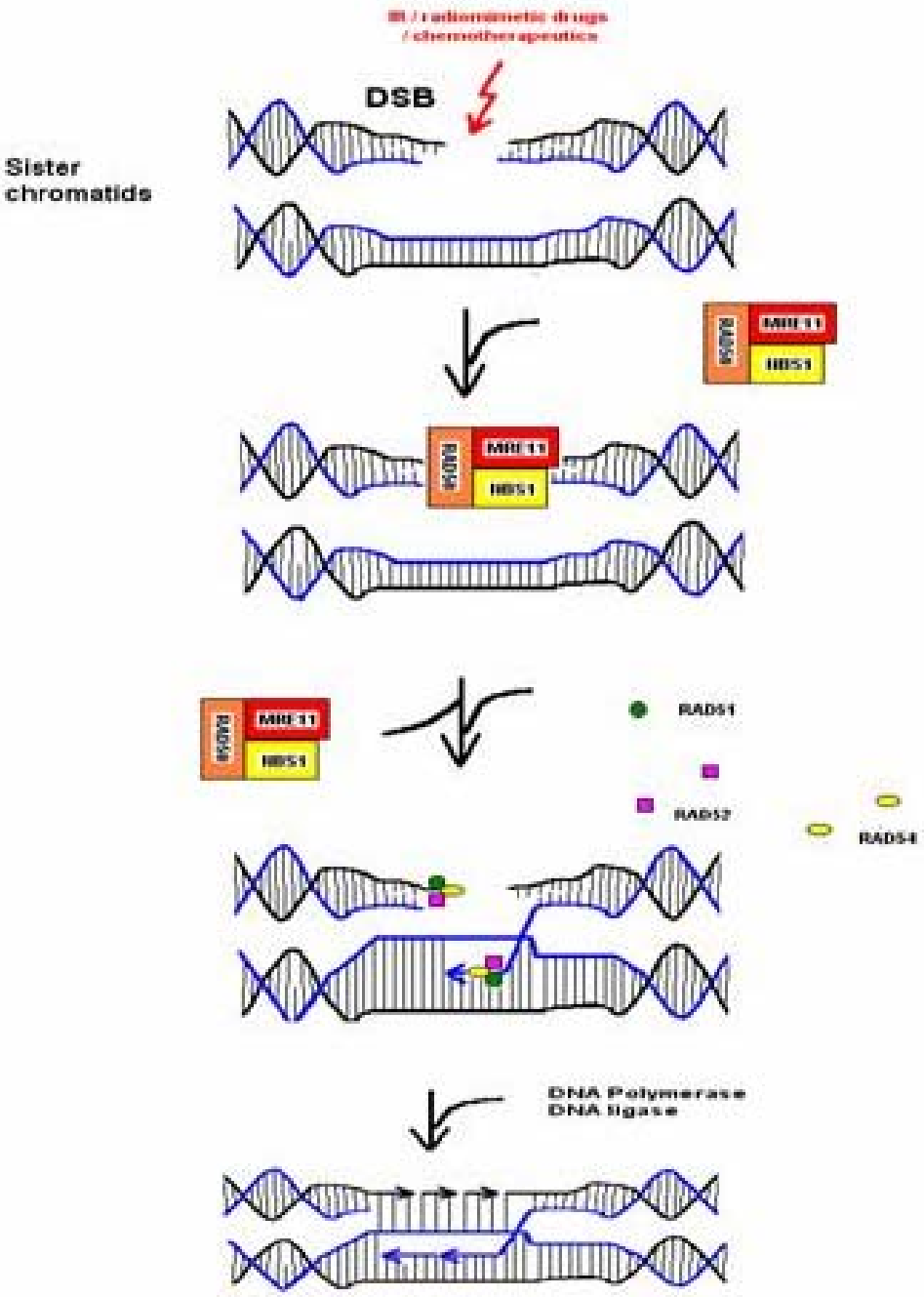

Figure 1.13: Homology directed recombinational repair (HRR). 1. End processing by Rad50/Mre11/Nbs1. 2. Rad51 binds. 3. Rad52 and Rad54 facilitate strand exchange. 4. DNA polymerase extends DNA and DNA ligase seals nick. 5. Crossovers are resolved resulting in intact DNA molecules.

annealing reactions without requiring Rad51 (Mortensen *et al*, 1996). Rad54 was shown to stimulate Rad51-catalysed pairing of homologous DNA molecules *in vitro* (Petukhova *et al*, 1998). However, exactly how Rad54 stimulates the process of strand invasion *in vivo*, remains unclear. Strand exchange proceeds with Rad51 mediating the search for homologous DNA sequences on the undamaged partner. When this sequence is found, the damaged molecule invades the other DNA duplex. A DNA polymerase extends the 3' end of the molecule by copying the DNA sequence of the undamaged partner.

In the final steps, both ends are ligated through DNA ligase I, and two intact DNA molecules are generated by resolving the DNA crossovers (or Holliday junctions). This process is well characterized in prokaryotic cells. However, it remains to be elucidated in eukaryotic systems. Fractionated mammalian cell free extracts have been showed to have the ability to resolve Holliday junctions (Constantinou *et al*, 2001). However, the identity of the factors responsible for this activity remains elusive.

As for most systems, HRR is probably more complex in human cells than in yeast cells. Since mammalian homologues exist for all of these HRR factors, the basic mechanism is thought to be conserved. However, mammalian cells possess additional factors not present in yeast that are likely to play regulatory roles. Two such factors are the breast cancer susceptibility proteins BRCA1 and BRCA2. Both proteins are required for efficient HRR in mammalian cells (Venkitaraman, 1999). Rad51 has been shown to interact with BRCA2 probably through a BRCA1 intermediary (Wong *et al*, 1997). Furthermore, as previously mentioned, these two tumour suppressor proteins colocalise with Rad51 in DNA damage induced foci. The pleiotropic phenotypes of BRCA1 and BRCA2 mutations suggests that they are involved in several aspects cell cycle control, chromatin remodeling, DNA damage detection and repair (Kerr and Ashworth, 2001). As

such, in the HRR process they have been suggested to play a role in the signal transduction from DSB recognition to DSB repair machineries as well as, serve as scaffolding proteins for Rad51 at break sites (West, 2003).

1.6.2 Non-homologous end-joining (NHEJ)

The non-homologous end-joining pathway is the more common DSB repair pathway in multicellular eukaryotes. Typically, when DNA DSBs are generated in the cell, the broken ends are very diverse and consequently generally incompatible. The use of this error-prone system is presumably due to the fact that it is likely difficult to bring homologous chromosomes together unless they are already in close proximity, as is the case in S and G_2 phase cells. It has also been suggested that HRR could be too dangerous and too slow in organisms that have a significant amount of repetitive DNA in their genome (Lieber *at al*, 2003). The individual steps of this pathway are summarized in Figure 1.14.

This pathway is carried out by a conserved set of proteins: Ku70, Ku80, DNA ligase IV and XRCC4 (X-ray cross complementing group 4) (Haber, 2000). In vertebrates, the DNA-dependent protein kinase catalytic subunit (DNA-PKcs) is also required (Smith and Jackson, 1999) (Figure 1.14). The process of NHEJ not only acts on DSBs induced by DNA damage, but also on DNA breaks arising during the course of immunoglobin gene rearrangement. Therefore, cells and animals deficient in DNA-PKcs are defective in both DSB repair and V(D)J recombination, the process by which antibody and T cell diversity is generated (Gellert, 2002). In fact, severe combined immunodeficiency (SCID) in several species (including humans, dogs, horses and mices) is the result of deficiencies in factors involved in NHEJ (reviewed in Bankert *et al*, 2002).

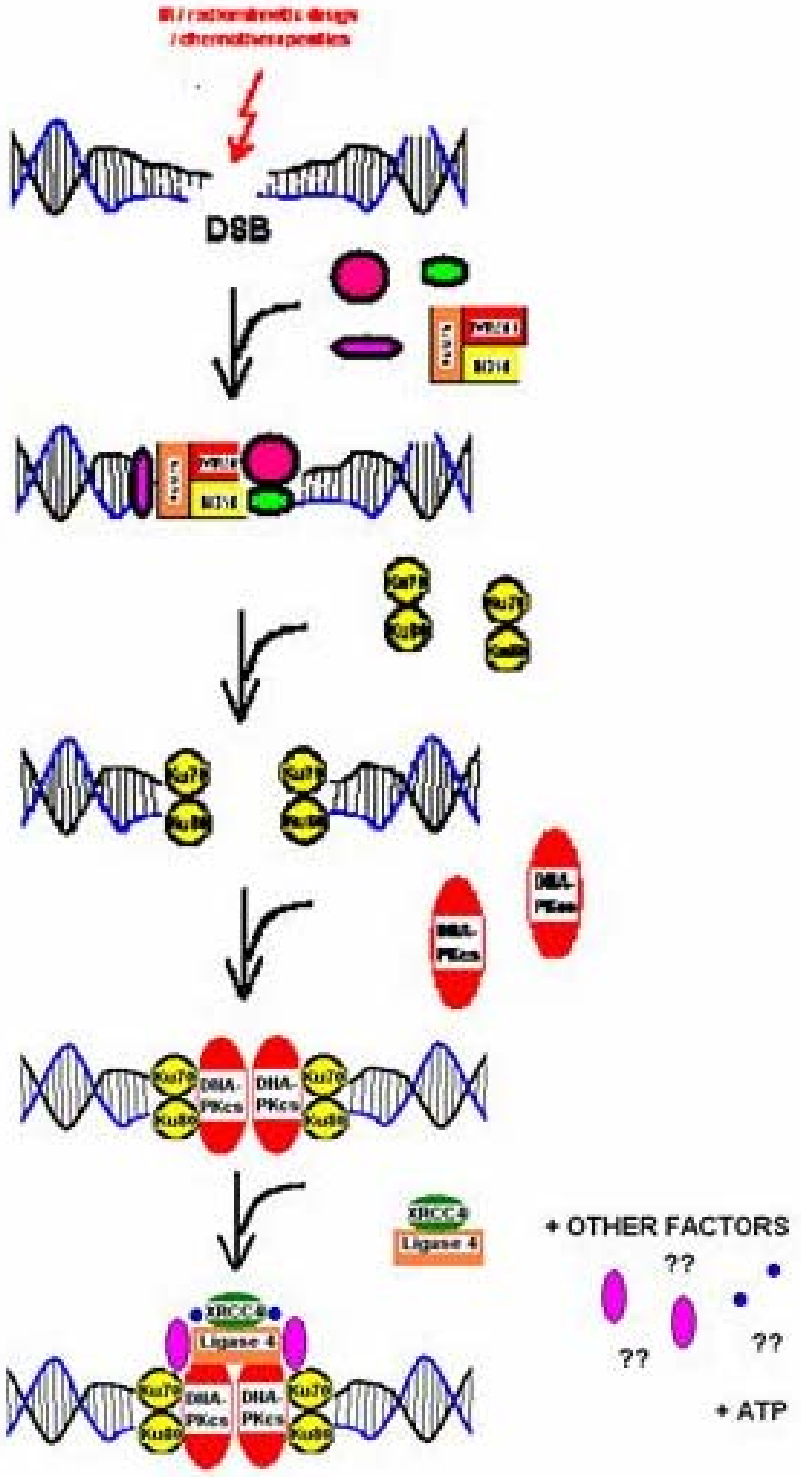

Figure 1.14: Non-homologous end-joining pathway (NHEJ). 1. End processing enzymes and the Ku heterodimer bind at the DSB. 2. DNA-PKcs binds 3. XRCC4/Ligase 4 is recruited along with other factors and ATP 4. DNA is repaired

NHEJ is initiated by the DNA-end binding activity of the Ku 70/80 heterodimer (Nick-McElhinny *et al*, 2000). Once Ku is loaded onto the DNA terminus, it can translocate to an internal DNA site. Walker *et al,* 2001 reported a Ku crystal structure which suggests that the heterodimer forms a ring structure which allows it to thread onto dsDNA. In mammalian cells, DNA-PKcs also binds at these sites, resulting in the activation of its serine/threonine kinase activity (Smith and Jackson, 1999). Although both DNA-PKcs and Ku can both bind DNA ends individually, studies have shown that the DNA termini are required for their association (Yaneva *et al*, 1997). While the mechanism by which DNA-PKcs functions in NHEJ is not entirely clear, it is likely that it plays a regulatory role by modulating the activities of the other components through phosphorylation events. However, although several *in vitro* DNA-PKcs substrates have been identified, very few have revealed themselves as relevant *in vivo* substrates. DNA-PKcs has been shown to phosphorylate itself (Chan *et al*, 2002; Douglas *et al*, 2002), the Werner syndrome helicase (WRN) (Karkamar *et al*, 2002a) and it is also thought to be involved in synapsis, a process by which the DNA ends are kept in close physical proximity to prevent them from diffusing away from each other (DeFazio *et al*, 2002).

Typically, in order for rejoining to occur, nucleases, RNA polymerases and other end processing enzymes are required to remove several nucleotides and fill in the gaps. There is evidence that the polynucleotide kinase (PNK) can phosphorylate the 5' end of the DNA when necessary (Chappell *et al*, 2002). Artemis was identified on the basis of its mutation in a subset of human SCID patients (Moshous *et al*, 2001). It was later shown to have nuclease activity, to be phosphorylated by, and form a physical complex with DNA-PKcs *in vivo* and *in vitro* (Ma *et al*, 2002). As such it has been proposed as a potential nuclease involved in NHEJ. DNA polymerase μ (pol-μ) is a good candidate for the

polymerase involved in the NHEJ reaction since it has been reporter to interact Ku-DNA-XRCC4-ligaseIV complex (Mahajan *et al*, 2002).

The problem of end processing remains an enigma in NHEJ. However, several other end processing factors have been suggested as potential players in this pathway. These suggestions are made based on their ability to interact with one of the components of NHEJ or their ability to stimulate NHEJ *in vitro*. The non- protein factor inositol hexakisphosphate (IP_6) has been shown to bind Ku and stimulate NHEJ *in vitro* (Hanakahi *et al*, 2000; Hanakahi and West, 2002). The MRN complex has nuclease activity used for the resection of DSBs in the 5' $\rightarrow$ 3' direction. It has been shown to stimulate DSB rejoining *in vitro* (Huang and Dynan, 2002). Finally, WRN has been shown to interact with the both DNA-PKcs and Ku (Karmakar *et al*, 2002b). It may be involved in DNA end processing through its DNA helicase or exonuclease activity. Furthermore, it has been identified as one of the rare *in vivo* substrates of DNA-PKcs, making it a good candidate for the NHEJ pathway (Karmakar *et al*, 2002a).

In the final step, the heterodimeric complex of DNA ligase IV/XRCC4 is recruited to break site by Ku to complete the annealing process (Nick McElhinny *et al*, 2000). DNA ligase IV was established as the ligase involved in NHEJ based on its interaction with XRCC4 (Grawunder *et al*, 1997). Furthermore, this interaction with XRCC4 appears to stabilize and enhance ligase IV activity. Additionally, XRCC4 deficiency results in lowered expression of DNA ligase IV *in vivo* (Bryans *et al*, 1999).

1.7 Human deficiencies in the DSB detection and repair proteins

Several of the proteins involved in the genotoxic stress response are associated with chromosomal instability disorders. Furthermore, several of these conditions show overlap in their clinical and cellular features. Ataxia-telangectasia (A-T) is a rare autosomal recessive disorder which results in progressive cerebellar ataxia, oculocutaneous telangectasias, immune deficiencies, radiation sensitivity, premature aging and increased cancer risk (mostly lymphomas) (Shiloh, 2003; Lavin and Shiloh, 1997). Typically, cells from these patients lack any detectable ATM protein. This results in abnormal telomere morphology, and abnormal responses to IR which exhibits itself through increased cell death, cell cycle defects and increased chromosomal breakage.

While *ATM* gene knock-outs are viable, null mutations in ATR are embryonic lethal and ATR negative cell lines could not be established. However, the protein has been studied in a conditional knockout allele or a dominant-negative kinase dead mutant. Seckel syndrome is characterized by mental retardation, microcephaly, dwarfism and intrataurine growth retardation (O'Driscoll *et al*, 2003). This condition shows shared phenotypic features with NBS (discussed next). This is the result of a founder mutation that affects splicing of the ATR gene transcript resulting in residual but markedly reduced levels of ATR protein.

The gene encoding *NBS1* is mutated is NBS. These patients show clinical phenotypes such as mental retardation, microcephaly, immunodeficiency and cancer predispositions (Varon *et al*, 1998; Tauchi *et al*, 2002). Furthermore, NBS cells are characterized by chromosomal instability, hypersensitivity to DSB inducing agents and radio-resistant DNA synthesis (RDS). Mutation in another component of the MRN complex, Mre11, causes the A-T like disorder (A-TLD) which is characterized by the later onset of a disease with similar phenotype to A-T (Stewart *et al*, 1999).

1.8 Inhibitors of the PIKK family

The steroid wortmannin, isolated from *Penicillium wortmanni*, specifically inhibits PI3K and its family members including ATM, ATR, hSMG-1/ATX and DNA-PK (Walker *et al*, 2000; Block *et al*, 2004). This specificity is due to the unique geometry of PI3K/PIKK active site. Wortmannin is an ATP non-competitive inhibitor, which can irreversibly bind to the ATP-binding site of these kinases. The concentration of wortmannin needed for inhibiting 50% of the kinase activity (IC_{50}) has been determined for DNA-PK, ATM and ATR. The IC_{50} for DNA-PK has been reported as 16 nM by Sarkaria *et al*, while Izzard *et al* report 120 nM. The values for ATM and ATR were determined to be 150 nM and 1.8 μM, respectively (Sarkaria *et al*, 1998), while hSMG-1/ATX is inhibited by 50% at 80 nM (Abraham, 2004). This provides a potential method for distinguishing between ATM and ATR mediated signaling in cell extracts.

Caffeine, an inhibitor of both ATM and ATR, completely inhibits p53 serine 15 phosphorylation in A549 lung cancer cells at a concentration of 3mM (Sarkaria *et al*, 1999). The IC_{50}s for ATM and ATR were determined to be 0.2 mM and 1.1 mM, respectively (Sarkaria *et al*, 1999). However, the reported caffeine concentration necessary for inhibition of DNA-PK varies. It has been reported by one group as IC_{50}= 10 mM (Sarkaria *et al*, 2001) while another reports IC_{50}= 0.2-.0.6 mM (Block *et al*, 2004). Therefore, caffeine can be used to inhibit PIKKs but cannot be used to distinguish ATM, ATR and DNA-PKcs.

1.9 Substrates of ATM and ATR

The signaling pathways triggered by ATM and ATR in response to DNA damage have been described. This section will focus on the description of some of the characterized ATM and ATR substrates examined in this study.

1.9.1 Overview of p53 structure and function

The p53 protein is involved in several molecular signal transduction pathways. Under normal physiological conditions, the p53 protein is present at a low concentration, with a very short half-life (approximately 20 minutes). Although it has a NLS (nuclear localization sequence) (Shaulsky *et al*, 1990), its preferred location appears to be cytoplasmic due to a NES (nuclear export signal), which directs it to the cytoplasm (Freedman *et al*, 1998). The binding of p53 to its negative regulator MDM2 also participates in its cytoplasmic localization since MDM2 also has a NES sequence. The activation of p53 induces its dissociation from MDM2 and its tetramerization, thereby hiding the NES. The protein therefore stays localized in the nucleus and activates transcription of target genes. This relocalization of p53 towards the nucleus and its subsequent effect on cell cycle regulation are made possible only after activation of the protein by post-translational modifications.

The p53 protein consists of six functional domains (Figure 1.15). Several phosphorylation sites as well as at least three acetylation sites have been identified. The majority of these phosphorylation sites are found in the first 40 a.a.s of the protein sequence, which corresponds to the MDM2 binding region (Prives, 1998). In its inactive state, the p53 protein is phosphorylated on ser376 and ser378. The inhibitor MDM2 binds to the N-terminal end, directing it to the cytoplasm for ubiquitin-mediated proteolysis. This negative regulatory loop serves to control the concentration of active p53 by targeting it for

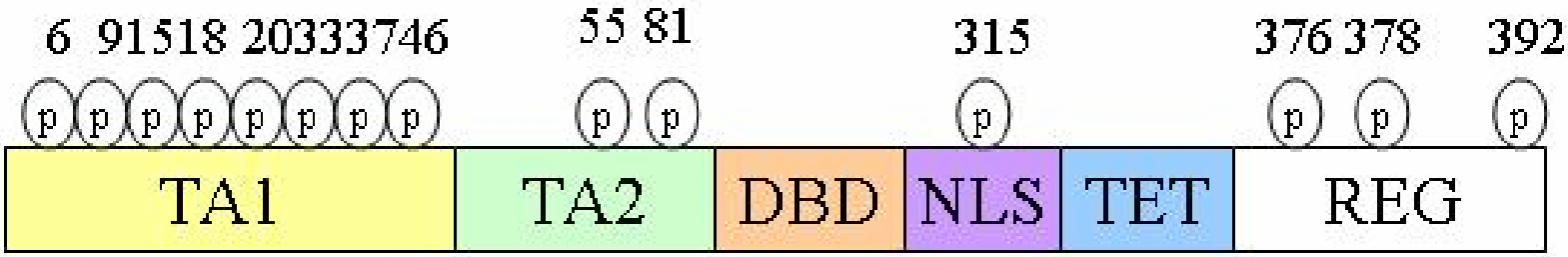

Figure 1.15: Structural organisation of the p53 tumour suppressor. The p53 tumour suppressor is divided into 6 domains. 1. Transactivation domain 1 (TA1), 2. Transactivation domain 2 (TA2), 3. DNA binding domain (DBD), 4. Nuclear localisation signal containing domain (NLS), 5. The tetramerisation domain (TET), and 6. The regulatory domain (REG). (Adapted from Anderson and Appella, 2001).

degradation. The first step in the stabilization and subsequent activation of the transcriptional activities of p53, involves a series of serine/threonine phosphorylation events in its N-terminal end *i.e*. transactivation domain. Seven serines, 6, 9, 15, 20, 33, 37, 46 and two threonines, 18 and 81 are known to be phosphorylated in response IR or UV induced DNA damage. Stress-activated phosphorylation of p53 at numerous site in the N-terminal region, near the MDM2 binding site, has led to the hypothesis that this may prevent the interaction of MDM2 thus stabilizing p53 (Shieh *et al*, 1997). The details surrounding the phosphorylation of individual sites are far from being known. However, recent studies have concentrated on trying to decipher the basis for the phosphorylation of individual sites, as well as multisite phosphorylation in the N-terminal region.

Mutational studies have been used to try and shed some light on the purpose of phosphorylation at individual sites in the N-terminus of p53. Serine to alanine mutations of several sites have been made. The serine 15 to alanine mutation resulted in decreased ability to activate transcription and increased apoptosis (Shieh *et al*, 1997; Unger *et al*, 1999a), while the serine 20 mutation to alanine interfered with stabilisation in response to DNA damage (Chehab *et al*, 1999; Unger *at al*, 1999b). In conjunction with structural data, these results indicate an indirect role for the phosphorylation of serine 15 and 20 in complex formation with MDM2. Changing serine 6, serine 9, serine 15 or threonine 18 to alanine showed a decrease in acetylation of lysine 382, which is involved in transcriptional activation (acetylation is described later) (Saito *et al*, 2002).

Although post-translation modifications of p53 occur at most sites in response to genotoxic stress, clear differences at individual sites have been observed in response to different damaging agents. For example, increased phosphorylation of serine 15 was observed in response to IR, UV, cisplatin, camptothecin, arsenite, genistein, deferoxamine

mesylate, but not actinomycin D (reviewed in Appella and Anderson, 2001). The delay in response has also been shown to be specific for the type of DNA damage or genotoxic stress. IR increases phosphorylation at serine 6, 9 and 15 as soon as 30 minutes while the UV damage response is significantly slower (Higashimoto *et al*, 2000). The effect of damage induced by chemotherapeutic agents on phosphorylation of p53, remains largely unknown.

1.9.2 Overview of H2AX structure and function

Histone proteins form a central protein core around which DNA is wrapped. This DNA- histone structure is termed the nucleosome. The nucleosome core is formed by an octomer of protein molecules consisting of two copies of each histone 2A, 2B, 3 and 4 (H2A, H2B, H3 and H4) (Luger *at al*, 1997). Each of the histones contains a core/globular domain required for both, histone-histone and DNA-histone contacts. Furthermore, histones also contain amino-terminal and carboxy-terminal tails which undergo extensive post-translational modifications. Although the histone core proteins are highly conserved, there exist several histone variants with distinctive a.a. sequences. Studies indicate that these variants have functions other than the encasing of DNA into nucleosomes. For example, the H2A variant H2AX was identified as a member of the DNA damage signaling pathway and is important in maintenance of genome stability.

The H2AX isoform constitute a major portion of the H2A species. Depending on the cell line examined, it can represent up to 25% of the H2A pool (Rogakou *et al*, 1998). H2AX is characterized by a short, distinct carboxy-terminal tail (Redon *et al*, 2002). This tail region contains a phosphorylation site, serine 139, which is rapidly phosphorylated in response to DNA damage (Rogakou *et al*, 1998). The same study also showed that a very

large region of DNA (approximately 2 Mbp) was phosphorylated on H2AX in response to a single DSB. These findings have lead researchers to accept the phosphorylation on H2AX as a "gold standard" for the formation of IRIF (previously discussed). Furthermore, the phosphorylation of H2AX has been shown to result from DSBs of diverse sources including "accidental" and programmed DSBs (Redon *et al*, 2002). Replication fork collisions (Furuta *et al*, 2003), abnormal telomeres (d'Adda di Fagagna *et al*, 2003), several exogenous sources of DNA DSBs and apoptosis (Rogakou *et al*, 2000) have all been shown to result in H2AX phosphorylation. This phosphorylation has been shown to be dependent on ATR in response to replication stress (Ward and Chen, 2001) while ATM was responsible in reponse to ionizing radiation (Burma *et al*, 2001). However, there appears to be some redundancy in the phosphorylation of H2AX on serine 139 since both ATM and ATR kinase dead expressing cell lines still show detectable H2AX phosphorylation. It has recently been shown that DNA-PKcs is also involved in phosphorylation at this site (Stiff *et al*, 2004).

The H2AX deficiency mouse model shows a phenotype characteristic of other genome instability disorders (Celeste *et al*, 2002). The use of this model and H2AX negative cell lines has shown that although H2AX is essential for the recruitment of several factors to IRIFs, it is not essential for the repair of DSBs. However, it has been suggested that the phosphorylation of H2AX serves to concentrate DSB signal and repair factors in close vicinity to the break (Celeste *et al*, 2003). Furthermore, it has also been suggested that this phosphorylation event serves to change chromatin structure to provide a means of recognition for other signaling and repair factors (Fernandez-Capetillo *et al*, 2004).

1.9.3 Overview of CHK2 structure and function

The Chk2 kinase is a highly conserved kinase involved in the signal transduction of DSBs to delay cell cycle progression. Its kinase activity is well established to increase in response to DNA damage induced by IR and chemotherapeutic drugs. It has recently been shown that senescence-triggered telomere erosion also activates Chk2 (d'Adda di Fagagna *et al*, 2003). ATM activates Chk2 in response to IR, while ATR activates it in response to ultraviolet radiation (UV) or hydroxyurea (HU) (Brown *et al*, 1999; Matsuoka *et al,* 2000). Furthermore, Chk2 is not activated in cells derived from A-T patient (Chaturvedi *et al*, 1999). ATM was shown to phosphorylate Chk2 directly on threonine 68 (Ahn *et al*, 2000). This site was further identified as being essential for Chk2 activation (Melchionna *et al*, 2000). Chk2 has been shown to localize to IRIF, but unlike several other factors, Chk2 does not remain at the DSB site after being activated. On the contrary, Chk2 spreads away from the damage site to find and phosphorylate its downstream effectors responsible for the initiation of cell cycle arrest or apoptosis (Lukas *et al*, 2003)

The Chk2 protein is divided into three functional domains: (1) an SQ/TQ cluster domain (SCD), (2) a forkhead associated domain (FHA) and, (3) serine/threonine kinase domain. Chk2 is found as an inactive monomer in the cell. A model for Chk2 activation has been proposed (Ahn *et al*, 2004). Phosphorylation of threonine 68 by ATM or ATR is likely the initiating event which results in Chk2 dimerization by binding of both molecules at a region spanning this phosphorylation site. Full activation is then achieved by a series of autophosphorylation and transphosphorylation events. These phosphorylation events are likely to be mediated by different stresses according to the extent of activation required.

1.9.4 Overview of CHK1 structure and function

The Chk1 and Chk2 serine/threonine kinases have overlapping functions in response to DNA damage, while being structurally unrelated. The Chk1 kinase has two identified domains: (1) a serine/threonine kinase domain and, (2) an SQ/TQ cluster domain (SCD) in the C-terminus. Several studies have demonstrated that Chk1 is phosphorylated and activated in response to both DNA damage and replication stress (Sanchez *et al*, 1999; Liu *at al*, 2000; Gatei *et al*, 2003). As previously mentioned, the original concept suggested that Chk1 was phosphorylated by activated ATR while Chk2 required ATM activation. However, ATM has been shown to be required for the phosphorylation of serines 317 and 345 in response to IR (Gatei *et al*, 2003; Sapkota *et al*, 2002). These two sites have been identified as being particularly important for the DNA damage response, they are also phosphorylated in response to HU and UV (Liu *et al*, 2000). Cells expressing Chk1 with an alanine substitution at serine 345 show defects in cell cycle checkpoints and hypersensitivity to IR, UV and other DNA damaging agents (Lopez-Girona *et al*, 2001). These phosphorylation events have been suggested to help mediate the checkpoint response by increasing the ability of Chk1 to bind other proteins (Chen and Sanchez, 2004). Based on experiments performed in yeast, Chk1 is suggested to function in the G_2 checkpoint. Disruption of the Chk1 gene causes cells to bypass this checkpoint and enter mitosis event in the presence of DNA damage (Walworth *et al*, 1993).

1.9.5 Overview of NBS1 structure and function

NBS1 has previously been described as a member of the HRR MRN complex, and identified as a good candidate for the primary sensor of DNA DSBs. However, it has also been identified as an ATM substrate in response to IR-induced DNA damage (Gatei *et al*,

2000). ATM is responsible for phosphorylation of NBS1 on serine 278 and 343 in response to IR both *in vitro* and *in vivo* (Gatei *et al*, 2000). These phosphorylation events are associated with the role of NBS1 in the intra-S-phase cell cycle function. As previously mentioned, these specific phosphorylation events likely result in a change in function for this protein. The function of the NBS1 protein in the MRN complex as a DNA damage sensor has previously been discussed; therefore, this section will focus mostly on its function in the intra-S-phase checkpoint.

The NBS1 protein is composed of three functional domains: (1) the N-terminal domain, (2) a central region and, (3) the C-terminal domain. The N-terminal region contains a forkhead-associated (FHA) domain and a BRCA1 C-terminal (BRCT) domain. Both of these protein domains are typically associated with nuclear eukaryotic proteins related to DNA repair or cell cycle arrest. It has been demonstrated that the FHA and BRCT domains of NBS1 directly bind γ-H2AX to recruit the MRN complex to DSB sites (Kobayashi *et al*, 2002). The central region includes several SQ motifs containing the PIKK consensus sequence, including the highly conserved serines 278 and 343 which are phosphorylated by ATM in response IR. It is suggested that this region is associated with the role that NBS1 plays in the intra-S checkpoint (Kobayashi *et al*, 2004). The C-terminal region is associated with the formation of the MRN complex. This region of NBS1 is known to bind MRE11 and is essential for the nuclear transport of the MRN complex (Desai-Mehta *et al*, 2001).

When NBS1 cells were characterized, it was determined that they underwent RDS. Continued DNA synthesis in response to IR-induced damage, is a phenotype representative of cells which have an abrogated intra-S-phase checkpoint. This hypothesis is supported by the fact that the yeast Xrs2/Rad32/Rad50 complex (homolog of the human

Nbs1/Mre11/Rad50 complex) acts specifically in the intra-S-checkpoint (Chahwan *et al*, 2002). Three parallel ATM-dependent pathways have been described as participants in the intra-S-phase checkpoint, two of which are NBS1 dependent. The first requires ATM, NBS1 and SMC1. Phosphorylation of NBS1 on serines 276 and 343 are required for the ATM-dependent phosphorylation of SMC1 (Kim *et al,* 2002; Yazdi *et al*, 2002). The second pathway requires the phosphorylation of NBS1 on serine 343 for ATM-dependent phosphorylation of the mutated in chromosomal instability syndrome Fanconi's anemia (FANCD2) protein on serine 222 (Nakanishi *et al*, 2002). However, the third pathway, the ATM/CHK2/CDC25A/CDK2 pathway does not require the NBS1 protein.

1.9.6 Overview of SMC1 structure and function

SMC proteins carry out several biological functions. They are established to be involved in chromosome condensation, sister chromatid cohesion, DNA recombination, DNA repair and more recently DNA damage signaling (Strunnikov and Jessberger, 1999; Yazdi *et al,* 2002). More specifically, SMC1 and SMC3 are believed to form a heterodimer to form the cohesin complex, required for sister chromatid cohesion. Furthermore, this complex has also been shown to be involved in postreplicative DSB repair (Sjogren and Nasmyth, 2001). All SMC proteins possess two coiled-coil domains of 300 to 400 a.a. These domains flank a moderately conserved flexible hinge region in the protein. The N-terminal and C-terminal both consist of globular nucleotide-binding motifs, a Walker A (Walker A box) and Walker B (DA box) motif, respectively. The SMC1-SMC3 heterodimer forms in an anti-parallel fashion with the N-terminal coiled-coil domain of SMC1 interacting with the C- terminal coiled-coil domain of SMC3 and *vice versa*.

More recently, SMC1 was identified as a component of DNA damage signaling pathways. It was established that ATM is required for the phosphorylation of two sites on SMC1 in response to IR induced DNA damage, serine 957 and serine 966 (Yazdi *et al,* 2002). Furthermore, this response was shown to require functional NBS1, identifying SMC1 as a downstream effector of both ATM and NSB1. These studies identified SMC1 as a component of one of the pathways responsible for intra-S-phase arrest, the ATM-NBS1-SMC1 pathway.

2.0 Thesis Goals

Hypothesis: The hypothesis to be tested is whether DSB induced by the epipophyllotoxin chemotherapeutic agent etoposide are detected through the ATM signal transduction pathway.

Statement of aims : To investigate and characterize the molecular response to the DNA damaging effects of the antineoplastic drug etoposide. The goal is to identify the pathways, which detect and respond to this type of damage, in order to compare with other classes of drugs.

Specific objectives : We propose to investigate the DNA damage response induced by etoposide by:

(1) determining whether ATM undergoes autophosphorylation at serine 1981 and has increase protein kinase activity in response to etoposide,

(2) examining the role of ATM in the phosphorylation of NBS1, SMC1, Chk1, Chk2, and H2AX in response to etoposide,

(3) characterization of the p53 phosphorylation status in response to this drug,

(4) determining the effect of the damage on the ability of p53 to bind to its specific DNA binding sequence,

(5) determine the involvement of other PIKK family members in the phosphorylation of p53 on serine 15 in response to etoposide.

SECTION II : MATERIAL AND METHODS

2.1 Cells and cell culture

Experiments were performed using Epstein Barr transformed human lymphoblastoid cell lines, which have previously been characterised as to their ATM status (Kozlov *et al*, 2003). Cell lines were maintained as suspension cultures in RPMI 1640 (GibcoBRL, Gaithersburg, MD) (BT and L3) or DMEM/F12 (C3ABR and AT1ABR) media containing 10% (v/v) fetal calf serum (Hyclone, Logan, UT), 50 U/ml penicillin (GibcoBRL) and 50 µg/ml streptomycin sulphate (GibcoBRL). The glioma cell lines M059K, M059J were maintained in DMEM/F12 media containing 10% fetal calf serum (Hyclone), 50 U/ml penicillin and 50 µg/ml streptomycin sulphate. Attached cells lines were subcultured by treating cells with pre-warmed (at 37^{o}C) trypsin/EDTA (TE; 0.05% (w/v) trypsin, 0.53 mM EDTA, GibcoBRL) to allow them to detach from culture dishes. Cells were maintained at 37^{o}C in a humidified atmosphere containing 5% CO_2. The suspension cell concentrations were maintained at less than $1x10^6$ cells/ml while adherent cells were used at 70% confluence, to ensure that the cells were used in logarithmic growth phase.

2.2 Cell treatments

Cells were pretreated with wortmannin (Sigma, Oakville, ON), or caffeine (Sigma), for 30 minutes before treatment with a DNA damaging agent. Stock solutions of etoposide (VP-16) (Sigma) were prepared in dimethyl sulfoxide (DMSO). Etoposide was applied to cells at indicated concentrations for the duration of the experiment and washed off during harvesting. In other experiments, radiation from a ^{137}Cs source (Gammacell 1000, MDS Nordion, Ottawa, CA) was delivered at 3.7 Gy per minute for a total of 10 Gy.

2.3 Cell extract preparations

After treatment, each 10 cm^2 plate of cells was collected by centrifugation at 2,000 rpm (700 x g) at 4^oC in the JS5.2 rotor of a Beckman J-6B centrifuge. Media was removed and cell pellets were washed twice in 15-20 ml of ice cold phosphate buffered saline (1x PBS, 136.8 mM NaCl, 2.6 mM KCl, 10.2 mM Na_2HPO_4, 1.8 mM KH_2PO_4, pH 7.4). Adherent cells were treated with Trypsin/EDTA before havesting by centrifugation. In this case, 0.2 mM of phenylmethylsulfonyl fluoride (PMSF) (Sigma) was added to the PBS washes to inhibit any residual trypsin activity. Cell pellets were resuspended in lysis buffer as per the individual methods described below.

2.3.1 Cytoplasmic and nuclear extraction

After the cells were washed twice in 1x PBS, cell pellets were resuspended in 10-15 ml of ice cold low salt buffer (1x LSB: 10 mM HEPES, 25 mM KCl, 10 mM NaCl, 1 mM $MgCl_2$, 0.1 mM EDTA, pH 7.2) containing 0.1 mM dithiothreitol (DTT) and 0.2 mM PMSF. The cells were immediately pelleted at 700 x g. The cell pellet was resuspended in 1.5-2.5 times the packed cell volume (PCV) (usually 150-350 µl) of 1x LSB containing 0.1 mM DTT. The cells were left to swell on ice for 5-10 minutes, then snap frozen by immersing them in liquid nitrogen. The samples were quick thawed at 37^oC until they just began to melt. Protease inhibitors (2 mM PMSF, 2 µg/ml aprotinin (Sigma), 2 µg/ml leupeptin (Roche Diagnostics, Laval, Qc), 1 µg/ml pepstatin A (Roche Diagnostics), in methanol), and phosphatase inhibitors (20 mM β-glycerophosphate, 1 mM Na_3VO_4, 25 mM NaF) plus 1µM microcystin-LR, were added and the samples were placed on ice and allowed to thaw completely. The samples were then centrifuged at 10,000 x g for 10 minutes at 4^oC in a desktop Eppendorf centrifuge. The supernatant was removed,

transferred to a new microfuge tube, snap frozen and stored at -80^{o}C. This fraction represents a crude cytoplasmic fraction (S10) containing some nuclear proteins and soluble cytoplasmic proteins. The remaining pellet was resuspended in one PCV (approximately 100 µl) of high salt buffer (1x HSB: 10 mM HEPES, 25 mM KCl, 500 mM NaCl, 10 mM $MgCl_2$, 0.1 mM EDTA, pH 7.4) containing protease inhibitors, and phosphatase inhibitors including microcystin-LR as described above. The cells were left on ice for 5-10 minutes. The samples were then centrifuged at 10,000 x g for 10 minutes at 4^{o}C. The supernatant was removed and snap frozen in liquid nitrogen. This represents the nuclear fraction (P10) which contains the nuclear/chromatin associated fraction. Protein concentrations of the S10 and P10 fraction were determined using a protein concentration assay (Biorad, Hercules, CA) using Bovine Serum Albumin (BSA) (Sigma) as standard. The P10 fraction was then used in the electromobility shift assay (EMSA) for p53 (see section 2.7).

2.3.2 NP-40 or Triton X-100 whole cell extraction

After cells were washed twice in 1x PBS, cell pellets were resuspended in 4-5 PCV (400-500 µl) of a Nonidet P-40 (NP-40) or Triton X-100 containing lysis buffer (NET-N/T, 150 mM NaCl, 1 mM EDTA, 20 mM TRIS-HCl pH 8.0, 1% (v/v) NP-40 or 1% (v/v) Triton X-100, 2 mM PMSF, 2 µg/ml aprotinin, 2 µg/ml leupeptin, 1 µg/ml pepstatin A, 20 mM β-glycerophosphate, 1 mM Na_3VO_4, 25mM NaF, 1µM microcystin-LR). Cells were left on ice for 5-10 minutes then sonicated on ice for 2 X 5 seconds. Samples were centrifuged in a microcentrifuge at 10,000 g for 20 minutes at 4^{o}C. The supernatant was collected and snap frozen in liquid nitrogen. Whole cell extracts were stored at -80^{o}C. Protein concentrations of NP-40 or Triton X-100 whole cell extracts were determined using the Detergent Compatible (DC) protein concentration assay (Biorad, Gaithersburg MD)

using BSA as a standard. These extracts were subsequently used in immunoblots (see sections 2.5.1 and 2.5.2).

2.3.3 Histone preparations

After the cells were washed twice in 1x PBS, cell pellets were resuspended in 10-15 ml of ice cold LSB containing 0.1 mM DTT and 0.2 mM PMSF. The cells were immediately pelleted at 700 x g (as above). The cell pellet was resuspended in 100-150 µl of 1 X LSB containing 0.1 mM DTT. The cells were snap frozen by immersing in liquid nitrogen. The samples were quick thawed at 37^{o}C until they just began to melt. Protease inhibitors and phosphatase inhibitors including microcystein-LR, were added as described in section 2.3.1, and samples were placed on ice and allowed to thaw completely. The samples were then centrifuged at 10,000 x g for 5 minutes at 4^{o}C in a desktop centrifuge. The supernatant was removed and discarded. The pellet was resuspended in 6-8 PCV of 1 x LSB containing 0.1 mM DTT, protease inhibitors and phosphatase inhibitors. Sulphuric acid was added to each sample to a final concentration of 0.2 M sulfuric acid. Tubes were kept on ice for 30 min, then samples were spun at 11,000 x g for 10 min at 4^{o}C. The supernatants were dialysed using Spectropore® (MWCO 6-8000 cut off) dialysis tubing against 1 litre of 0.1M glacial acetic. The dialysis buffer was changed twice after 1 hour and 3 hours respectively. The samples were then dialysed against three 2L changes of cold dd$H_2$0 at 1 hour, 3 hours and overnight. After dialysis, protein concentrations were determined using the standard protein concentration assay as described above. The total volume of the samples was measured. Known aliquots of samples were lyophilized to dryness in a speed-vac concentrator. Dried samples were resuspended in 2x SDS sample

buffer (125 mM Trsi-HCl at pH6.8, 20% (v.v) glycerol, 5.3% (w/v) SDS, 0.05% (w/v) bromophenol blue, β-mercaptoethanol) to a final concentration of 4 μg/ml.

2.4 Immunoprecipitations

Cell extracts prepared for immunoprecipitations were centrifuged and washed in 1x PBS as per section 2.3 (Cell extract preparations). Different methods were used for immunoprecipitation of ATM and p53. These methods are described below.

2.4.1 p53 multisite phosphorylation

Each 10 cm^2 plate of cells was washed twice in 1x PBS, and cell pellets were resuspended in 4-5 PCV (400-500 μl) of a Triton X-100 containing lysis buffer (NET-T, 150mM NaCl, 5 mM EDTA, 50 mM TRIS-HCl pH 7.5, 1% (v/v) Triton X-100, 2 mM PMSF, 2 μg/ml aprotinin, 2 μg/ml leupeptin, 1 μg/ml pepstatin A, 20 mM β-glycerophosphate, 1 mM Na_3VO_4, 25mM NaF). Cells were left on ice for 5-10 minutes then sonicated on ice for 2x 5 seconds (as above). Samples were centrifuged at 14,000 rpm for 20 minutes at 4^oC. Protein concentrations of the supernatants were measured using the Detergent Compatible (DC) protein concentration assay using BSA as a standard. For each individual phosphorylation site analysed, 5 μg of agarose conjugated DO-1 (Santa Cruz, cat. # SC-126AC) and 5 μg of agarose conjugated Pab1801 (Santa Cruz Biotechnologies, Santa Cruz, CA, cat. # SC-98AC) was added to lysate containing 1 mg total protein. Samples were incubated overnight at 4^oC on an end-over-end rotator. Immune-complex were collected by centrifugation and washed five times with NET-T lysis buffer (1ml per wash). The beads were resuspended in 50 μl of 2x SDS sample buffer and boiled for 5 minutes. The samples were spun at 14,000 rpm for 5 minutes and the supernatant was

transferred to a new microfuge tube. Analysis of the proteins was by SDS-PAGE as described in section 2.5 (immunoblotting).

2.4.2 Immunoprecipitated ATM kinase assay

After the cells were washed twice in 1x PBS, cell pellets were resuspended in 4-5 PCV (400-500 µl) of a Tween-20 containing lysis buffer (TGN: 50 mM TRIS-HCl pH 7.5, 150 mM NaCl, 10% (v/v) glycerol, 1% (v/v) Tween-20, 2 mM PMSF, 2 µg/ml aprotinin, 2 µg/ml leupeptin, 1 µg/ml pepstatin A, 20 mM β-glycerophosphate, 1 mM Na_3VO_4, 25 mM NaF, 1 µM microcystin-LR, and 1 mM DTT). Samples were centrifuged at 14,000 rpm for 20 minutes at 4^oC in a refrigerated desktop micro centrifuge. Supernatant protein concentrations were measured using the Detergent Compatible (DC) protein concentration assay. Each immunoprecipitation reaction was prepared with 500 µg of total protein. Extracts were precleared with with 25µl of 1:1 protein A sepharose (Pharmacia) equilibrated in TGN buffer for 20 minutes at 4^oC on an end over end shaker. Samples were centrifuged for 5 minutes at 5,000 rpm at 4^oC in a desktop microcentrifuge. Five µl of ATM Ab-3 antibody (Oncogene research products, LaJolla, CA, cat # PC116) was added to each reaction. Samples were incubated overnight at 4^oC with end over end shaking. The following day, 25 µl of the protein A sepharose slurry was added to each reaction for 1 hour. The immune-complex was washed twice with TGN lysis buffer, once with 0.6M NaCl/100 mM Tris-HCl pH 7.5 and twice in pre-kinase buffer (10 mM HEPES pH 7.4, 50 mM β-glycerophosphate, 50 mM NaCl, 1 mM DTT). The reactions were incubated in kinase buffer (10 mM HEPES pH 7.4, 50 mM β-glycerophosphate, 50 mM NaCl, 10mM $MgCl_2$, and 1µM microcystein-LR) with 0.25µg of PHAS-I in the presence of 50 µM unlabelled ATP and 5 µCi of γ-^{32}P-ATP for 30 minutes at 30^oC. The kinase reaction was

stopped by addition of 15 µl of 2x SDS sample suffer. Samples were boiled for 5 minutes and centrifuged at 10 000 x g for 5 minutes in a desktop microcentrifuge. The supernatant was removed and resolved on a 15% SDS-PAGE. The PAGE gels were dried and exposed to X-ray film (Fuji SuperRX) overnight.

2.5 Immunoblotting

All SDS-Polyacrylamide gels were prepared according to lab protocols. Table 2.1 describes the composition of gels used. These are standard protocol for all SDS-PAGE unless otherwise indicated in the text.

Individual transfer conditions are indicated in the following sections. However, in all cases, the membranes were blocked in 25% skim milk powder in Tween-Tris Buffered Saline (TTBS: 20 mM Tris HCl pH 7.5, 0.5 M NaCl, 0.1% (v/v) Tween-20). After incubation in the primary antibody, the immunoblots were washed 1x for 15 minutes in TTBS followed by the incubation in the secondary antibody. The membranes were washed 4X in TTBS for 15 minutes, incubated with ECL reagent (Amersham Biosciences, Baie d'Urfé, Qc) for 1 minute and exposed to X-ray film.

After developing with ECL, the immunoblots were stripped with one of two methods. In the first method, the membrane was placed in 20 ml of ddH_2O (10 minutes), then 20 ml of 0.2N NaOH (10 minutes), 20 ml of ddH_2O (10 minutes), 20ml of TTBS (10 minutes), and was blocked as usual with 25% skim milk powder in TTBS. In the second method the membrane was placed in 50 ml of stripping solution (60 mM Tris HCl pH 6.8, 2% (w/v) SDS, 0.7% (v/v) β-mercaptoethanol) at 65^{o}C for 30 minutes with occasional shaking. The membrane was then washed 3x quickly with TTBS and washed one more

Solution (ml)	8% (low bis)	10%	16%	EMSA
30% acrylamide	3.0	5.0	8.0	4.0
2% bisacrylamide	0.4	1.0	0.625	1.3
1M Tris-HCl pH 8.8	4.2	5.6	5.6	--
5x Tris-Glycine*	--	--	--	5.0
ddH_2O	3.0	3.3	0.60	14.7
20% SDS	0.056	0.075	0.075	--
TEMED	0.004	0.015	0.015	0.030
10% APS	0.040	0.050	0.050	0.300

* 5x Tris-Glycine: 250 mM Tris, 1.9M Glycine, 10.5 mM EDTA

Table 2.1: Solutions used for gel electrophoresis

Name	Sequence
p53U	5’AGCTTAGACATGCCTAGACATGCCAAGCT-3’
p53L	5’AGCTTGGCATGTCTAGGCATGTCTAAGCT-3’

Table 2.2: Oligonucleotides used for p53 electomobility shift assay

time with TTBS for 15 minutes. The membrane was then blocked as usual with 25% skim milk powder in TTBS.

2.5.1 High molecular weight proteins: ATM, DNA-PK, SMC1

Samples were prepared as per section 2.3.2 (NP-40 or Triton X-100 whole cell extraction). For each sample, 60 µg of protein was loaded onto a 8% acrylamide SDS-PAGE. Pre-stained mid-range molecular weight markers (Biorad) were also loaded on the gel. Samples were run initially for 20 minutes at 80V followed by $1^1/_2$ hours at 150V. The proteins were transferred to nitrocellulose membrane for 1 hour at 100V in high molecular weight transfer buffer (48 mM Tris base, 39 mM glycine, 20% (v/v) methanol, 0.03% (w/v) SDS). Membranes were blocked in 25% (w/v) skim milk powder prepared in TTBS for a minimum of 1 hour, or up to overnight. Membranes were incubated overnight at room temperature with a phosphospecific antibody to serine 1981 of human ATM (Rockland Immunochemicals, Gilbertsville, PA) at a dilution of 1:500, a phosphospecific antibody to serine 957 of SMC1 (Novus Biologicals, Littleton, CO) at a dilution of 1:1000 or with the DPK1 antibody to DNA-PKcs (described in Lees-Miller *et al*, 1995) at a dilution of 1:3000. The following day, the membrane was incubated with the secondary goat anti rabbit antibody (Biorad) at a dilution of 1:2000 for 1 hour. After developing with ECL reagent, the blot was stripped using the β-mercaptoethanol method and probed overnight with a rabbit polyclonal antibody to ATM (4BA) (generously provided by Dr. Martin Lavin) at a dilution of 1:1000. The ATM-4BA antibody was raised in rabbits against a.a. 2323-2740 of full lenght ATM and has been previously characterised (Watters *et al*, 1997). Alternatively, after stripping, the blots were probed with SMC1 (Novus

Biologicals) at a dilution of 1:1500. The secondary HRP conjugated goat anti rabbit antibody (Biorad) antibody was incubated at a dilution of 1:2000 for 1 hour.

2.5.2 Low molecular weight proteins: p53, Chk2, Chk1, NBS1

Samples were prepared as per section 2.3.2 (NP-40 or Triton X-100 whole cell extraction). For each sample, 30 μg of protein was loaded onto a 10% acrylamide SDS-PAGE for p53 immunoblots or 60 μg for all other immunoblts. Pre-stained mid-range molecular weight markers (Biorad) were also loaded on the gel. Samples were run initially for 20 minutes at 80V followed by $1^1/_2$ hours at 150V. The proteins were transferred to nitrocellulose membrane for 1 hour at 100V in low molecular weight transfer buffer (48 mM Tris base, 39 mM glycine, 20% (v/v) methanol). Membranes were blocked in 25% (w/v) skim milk powder prepared in TTBS for a minimum of 1 hour, or up to overnight. Membranes were incubated overnight at room temperature with a phosphospecific antibody to serine 15 of p53 (Santa Cruz, Santa Cruz, CA) at a dilution of 1:3000, a phosphospecific antibody to serine 345 of Chk1 (Cell Signaling Technology, New England Biolabs, Beverly, MA) at a dilution of 1:500, a phosphospecific antibody to threonine 68 of Chk2 (Cell Signaling Technology) at a dilution of 1:1000, or, with a phosphospecific antibody to serine 343 of NBS1 at a dilution of 1:500. The following day, the membrane was incubated with the secondary goat anti rabbit antibody (Biorad) at a dilution of 1:2000 for 1 hour. After developing with ECL reagent, the blot was stripped using the β-mercaptoethanol method and probed overnight with the mouse monoclonal to p53 at a dilution of 1:3000, Chk1 (Cell Signaling Technology) at a dilution of 1:750, Chk2 (Novus Biologicals) at a dilution of 1:1500 or, NBS1 at 1:6000. The secondary HRP conjugated

goat anti mouse/rabbit antibody (Biorad) antibody was incubated at a dilution of 1:2000 for 1 hour.

2.5.3 H2AX, H2A

Samples were prepared as per section 2.3.3 (Histone preparations). For each sample, 60 μg of protein was loaded onto a 16% acrylamide SDS-PAGE. Pre-stained low-range molecular weight markers (Biorad) were also loaded on the gel. Samples were run initially for 20 minutes at 80V followed by $1^1/_2$ hours at 150V. The proteins were transferred to nitrocellulose membrane for 1 hour at 100V in histone transfer buffer. Membranes were blocked in 25% (w/v) skim milk powder prepared in TTBS for a minimum of 1 hour, or up to overnight. Membranes were incubated at room temperature with a phosphospecific antibody to serine 139 of human histone -H2AX (Upstate, Lake Placid, NY, cat # 05-636) at a dilution of 1:500 overnight. The following day, the membrane was incubated with the secondary goat anti mouse antibody (Biorad) at a dilution of 1:2000 for 1 hour. After developing with ECL reagent, the blot was stripped using the β-mercaptoethanol method and probed with a rabbit/mouse polyclonal antibody to Histone 2A (Santa Cruz) at a dilution of 1:200 overnight. The secondary HRP conjugated goat anti rabbit antibody (Biorad) antibody was incubated at a dilution of 1:2000 for 1 hour.

2.6 Quantification of Western blots

Western blot films were scanned and quantitated using ImageQuant software (version 4.0) (Molecular Dynamics, Amersham Pharmacia Biotech). Phosphorylation levels were estimated based on the intensity of the signal measured from westernblots. In

each case, the level of phosphorylation was normalised to total protein levels by dividing measured phospo-signal by the total protein signal.

2.7 Electromobility shift assay

Table 2.2 describes the DNA oligonucleotides used for detection of p53 DNA binding. Equal molar ratios of the upper and lower strand oligonucleotide were used in an annealing reaction to generate a 5 pmole/µl solution of dsDNA binding duplex. The annealing reaction was performed by placing the upper and lower oligonucleotide in Tris-EDTA (TE: 10 mM Tris-HCl, pH 7.5, 1 mM EDTA, 50 mM NaCl) to a final concentration of 5 pmole/µl. The mixture was placed in boiling water and allowed to cool to room temperature without disturbing. Five pmoles of the dsDNA duplex was radioactively labelled using T4 polynucleotide kinase (PNK) (Calbiochem, LaJolla, CA) using 30 µCi of γ-^{32}P-ATP. The labelling reaction was performed at 37^{o}C for 30 minutes. The probe was isolated on a G50 spin column (Pharmacia) using the manufacturers specifications. To determine the amount of ^{32}P incorporated, the probe was counted in a Beckman LS6500 scintillation counter using the Cerenkov counting protocol. The probe was diluted to 10,000 cpm/µl for use. The probe was used with 5-10 fmoles of dsDNA labelled with 20,000 cpm of radioactive γ-^{32}P-ATP. The probe was stored at -20^{o}C and used before 5 days. Protein-DNA binding reactions were carried out with 12 µg of the nuclear (P10) fraction of cell extracts in binding buffer (25 mM HEPES pH 7.5, 1mM EDTA, 10% glycerol, and 1 mM DTT), in the presence of 1 µg of poly (dI-dC) (Roche Diagnostics) to prevent non-specific interactions, and 4µl of the p53 monoclonal antibody pAb421 (Tissue culture supernatant, University of Calgary, Hybridoma facility) The reactions were incubated at room temperature for 15 minutes before loading on a non-denaturing

Tris/Glycine PAGE. The composition of the non-denaturing Tris/Glycine PAGE is indicated in Table 2.1. The gel was run at 200V for 2hours. The gel dried down on Whatman chromatography paper for 1 hour and exposed to X-ray film overnight.

SECTION III : RESULTS

3.1 Cell line characterisation

In order to study the effect of etoposide on DNA damage signaling pathways, this study made use of three pairs of cell lines. All cell lines have been characterised previously as to their ATM and DNA-PK status. The BT and L3 lymphoblastoid cell line pair were previously described. The BT cell line was characterised as ATM positive and was age and gender match to the ATM negative L3 cell line (Ye *et al*, 2001; Beamish *et al*, 2002; Kozlov *et al*, 2003). The L3 cell line contains a homozygous mutation at codon 103 of *ATM* resulting in a premature termination of the ATM protein at a.a. 34 (Kozlov *et al*, 2003). Similarly, the C3ABR and AT1ABR cell lines were characterized and age and gender matched. These cells lines have been described in Beamish *et al*, 2002. The AT1ABR cell line contains a three a.a. deletion outside the kinase domain resulting in the destabilisation of the ATM protein (Beamish *et al*, 2002). The M059K and M059J cell lines were derived from a single malignant glioma tumour, however M059J were shown to lack DNA-PKcs and be radiosensitive, while M059K were not radiosensitive and had normal DNA-PKcs activity (Lees-Miller *at al*, 1995). The M059J cell line was later found to contain a mutation in the *ATM* gene which led to expression of low levels of ATM in this cell line (Chan *et al*, 1999; Tsuchida *et al*, 2002).

The first figure (Figure 3.1) demonstrates the levels of ATM and DNA-PKcs expression in each of the cell lines used in the subsequent experiments. Extracts from BT, L3, C3ABR, AT1ABR, M059K and M059J cells were prepared, as described in Section II: Material and Methods, and characterized for their ATM and DNA-PKcs status. In lanes 1, 3, 5, and 6, BT, C3ABR, M059K, M059J, respectively, were shown to express the ATM protein, while in lanes 2 and 4, L3 and AT1ABR, respectively, did not express the ATM protein. As seen by Tsuchida *et al* and Chan *et al*, ATM levels are reduced in M059J cells.

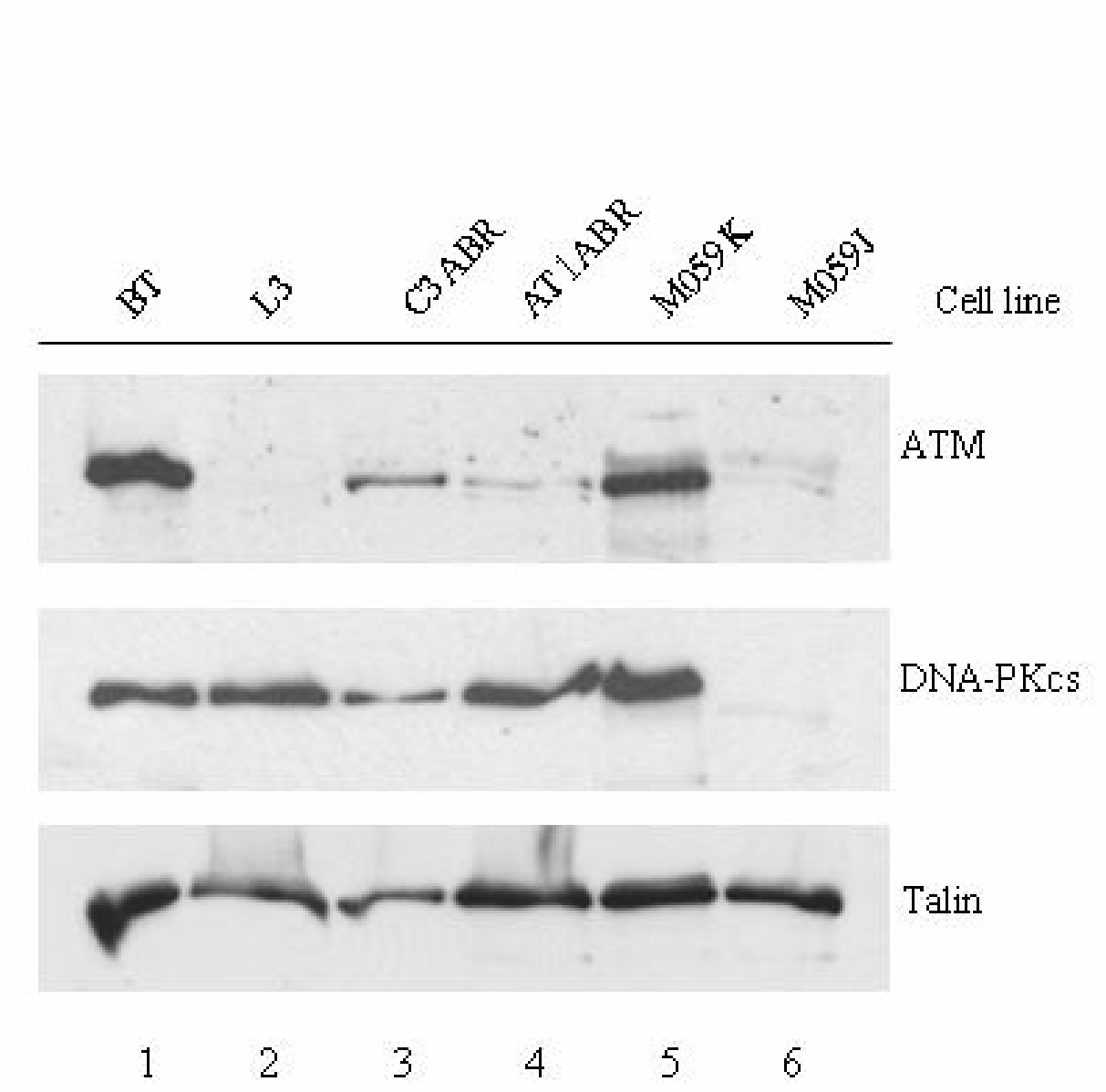

FIGURE 3.1: Characterization of ATM and DNA-PK status in cell lines. BT, L3, C3ABR, AT1ABR, M059K, and M059J cell extracts were prepared for characterization of ATM and DNA-PK status. Each lane represents 60 μg of a NET-N whole cell extracts. Lanes 1 through 6 represent respectively, BT, L3, C3ABR, AT1ABR, M059K, M059J cell lines. Immunoblots were probed with 4BA (ATM), DPK1 (DNA-PKcs) and Talin antibodies, as described in Section II: Material and Methods.

All cell lines, excluding the MO59J cell line, expressed the DNA-PKcs protein. Levels of Talin, a cytoskeletal protein, was used as a loading control in figure 3.1.

3.2 ATM activation in response to etoposide

As previously mentioned, *in vitro* the protein kinase activity of ATM is increased 2-3 fold in response to IR (Canman *et al*, 1998). Furthermore, the generation of an antibody that recognises the phosphorylated form of ATM (Bakkenist and Kastan, 2003), provides a powerful tool to measure ATM phosphorylation in cells exposed to DNA damaging agents. ATM is phosphorylated on serine 1981 within a very short delay after exposure to low doses of IR (Bakkenist and Kastan, 2003). In this study, we were interested in examining the effect of etoposide on the phosphorylation of ATM on serine 1981 as well as, its protein kinase activity in an immunoprecipitated kinase assay towards the PHAS-I substrate as per Canman *et al*, 1998.

In order to investigate the dose dependence of etoposide treatment on ATM phosphorylation at serine 1981, BT, L3, C3ABR and AT1ABR cells were exposed to 0, 1, 5, 10, 50 μM of etoposide for a 2 hour period. Figure 3.2 represents phosphorylation of ATM on serine 1981 in response to increasing doses of etoposide. In short, cells were treated with the previously mentioned doses of etoposide for 2 hours, and were harvested in NET-N extraction buffer as WCEs (described in Chapter II: Materials and Methods). Each lane represents 60 μg of protein as established by the Biorad© DC reagent for determining protein concentration. The Western blot was probed first with the ATM phospho-specific antibody, then stripped and reprobed for total ATM content (as described in Chapter II: Material and Methods). In Panel A, lane 1 shows that ATM was not phosphorylated at serine 1981 in untreated BT cells. Lanes 2 through 5 show ATM phosphorylation at this

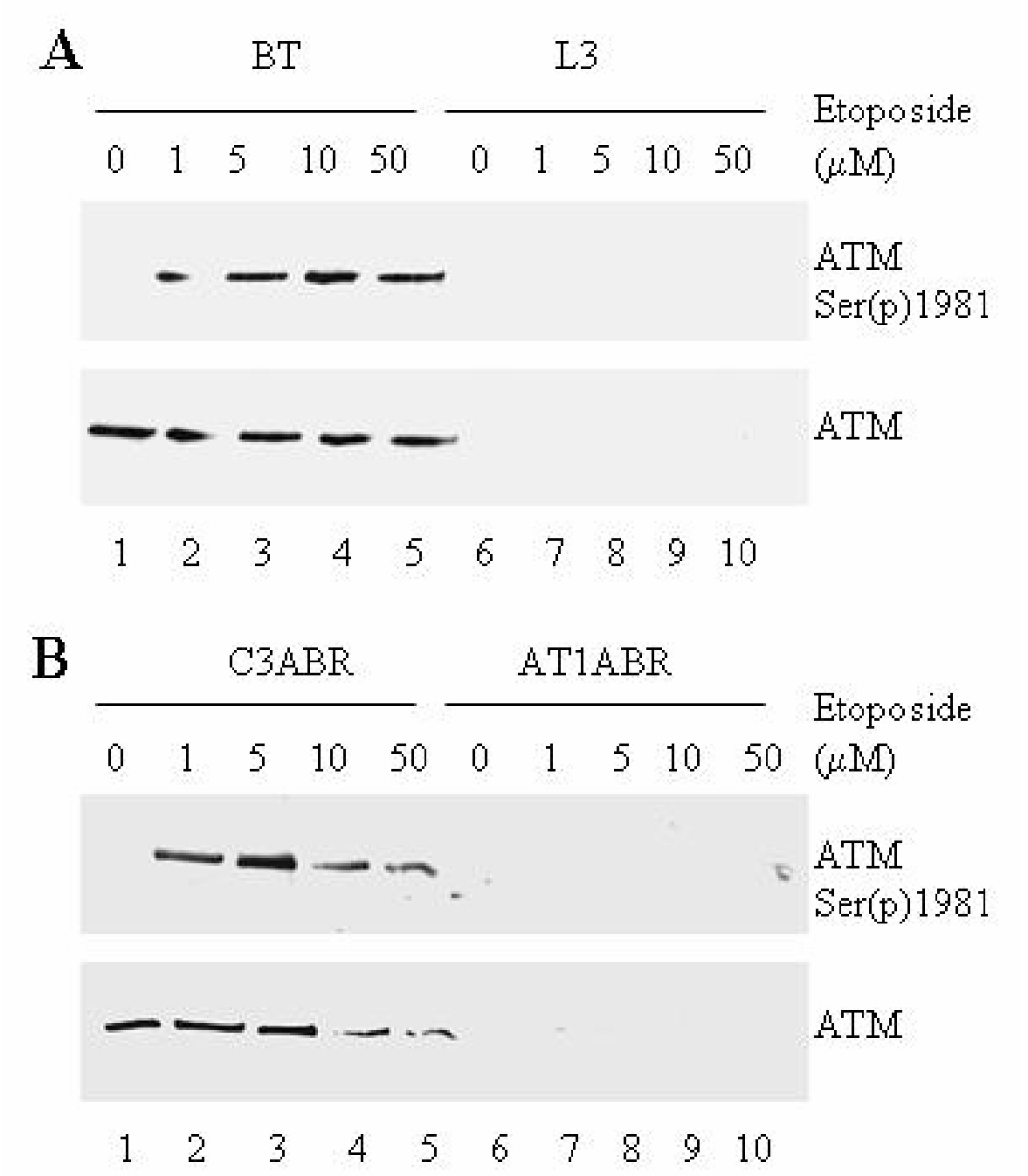

FIGURE 3.2: Phosphorylation of ATM on serine 1981 in response to different concentrations of etoposide. BT, L3, C3ABR and AT1ABR cells were exposed to 0, 1, 5, 10, 50 μM etoposide for 2 hours. Each lane represents 60 μg of a NET-N WCE. In panel A, lanes 1 through 5 represent BT extracts of cells treated with increasing concentrations of etoposide. Lanes 5 through 10 represent L3 cell extracts treated with increasing concentrations of etoposide. Panel B shows a similar experiment in the C3ABR and AT1ABR cell lines. Immunoblots were probe with 4BA (ATM) and a phosphospecific antibody to serine 1981 of human ATM.

site in response to all tested concentrations of etoposide. As expected, lanes 6 through 10 show no phosphorylation in the ATM negative L3 cell line. Panel B shows similar results in the C3ABR and AT1ABR cell lines.

The next figure examined the time course of ATM phosphorylation on serine 1981 in response to low doses of etoposide. BT, L3, C3ABR and AT1ABR cells were exposed to 0.8 μM of etoposide over a time course of 2 hours. The cell extracts were prepared, the protein concentration was determined and the Western blot was probed and stripped, as described in the previous experiment. Figure 3.3 also represents 60 μg of protein loaded in each lane probed for ATM phosphorylated on serine 1981 followed by total ATM content. In panel A, lane 1 shows that ATM was unphosphorylated at serine 1981 in untreated BT cells. Lanes 2 through 5 show ATM phosphorylation at this site occurs within 30 minutes and is substained after exposure to etoposide. Lanes 6 through 10 show no phosphorylation in the ATM negative L3 cell line. Panel B shows similar results in the C3ABR and AT1ABR cell lines. Panel C shows the increase in ATM serine 1981 phosphorylation based on the quantified data.

In order to determine whether ATM phosphorylation on serine 1981 at low concentrations of etoposide also resulted in increased ATM protein kinase activity, ATM was immunoprecipitated from etoposide treated cells, and assayed towards the PHAS-I substrate *in vitro*. In short, BT and C3ABR cells were exposed to 0.8 μM of etoposide over a 1 hour time course, WCEs were prepared in TGN buffer, ATM was immunoprecipitated and its kinase activity was assessed towards the PHAS-I substrate in the presence of radiolabelled γ-^{32}P-ATP and kinase buffer (as described in Chapter II: Materials and Methods). Audioradiograms are presented in Figure 3.4. In panel A, lane 1 represents a positive control for the ATM kinase activity towards PHAS-I. This lane demonstrates that

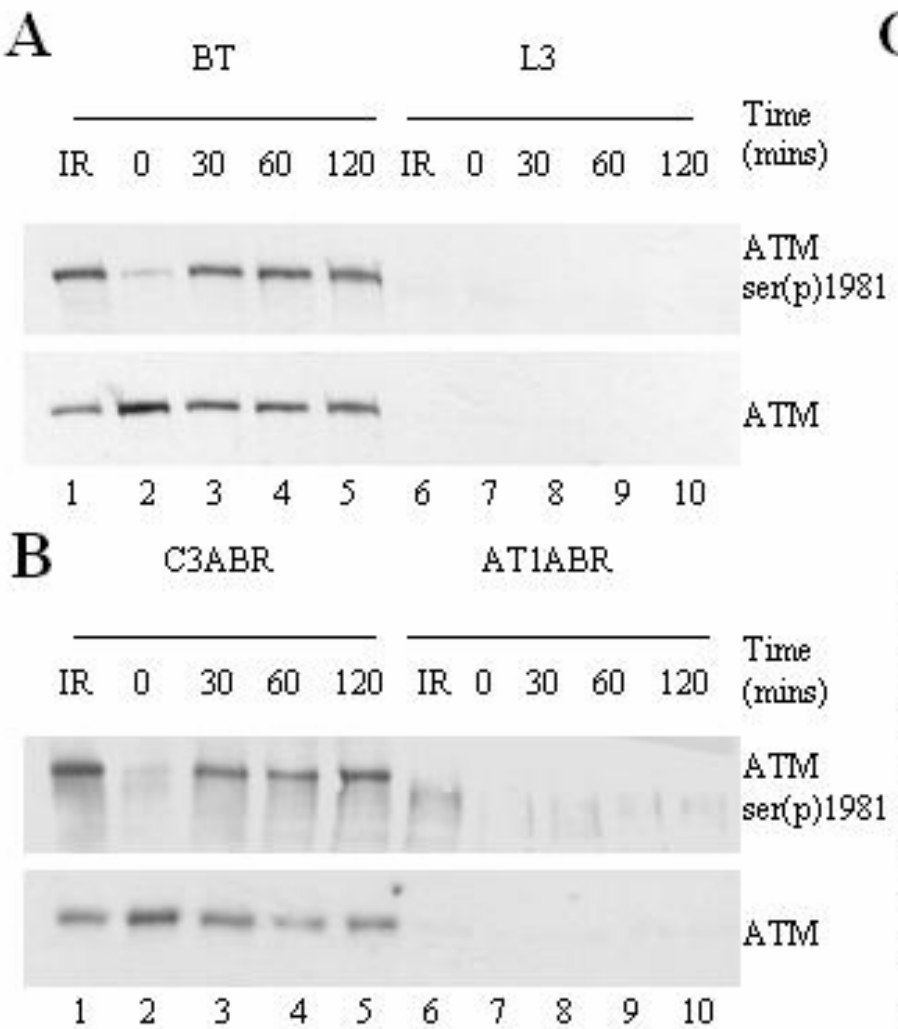

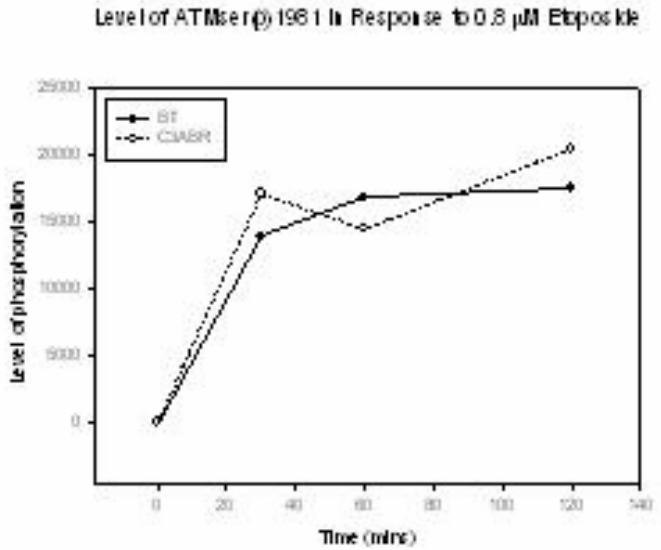

FIGURE 3.3: Time course of ATM phosphorylation on serine 1981 in response to 0.8µM etoposide. BT, L3, C3ABR and AT1ABR cells were exposed to 0.8 µM of etoposide over a time course of 2 hours. Each lane represents 60 µg of a NET-N WCE. In panel A, lanes 1 through 5 represent BT cell extracts treated with etoposide for an increasing period of time. Lanes 5 through 10 represent L3 cell extracts treated with etoposide for an increasing period of time. Panel B shows a similar experiment in the C3ABR and AT1ABR cell lines. Panel C shows ATM serine 1981 phosphorylation based on the quantified data.

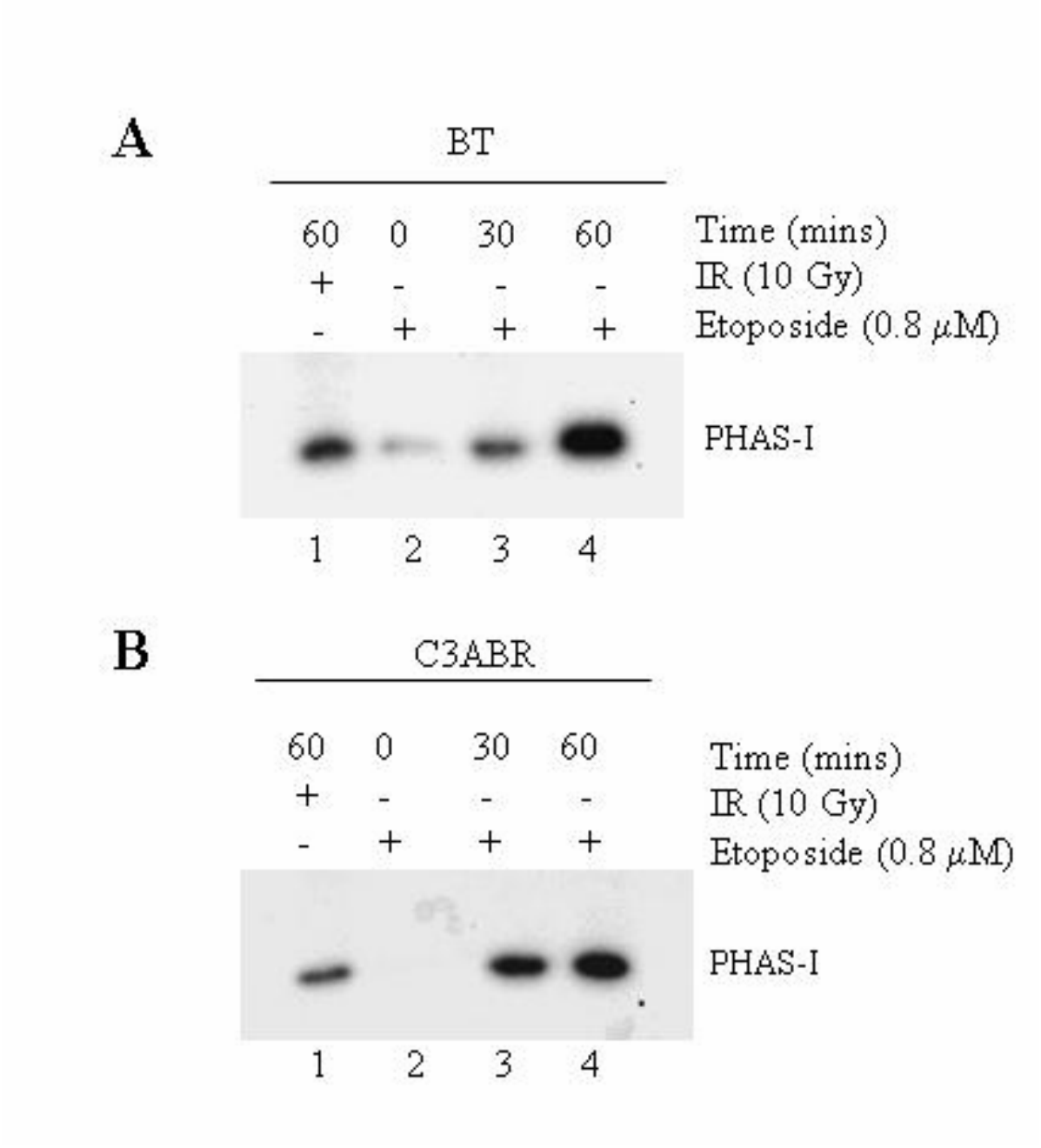

FIGURE 3.4: Activation of the protein kinase activity of immunoprecipitated ATM in response to 0.8 μM etoposide. BT, L3, C3ABR and AT1ABR cells were exposed to 0.8 μM of etoposide over a time course of 1 hour. ATM was immunoprecipitated from the cell extracts and assayed for its kinase activity towards the PHAS-I substrate. In panel A, the positive control in lane 1 represents cells treated with 10 Gy of IR, and harvested 60 minutes later. Lane 2 to 4 show the ATM kinase activity towards PHAS-I after treatment with etoposide over an increased period of time. Panel B shows similar results in the C3ABR cell line.

IR treated cells had detectable ATM kinase activity when incubated with the PHAS-I substrate. Lanes 2 to 4 show increased ATM kinase activity towards PHAS-I over time in response to treatment with 0.8 μM etoposide. Similar results were observed in C3ABR treated cells (in panel B).

3.3 Phosphorylation of ATM substrates in response to etoposide

DSBs induced by IR result in the activation of several ATM-dependent pathways (reviewed in Kurz and Lees-Miller, 2004). Activation of these pathways subsequently results in the ATM-dependent phosphorylation of substrates. As previously mentioned, these pathways have been extensively studied in response to IR. However, they have been studied to a much lesser extent in response to other DSB inducing agents such as etoposide. This section examines the phosphorylation of substrates known to be ATM-dependent in response to IR to determine the DNA damage signaling pathways activated in response etoposide.

3.3.1 Phosphorylation of H2AX in response to etoposide

H2AX is known to be rapidly phosphorylated on serine 139 in response to IR (Rogakou *et al*, 1998). It has also been shown that H2AX is phosphorylated in response to high doses of etoposide (Burma *et al*, 2001). However, it is unknown whether low doses of etoposide cause H2AX phosphorylation and if ATM is required for this phosphorylation event. Figure 3.5 examines phosphorylation of H2AX on serine 139 in response to increasing concentrations of etoposide. In short, BT and L3 cells were exposed to 0, 1, 5, 50 μM etoposide for 2 hours. Extracts were prepared by sulphuric acid precipitation and dialysis in acetic acid and water (as described in Chapter II: Materials and Methods). The

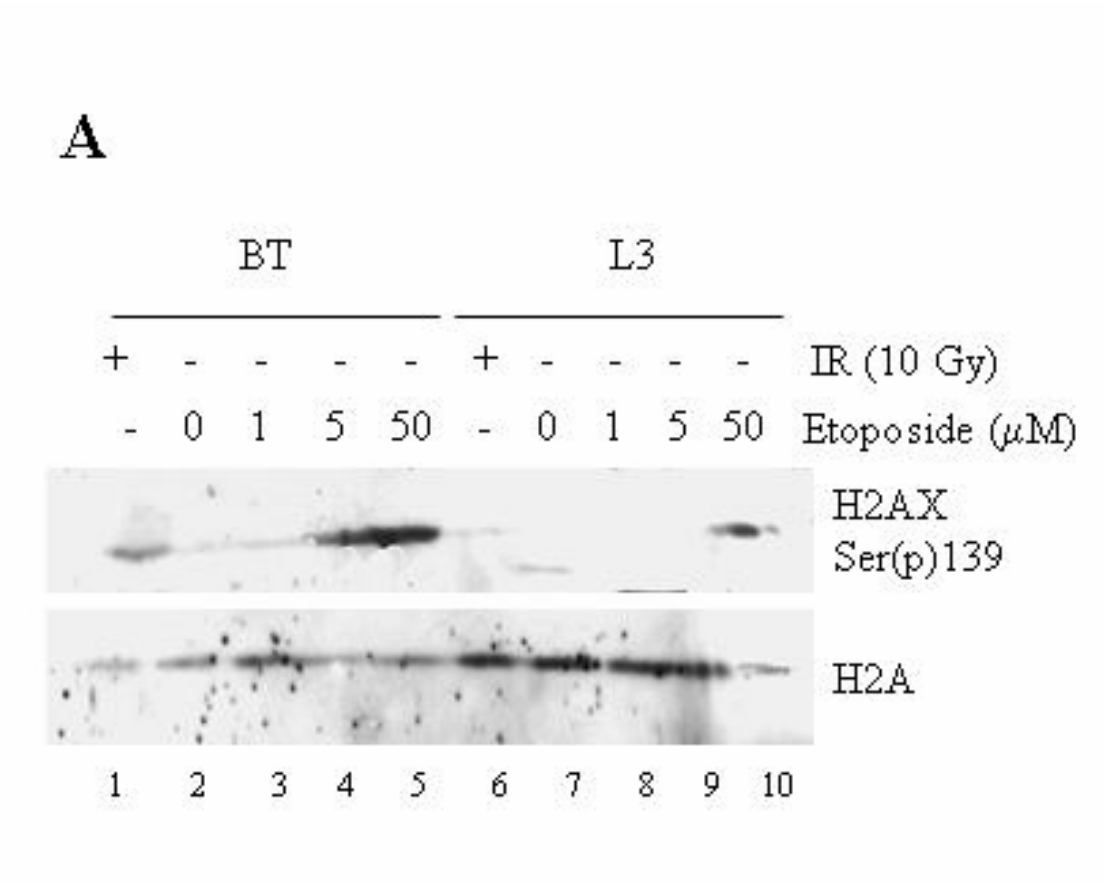

FIGURE 3.5: Phosphorylation of the ATM downstream effector H2AX in response to different concentrations of etoposide. BT and L3 cells were exposed to 0, 1, 5, 50 μM of etoposide for 2 hours. In panel A, the positive control for phosphorylation at serine 139 in lane 1 represents cells treated with 10 Gy of IR, and allowed to recover for 2 hours. Lanes 2 through 5 represent BT extracts of cells treated with increasing concentrations of etoposide. Lane 6 represent IR treated cells (similar treatment as lane 1) in L3 cells. Lane 7 through 10 represent L3 extracts of cells treated with increasing concentrations of etoposide. Immunoblots were probed with a phosphospecific antibody to serine 139 of human histone γ-H2AX and the H2A antibody.

immunoblot was initially probed with a H2AX phosphospecific antibody to serine 139, then stripped and reprobed with a H2A antibody to estimate total H2AX content. In Panel A, lane 1 represents a positive control for H2AX phosphorylation at serine 139. BT cells treated with 10 Gy of IR, and allowed to recover for 2 hours showed phosphorylation at serine 139 of H2AX. Lanes 2 through 4 showed that H2AX was unphosphorylated in BT cells exposed to 0, 1, or 5 μM of etoposide for 2 hours. Lane 5 shows that H2AX is phosphorylated in BT cells exposed to 50 μM of etoposide for the same time period. The control experiment in lane 6 showed that phosphorylation in L3 cells in response to IR was reduced. However, lanes 7 through 10 show that the phosphorylation of H2AX in response to etoposide was the same in L3 cells as that observed in BT cells.

3.3.2 Phophorylation of NBS1 in response to etoposide

Phosphorylation of the NBS1 protein on serine 343 has been shown to be required for proper intra-S-phase arrest in response to IR (Lim *et al*, 2000). Similarly to ATM autophosphorylation and H2AX phosphorylation, this response has been determined in IR-treated cells but remains to be elucidated in response to other DSB-inducing agents. The experiments performed next investigated NBS1 phosphorylation on serine 343 in response to increasing concentrations of etoposide, as well as, a time course in cells treated with a low dose of etoposide (0.8 μM).

In Figure 3.6, BT, L3, C3ABR and AT1ABR cells were exposed to 0, 1, 5, 10, 50 μM of etoposide for 2 hours. NET-N WCEs were prepared and 60 μg of extracts was run and immunoblotted for phosphorylated NBS1. Immunoblots were then stripped and reprobed for total NBS1. Panel A, lane 1 and 6 show that both BT and L3 cells are unphosphorylated at serine 343 in untreated cells. Lanes 2 through 5 demonstrate that

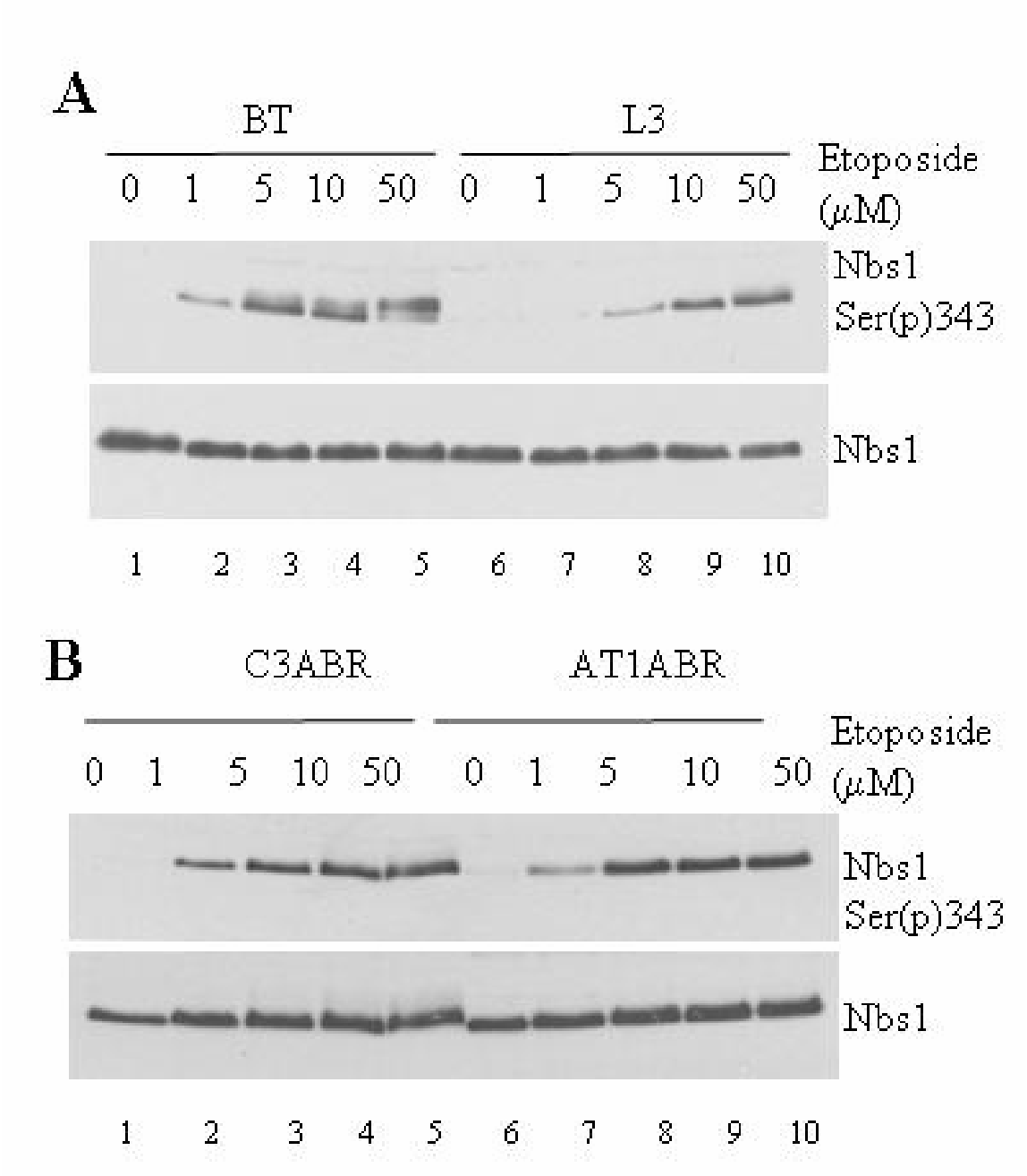

FIGURE 3.6: Phosphorylation of the ATM downstream effector Nbs1 in response to different concentrations of etoposide. BT, L3, C3ABR and AT1ABR cells were exposed to 0, 1, 5, 10, 50 μM etoposide for 2 hours. Each lane represents 60 μg of a NET-N WCE. In panel A, lanes 1 through 5 represent BT extracts of cells treated with increasing concentrations of etoposide. Lanes 5 through 10 represent L3 cell extracts treated with increasing concentrations of etoposide. Panel B shows a similar experiment in the C3ABR and AT1ABR cell lines. Immunoblots were probed with a phosphospecific antibody to serine 343 of human NBS and an NBS1 antibody for total protein.

NBS1 is phosphorylated in a dose-dependent manner at this site, in response to 1, 5, 10 and 50 μM etoposide. Lanes 7 and 8 show that phosphorylation at this site occurs but is reduced in the L3 cell line in response to 1 and 5 μM of etoposide, respectively. Phosphorylation of NBS1 at higher concentrations of etoposide was not markedly reduced in L3 cells, as demonstrated in lanes 9 and 10. Panel B shows similar results in the C3ABR and AT1ABR cell lines. However, phosphorylation at serine 343 in response to 5 μM of was not reduced in AT1ABR as it was in L3 cells.

In figure 3.7, BT, L3, C3ABR and AT1ABR cells were exposed to 0.8 μM of etoposide over a time course of 2 hours. In panel A, Lane 1 shows that cells allowed to recover from being exposed to 10 Gy of IR are phosphorylated on NBS1 serine 343. Lane 2 shows that NBS1 was unphosphorylated in untreated BT cells. Lanes 2 through 5 show NBS1 phosphorylation at this site increased over time with exposure to etoposide. Lanes 6 shows that by 2 hours, NBS1 was phosphorylated at serine 343 in IR treated L3 cells. Lanes 7 through 10 demonstrate that phosphorylation of NBS1 serine 343 is delayed in response to 0.8 μM etoposide. Panel B shows similar results in the C3ABR and AT1ABR cell lines. Panel C shows the increase in phosphorylation at NBS1 serine 343 based on the quantified data.

3.3.3 Phosphorylation of Chk1 in response to etoposide

Chk1 was long believed to be exclusively an ATR substrate. However, recent studies have suggested that Chk1 is also phosphorylated in an ATM-dependent manner in response to IR. ATM has been shown to be required for the phosphorylation of both serine 317 and 345 on Chk1 after exposure to IR (Gatei *et al*, 2003; Sapkota *et al*, 2002), suggesting that ATM and ATR pathways overlap in the phosphorylation of this checkpoint

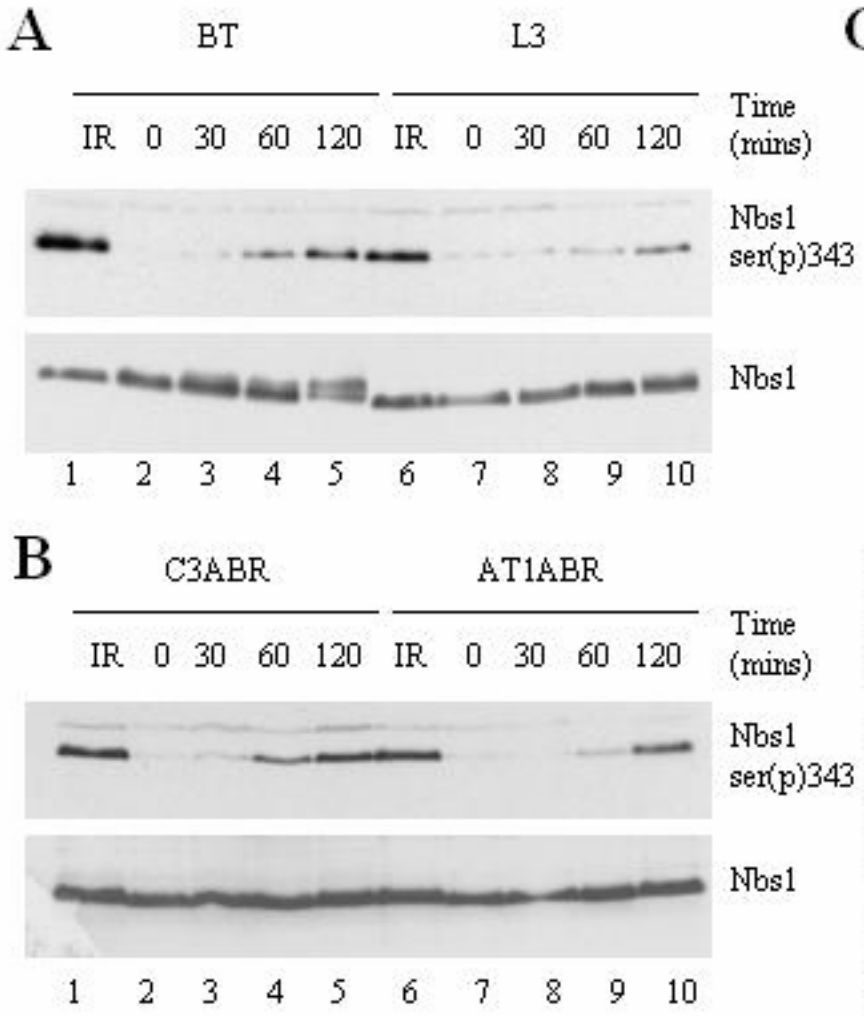

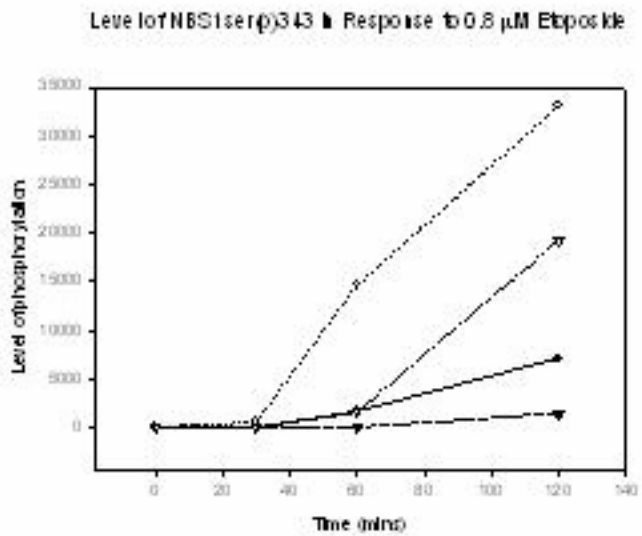

FIGURE 3.7: Time course of phosphorylation of the ATM downstream effector Nbs1 in response to etoposide. BT, L3, C3ABR and AT1ABR cells were exposed to 0.8 µM of etoposide over a time course of 2 hours. Each lane represents 60 µg of a NET-N WCE. In panel A, lanes 1 through 5 represent BT extracts of cells treated with etoposide for an increasing period of time. Lanes 5 through 10 represent L3 cell extracts treated with etoposide for an increasing period of time. Panel B shows a similar experiment in the C3ABR and AT1ABR cell lines. Panel C shows NBS1 serine 343 phosphorylation based on the quantified data.

kinase. Once again, this response has not been characterised for other DSB-inducing agents. Therefore, the experiments performed in this section examine the effect of increasing concentrations of etoposide, as well as, a time course of a low dose of etoposide (0.8 μM) on phosphorylation of Chk1 at serine 345.

In figure 3.8, BT, L3, C3ABR and AT1ABR cells were exposed to 0, 1, 5, 10, 50 μM etoposide for 2 hours. Cells were harvested and extracts were prepared for immunoblotting. Each lane represents 60 μg of NET-N WCE. Immunoblots were probed with a phosphospecific antibody to Chk1 serine 345, then stripped and reprobed for total Chk1 levels. In panel A, lanes 1 through 5 demonstrate that Chk1 is phosphorylated at serine 345 in a dose-dependent manner in response to etoposide. Lanes 6 through 10 demonstrate that this is also the case in L3 cells, indicating an ATM-independent phosphorylation event. Panel B shows similar results in the C3ABR and AT1ABR cell lines.

In Figure 3.9, BT, L3, C3ABR and AT1ABR cells were exposed to 0.8 μM of etoposide over a 2 hour time course. As a control, lane 1 shows that Chk1 was phosphorylated at serine 345 in BT cells, 2 hours after exposure to 10 Gy of IR. Lanes 2 through 5 show a time depedent increase, up to 2 hours, of phosphorylation on serine 345 in response to 0.8 μM etoposide. Lane 6 shows that this site is phosphorylated in L3 cells 2 hours after exposure to 10 Gy of IR. Similarly to BT cells, L3 cells also showed a time dependent increase of this phosphorylation event. Panel C shows the increase in phosphorylation of Chk1 serine 345 based on the quantified data.

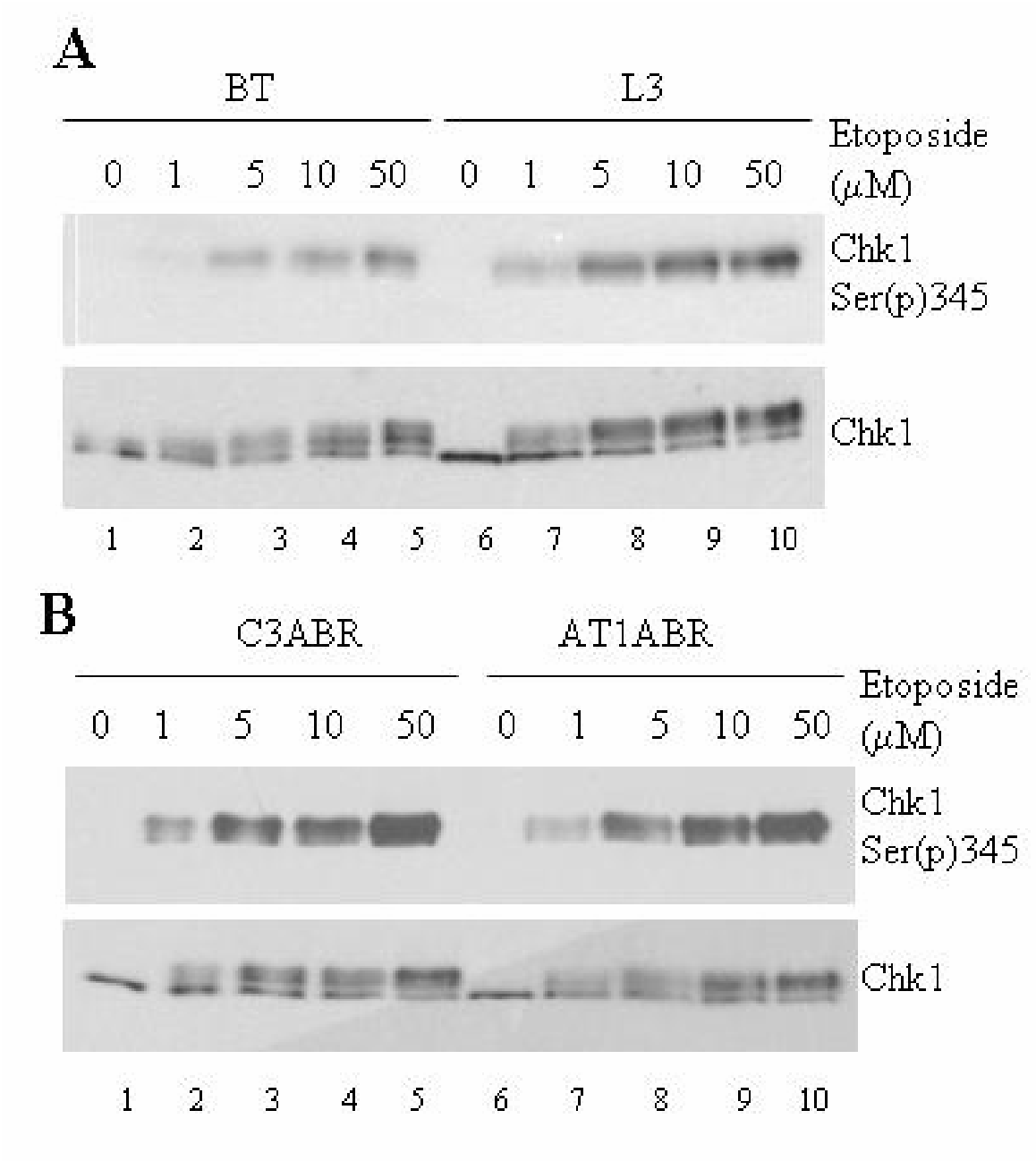

FIGURE 3.8: Phosphorylation of the ATM downstream effector CHK1 in response to different concentrations of etoposide. BT, L3, C3ABR and AT1ABR cells were exposed to 0, 1, 5, 10, 50 μM etoposide for 2 hours. Each lane represents 60 μg of a NET-N WCE. In panel A, lanes 1 through 5 represent BT extracts of cells treated with increasing concentrations of etoposide. Lanes 5 through 10 represent L3 cell extracts treated with increasing concentrations of etoposide. Panel B shows a similar experiment in the C3ABR and AT1ABR cell lines.

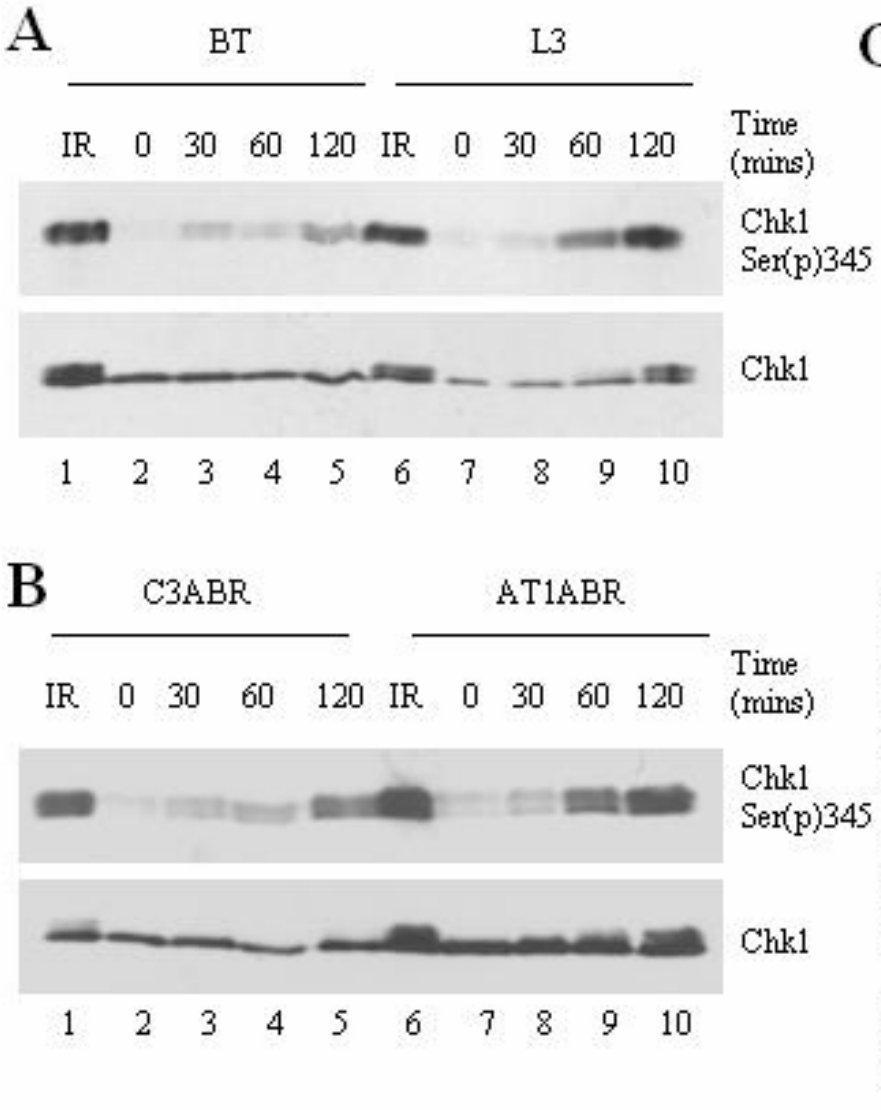

FIGURE 3.9 : Time course of phosphorylation of the ATM downstream effector Chk1 in response to etoposide. BT, L3, C3ABR and AT1ABR cells were exposed to 0.8 µM of etoposide over a time course of 2 hours. Each lane represents 60 µg of a NET-N WCE. In panel A, lanes 1 through 5 represent BT extracts of cells treated with etoposide for an increasing period of time. Lanes 5 through 10 represent L3 cell extracts treated with etoposide for an increasing period of time. Panel B shows a similar experiment in the C3ABR and AT1ABR cell lines. Panel C shows CHK1 serine 345 phosphorylation based on the quantified data.

3.3.4 Phosphorylation of SMC-1 in response to etoposide

SMC-1 has been recognized as an important ATM substrate in the intra-S-phase checkpoint pathway. Serines 957 and 966 have both been identified as ATM-dependent phosphorylation sites in response to IR (Kim *et al*, 2002; Yazdi *et al*, 2002). Futhermore, these events have also been shown to require functional NBS1 (Yazdi *et al*, 2002). In the following set of experiments, the effect of increasing concentrations of etoposide and a time course of a low dose of etoposide (0.8 μM) were examined to determine the pattern of phosphorylation on SMC-1 serine 957.

In Figure 3.10, BT, L3, C3ABR and AT1ABR cells were treated with 0, 1, 5, 10, 50 μM of etoposide for a 2 hour period. Cell extracts and immunoblots were prepared as previously described. Immunoblots were probed with an SMC-1 serine 957 phosphospecific antibody, stripped and reprobed for total SMC-1 content. In panel A, lanes 1 and 6 indicate that both in BT and L3 cells SMC-1 is unphosphorylated on serine 957. Lanes 2 through 5 show a dose-dependent increase in phosphorylation at this SMC-1 site in response to etoposide. This phosphorylation event was abolished in L3 cells except at 50 μM of etoposide, which resulted in a markedly reduced amount of phosphorylation in this cell line. Similar results were observed in panel B.

In Figure 3.11, BT, L3, C5ABR and AT1ABR cells were treated either with 10 Gy of IR for 2 hours or, with 0.8 μM etoposide over a time course of 2 hour. Cell extracts and immunoblots were prepared and probed as per the previous experiment. Lane 1 shows that SMC-1 is phosphorylated on serine 957 in response to IR radiation. This phosphorylation event is markedly reduced in L3 cells (lane 6) indicating that ATM is required for phosphorylation at this site. Lanes 2 through 5 demonstrate that SMC-1 is phosphorylated in a time-dependent manner in response to a low dose of etoposide (0.8 μM) and this

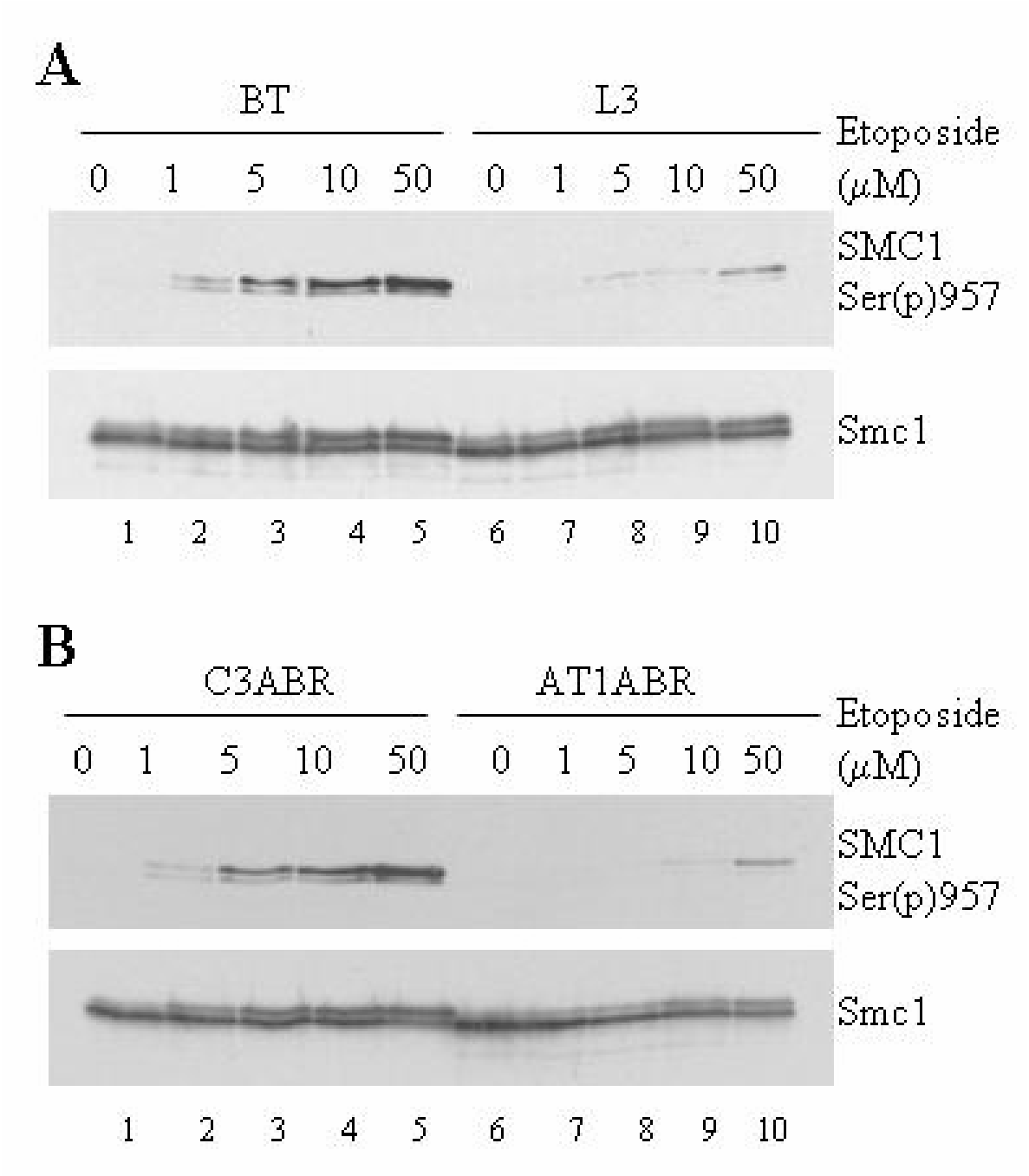

FIGURE 3.10: Phosphorylation of the ATM downstream effector SMC1 in response to different concentrations of etoposide. BT, L3, C3ABR and AT1ABR cells were exposed to 0, 1, 5, 10, 50 μM etoposide for 2 hours. Each lane represents 60 μg of a NET-N WCE. In panel A, lanes 1 through 5 represent BT extracts of cells treated with increasing concentrations of etoposide. Lanes 5 through 10 represent L3 cell extracts treated with increasing concentrations of etoposide. Panel B shows a similar experiment in the C3ABR and AT1ABR cell lines.

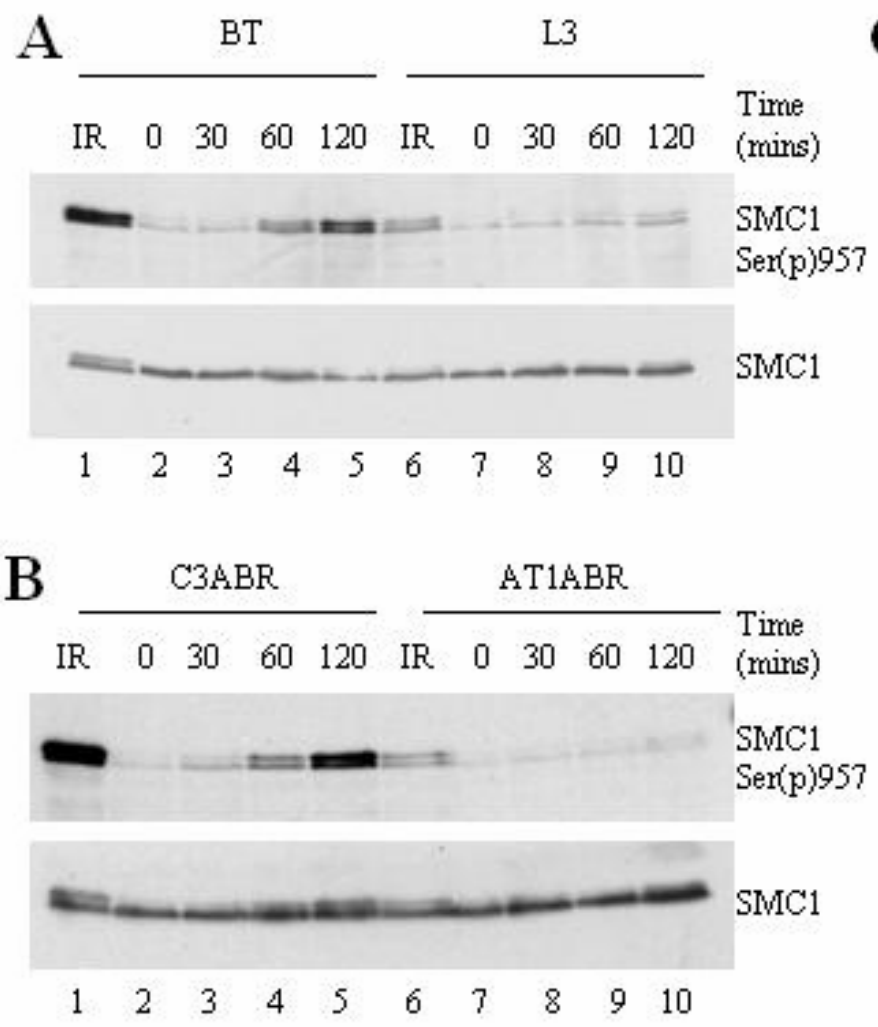

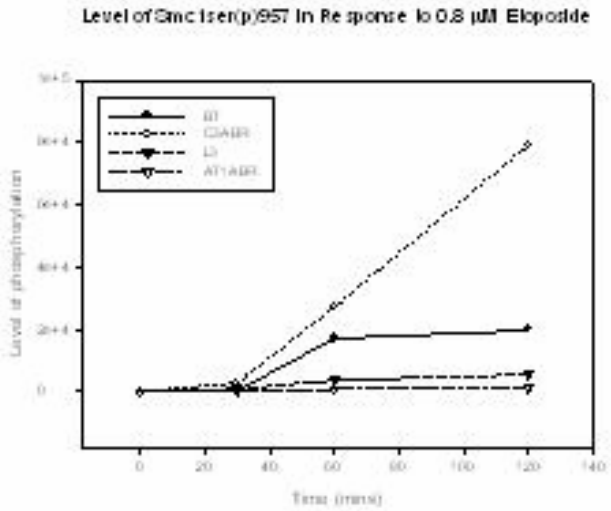

FIGURE 3.11 : Time course of phosphorylation of the ATM downstream effector SMC1 in response to etoposide. BT, L3, C3ABR and AT1ABR cells were exposed to 0.8 µM of etoposide over a time course of 2 hours. Each lane represents 60 µg of a NET-N WCE. In panel A, lanes 1 through 5 represent BT extracts of cells treated with etoposide for an increasing period of time. Lanes 5 through 10 represent L3 cell extracts treated with etoposide for an increasing period of time. Panel B shows a similar experiment in the C3ABR and AT1ABR cell lines. Panel C shows SMC1 serine 957 phosphorylation based on the quantified data.

phosphorylation event requires ATM (lanes 7 through 10). A similar result is presented in panel B. Panel C shows the increase in SMC1 phosphorylation on serine 957 based on the quantified data.

3.3.5 Phosphorylation of Chk2 in response to etoposide

The Chk2 kinase is a well established kinase involved in IR-induced cell cycle delay. As previously mentioned, ATM was shown to phosphorylate Chk2 directly on threonine 68, an essential site for proper Chk2 activation. These experiments look at the phosphorylation of Chk2 on threonine 68 in response to etoposide. The first set of experiments looks at increasing concentrations of etoposide while the second examines threonine 68 phosphorylation in response to a low dose of etoposide (0.8 μM) over a 2 hour time course.

In figure 3.12, BT, L3, C3ABR and AT1ABR cells were exposed to increasing concentrations of etoposide over a two hour period. WCEs were prepared as previously described. Two immunoblots were prepared for each cell line pair. Immunoblots were probed with either a phospho-specific Chk2 antibody against threonine 68 or total Chk2. They were then stripped and reprobed with an anti-actin antibody. Two sets of immunoblots were performed since experiments where the Chk2 phospho-specific was stripped and reprobed with the total Chk2 antiboby were inconsistent. In panel A, Lane 1 shows that Chk2 is unphosphorylated in untreated BT cells. Lanes 2 through 5 shows phosphorylation at this site in response to all tested concentrations of etoposide. This panel also shows that Chk2 becomes highly phosphorylated at higher doses of etoposide as indicated by the increase in the shifted band after treatment with 50 μM. Lane 6 shows that threonine 68 is unphosphorylated in untreated L3 cells. Lanes 7 indicates that this

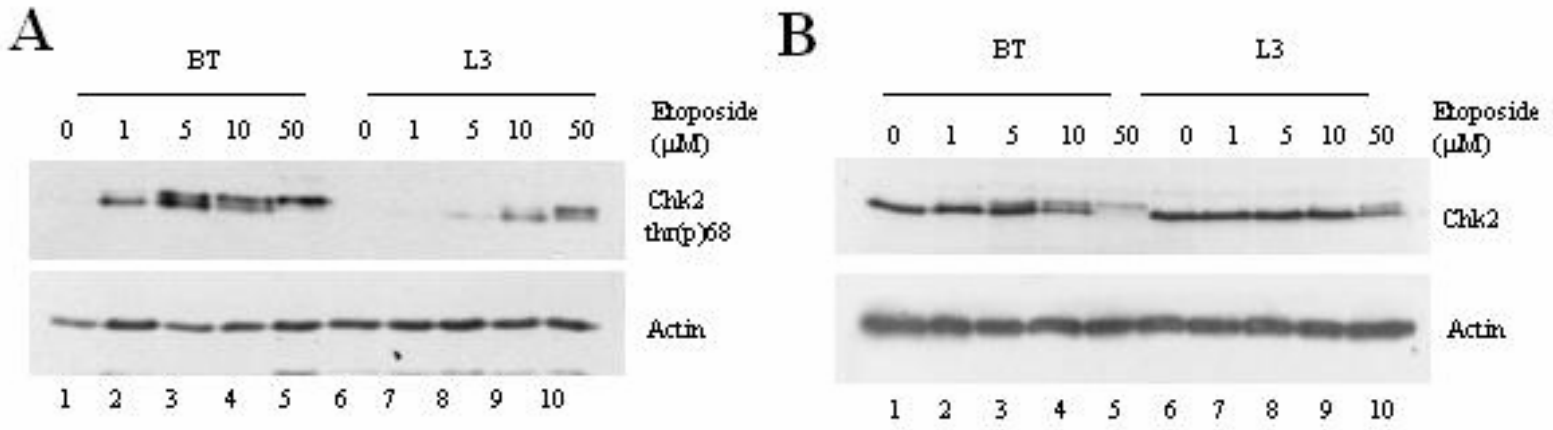

FIGURE 3.12: Phosphorylation of the ATM downstream effector Chk2 in response to different concentrations of etoposide.. BT and L3 cells were exposed to 0, 1, 5, 10, 50 μM for etoposide 2 hours. Each lane represents 60 μg of a NET-N WCE. In panel A, lanes 1 through 5 represent BT extracts of cells treated with increasing concentrations of etoposide. Lanes 5 through 10 represent L3 cell extracts treated with increasing concentrations of etoposide.

phosphorylation event is abrogated after treatment with 1 μM of etoposide. Lanes 8 through 10 show that this phosphorylation event is markedly reduced in the absence of ATM after treatment with 5, 10 or 50 μM etoposide. In panel B, Lanes 1 through 5 show a decrease in total Chk2 in response to treatment with increasing amounts of etoposide. However, lanes 6 through 10 show that this effect is decreased in the absence of ATM.

In figures 3.13 and 3.14, BT, L3, C3ABR and AT1ABR cells were exposed to 10 Gy of IR or 0.8 μM of etoposide over a time course of 2 hours. Cell extracts and immunoblots were prepared as per the previous experiment. In figure 3.13, panel A and B indicate that total Chk2 level are unaffected at low concentration of etoposide in all cell lines examined. Total Chk2 levels remained constant in BT (Panel A/Lanes 1through 5), L3 (Panel A/Lanes 6 through 10), C3ABR (Panel B/Lanes 1through 5) and AT1ABR BT (Panel B/Lanes 6 through 10). In figure 3.14, lane 1 shows that Chk2 was phosphorylated at threonine 68 in IR treated cells. This response was abrogated in L3 cells (lane 6). Lane 2 and 7 show that this site is unphosphorylated in untreated BT and L3 cells, respectively. Lanes 3 through 5 show that Chk2 is phosphorylated at threonine 68 in response to low doses of etoposide. Lanes 8 through 10 show that this phosphorylation event is abrogated in the absence of ATM in L3 cells. Panel B shows similar results in the C3ABR and AT1ABR cell lines. Panel C shows the increase in phosphorylation at Chk2 threeonine 68 based on the quantified data.

3.3.6 Phosphorylation of p53 in response to etoposide

p53 has been described as the nodal point of the DNA damage response. Serine 15 on p53 has been identified as a phosphorylation site for activation and stabilisation of this protein in response to DNA damage. Moreover, ATM, ATR and hSMG-1/ATX have all

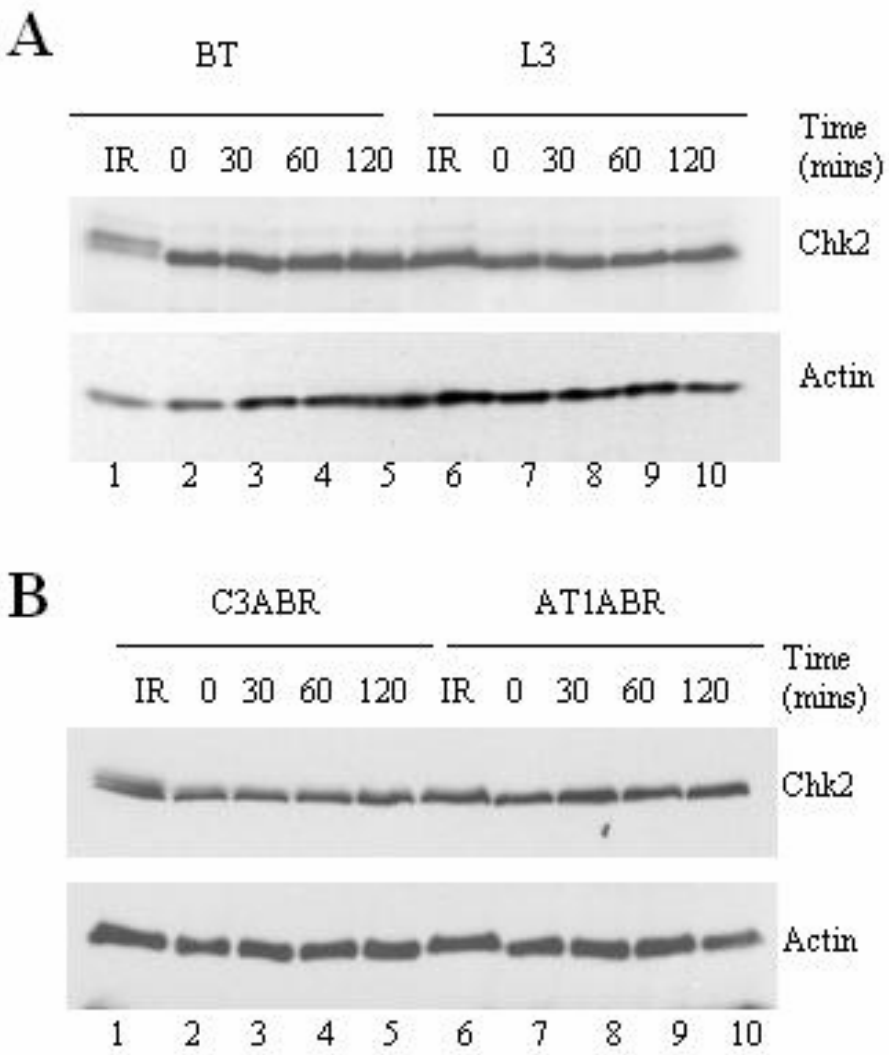

FIGURE 3.13: Time course of ATM downstream effector Chk2 in response to etoposide. BT, L3, C3ABR and AT1ABR cells were exposed to 0.8 μM of etoposide over a time course of 2 hours. Each lane represents 60 μg of a NET-N WCE. In panel A, lanes 1 through 5 represent BT extracts of cells treated with etoposide for an increasing period of time. Lanes 5 through 10 represent L3 cell extracts treated with etoposide for an increasing period of time. Panel B shows a similar experiment in the C3ABR and AT1ABR cell lines.

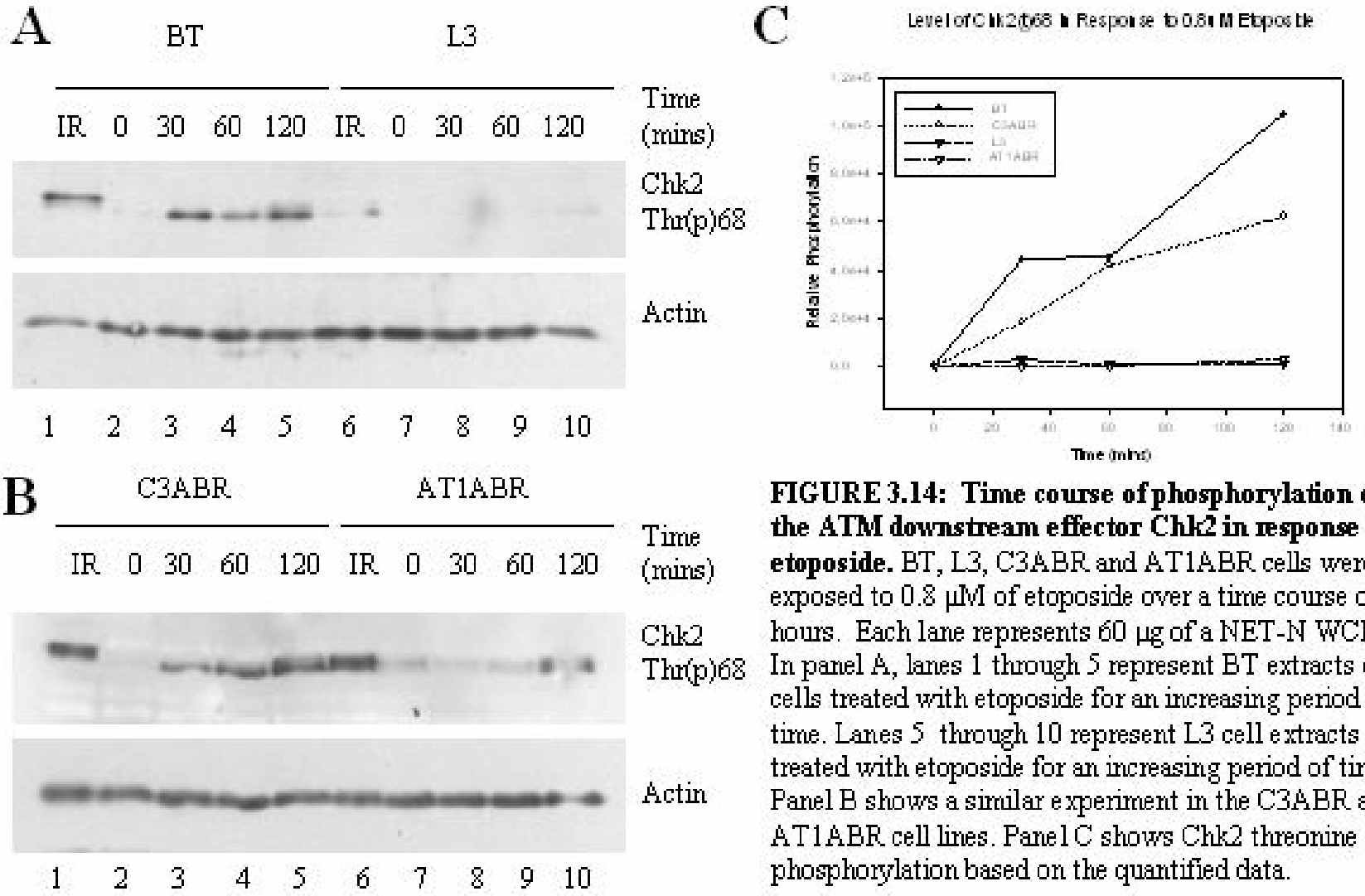

FIGURE 3.14: Time course of phosphorylation of the ATM downstream effector Chk2 in response to etoposide. BT, L3, C3ABR and AT1ABR cells were exposed to 0.8 μM of etoposide over a time course of 2 hours. Each lane represents 60 μg of a NET-N WCE. In panel A, lanes 1 through 5 represent BT extracts of cells treated with etoposide for an increasing period of time. Lanes 5 through 10 represent L3 cell extracts treated with etoposide for an increasing period of time. Panel B shows a similar experiment in the C3ABR and AT1ABR cell lines. Panel C shows Chk2 threonine 68 phosphorylation based on the quantified data.

been shown to phosphorylate this site upon different types of DNA damage, in some cases, in apparently redundant pathway (see Section I: Introduction). p53 has been shown to be phosphorylated on serine 15 after a 2 hour treatment with 68 μM etoposide (Ye *et al,* 2001). Furthermore, this response did not require the presence of ATM. The response to IR has been shown to cause multisite phosphorylation of p53 including serines 6, 9, 15, 20 and 46 (Saito *et al*, 2002). Moreover, ATM was shown to be implicated in the phosphorylation of all these sites and be absolutely required for the phosphorylation of serine 46. Therefore, we were interested in examining the phosphorylation of p53 at all these sites in response to different doses of etoposide and to further investigate the response to low doses of etoposide.

The first set of experiments investigates the phosphorylation of p53 on serine 15. In figure 3.15, BT, L3, C3ABR and AT1ABR cells were exposed to 0, 1, 5, 10, 50 μM etoposide for 2 hours. In panel A, lane 1 shows that p53 was unphosphorylated at serine 15 in untreated BT cells. Lanes 2 through 5 show p53 phosphorylation at this site in response to treatment with 1, 5, 10 and 50 μM etoposide. Lanes 6 shows that p53 was unphosphorylated at serine 15 in untreated L3 cells. Lanes 7 shows that at a low concentration of etoposide (1 μM), serine 15 on p53 was delayed in the L3 cell line. Lanes 8 through 10 show that phosphorylation on serine 15 occurs in response to 5, 10 or 50 μM etoposide in L3 cells. Panel B shows similar results in the C3ABR and AT1ABR cell lines.

To further examine the defect in phosphorylation at serine 15 in response to low etoposide concentration, cells were exposed to 0.8 μM etoposide over a 2 hour time course or to 10 Gy of IR. In short, BT, L3, C3ABR and AT1ABR cells were exposed to etoposide and WCE were prepared as previously described. Immunoblots from 30 μg of WCE were probed for p53 serine 15, stripped/reprobed for total p53 and stripped/reprobed for actin.

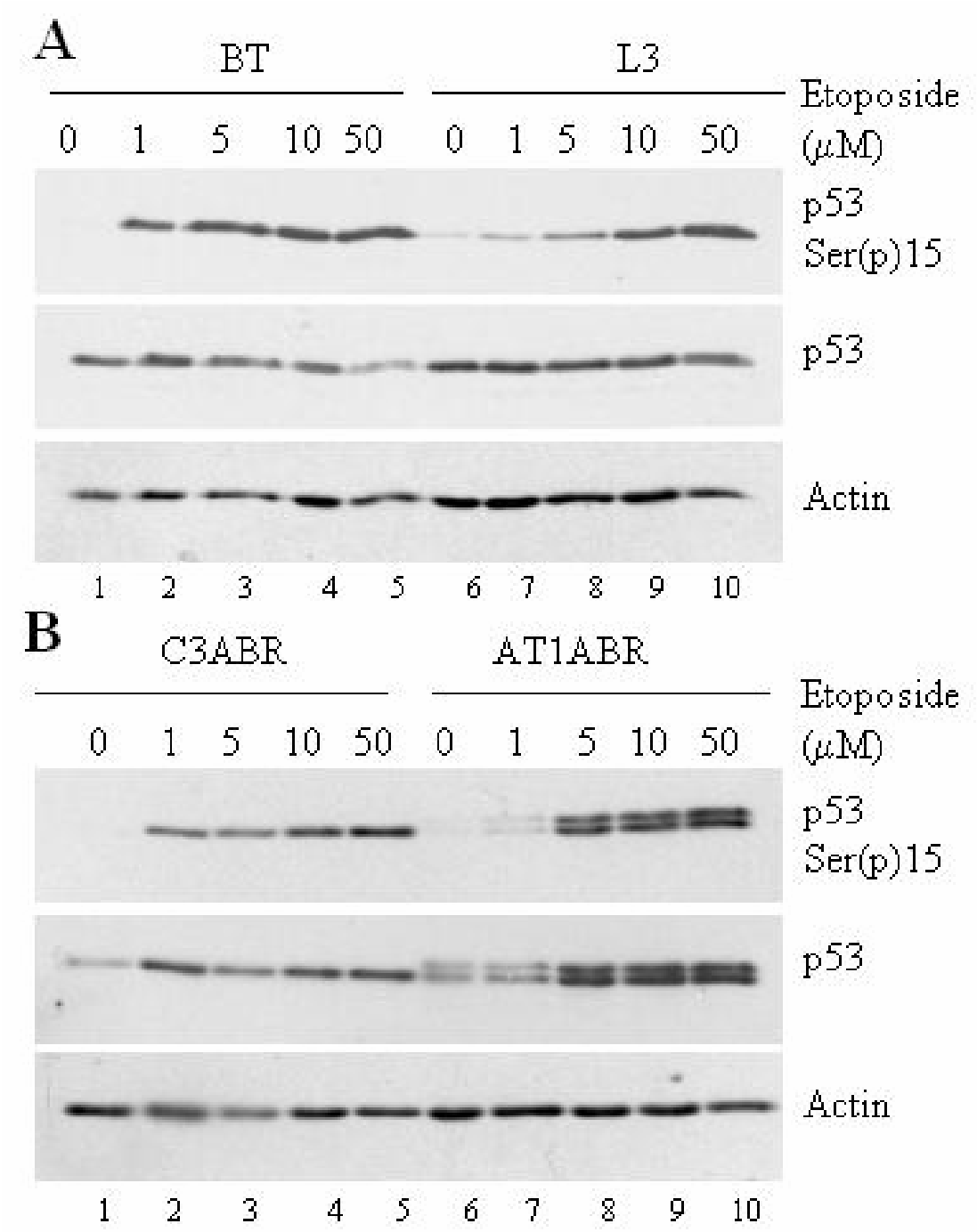

FIGURE 3.15: Phosphorylation of the ATM downstream effector p53 in response to different concentrations of etoposide. BT, L3, C3ABR and AT1ABR cells were exposed to 0, 1, 5, 10, 50 μM etoposide for 2 hours. Each lane represents 60 μg of a NET-N WCE. In panel A, lanes 1 through 5 represent BT extracts of cells treated with increasing concentrations of etoposide. Lanes 5 through 10 represent L3 cell extracts treated with increasing concentrations of etoposide. Panel B shows a similar experiment in the C3ABR and AT1ABR cell lines.

Results are presented in Figure 3.16. In panel A, lane 1 shows that p53 was phosphorylated at serine 15 in IR treated BT cells. Lane 2 shows that this site is unphosphorylated. Lanes 3 through 5 show p53 phosphorylation at this site increased over time with exposure toetoposide. Lanes 6 shows that p53 was phosphorylated at serine 15 in L3 cells 2 hours after exposure to IR. Lane 7 shows that p53 is unphosphorylated at this site in untreated L3 cells. Lanes 8 through 10 show that the increase in p53 phosphorylation is delayed in the L3 cell line. Panel B shows similar results in the C3ABR and AT1ABR cell lines. Panel C shows the increase in p53 serine 15 phosphorylation based on the quantified data.

In Figure 3.17, BT, L3, C3ABR and AT1ABR cells were exposed to 0.8 μM etoposide over a time course of 4 hours or to 10 Gy of IR. Briefly, WCEs were prepared in NET-T extraction buffer. p53 was immunoprecipitated and immunoblots were prepared and probed with antibodies specific to p53 phosphorylated at serine 6, 9, 15, 20, or 46. Lane 1 shows that p53 was phosphorylated at all serine residues in BT cells, 2 hours after treatment with 10 Gy of IR. Lanes 2 and 7 of the p53 serine 6 immunoblot indicate that this site in unphosphorylated in untreated BT and L3 cells, respectively. Lanes 3 through 5 indicate a time-dependent increase of phosphorylation at this same site. Lane 6 shows a low amount of phosphorylation at serine 6 in response to 10 Gy of IR suggesting a delay in phosphorylation or a redundant pathway for phosphorylation at this site. Lane 7 shows that serine 6 is unphosphorylated in untreated L3 cells. Lanes 8 through 10 show that ATM is required for the phosphorylation at this site in response to 0.8 μM of etoposide. The serine 9 immunoblot indicates this site is unphosphorylated in untreated BT and L3 cells (lanes 2 and 7, respectively). This site only appears to become phosphorylated after 4 hours of exposure to the low dose of etoposide (lane 5). In ATM deficient cells this site is not phosphorylated by either 10 Gy of IR (lane 6) or etoposide (lanes 7 through 10). The serine

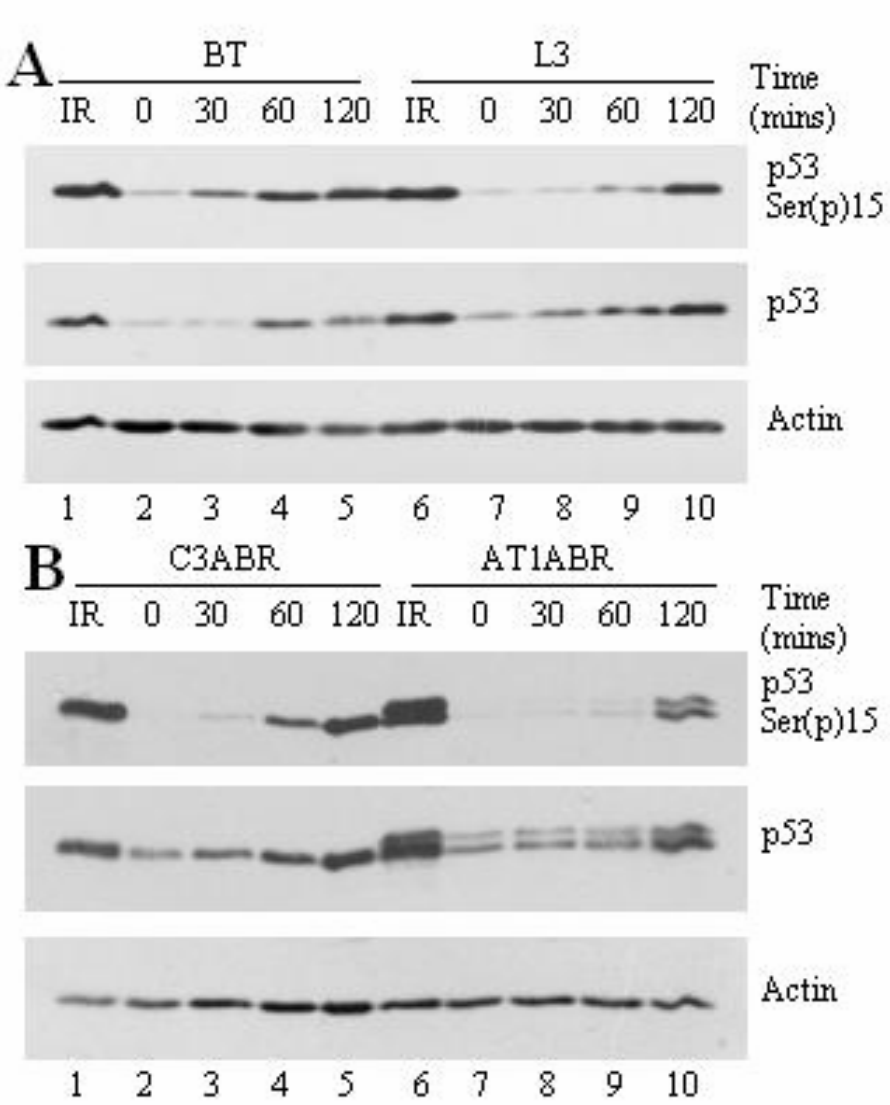

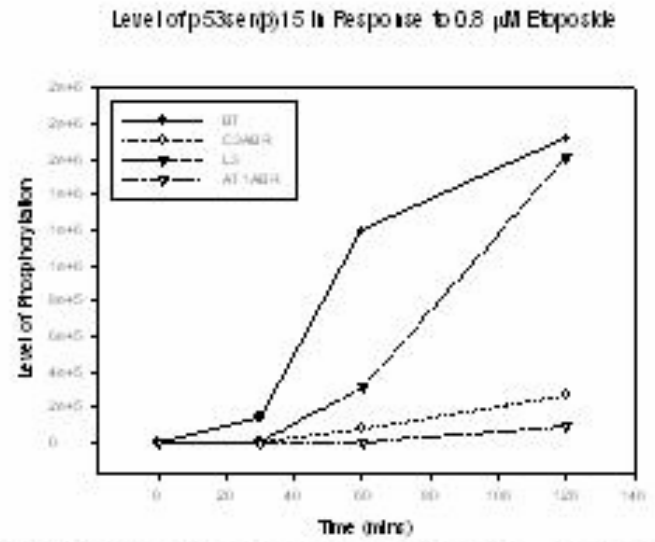

FIGURE 3.16: Time course of phosphorylation of the ATM downstream effector p53 at serine 15 in response to etoposide. BT, L3, C3ABR and AT1ABR cells were exposed to 0.8 µM of etoposide over a time course of 2 hours. In panel A, lane 1 shows that p53 was unphosphorylated at serine 15 in untreated BT cells. Lanes 2 through 5 show p53 phosphorylation at this site increased over time with exposure to etoposide. Lanes 6 shows that p53 was unphosphorylated at serine 15 in untreated L3 cells. Lanes 7 through 10 show that the increase in p53 phosphorylation is delayed in the L3 cell line. Panel B shows similar results in the C3ABR and AT1ABR cell lines. Panel C shows the increase in p53 serine 15 phosphorylation based on the quantified data.

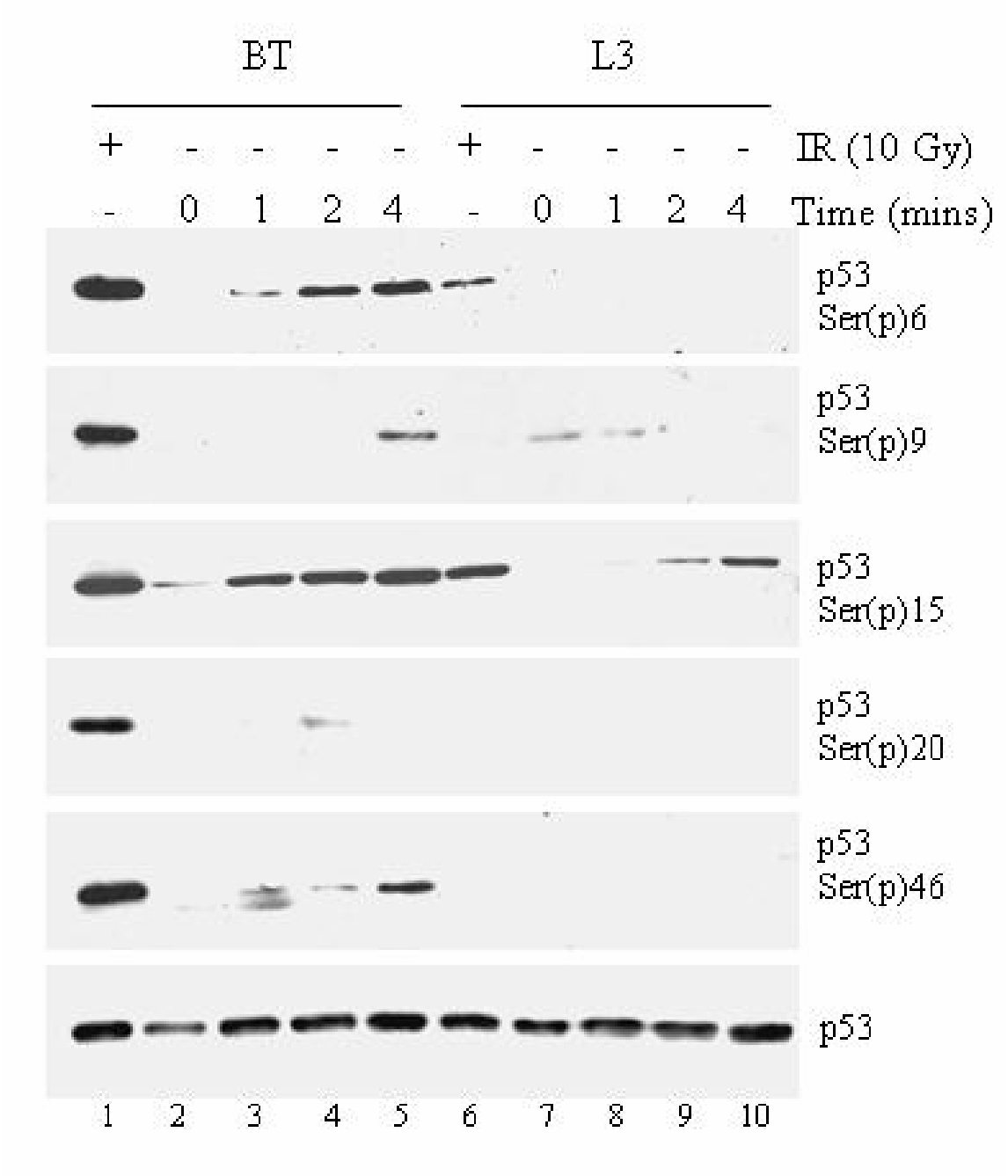

FIGURE 3.17: Time course of phosphorylation of the ATM downstream effector p53 at other serine residues in response to etoposide. BT, L3, C3ABR and AT1ABR cells were exposed to 0.8 μM of etoposide over a time course of 4 hours. Lane 1 and 6 represent cells treated with 10 Gy of IR and harvested 60 minutes later. Lanes 2 through 5 represent BT extracts of cells treated with etoposide for an increasing period of time. Lanes 6 through 10 represent L3 cell extracts treated with etoposide for an increasing period of time.

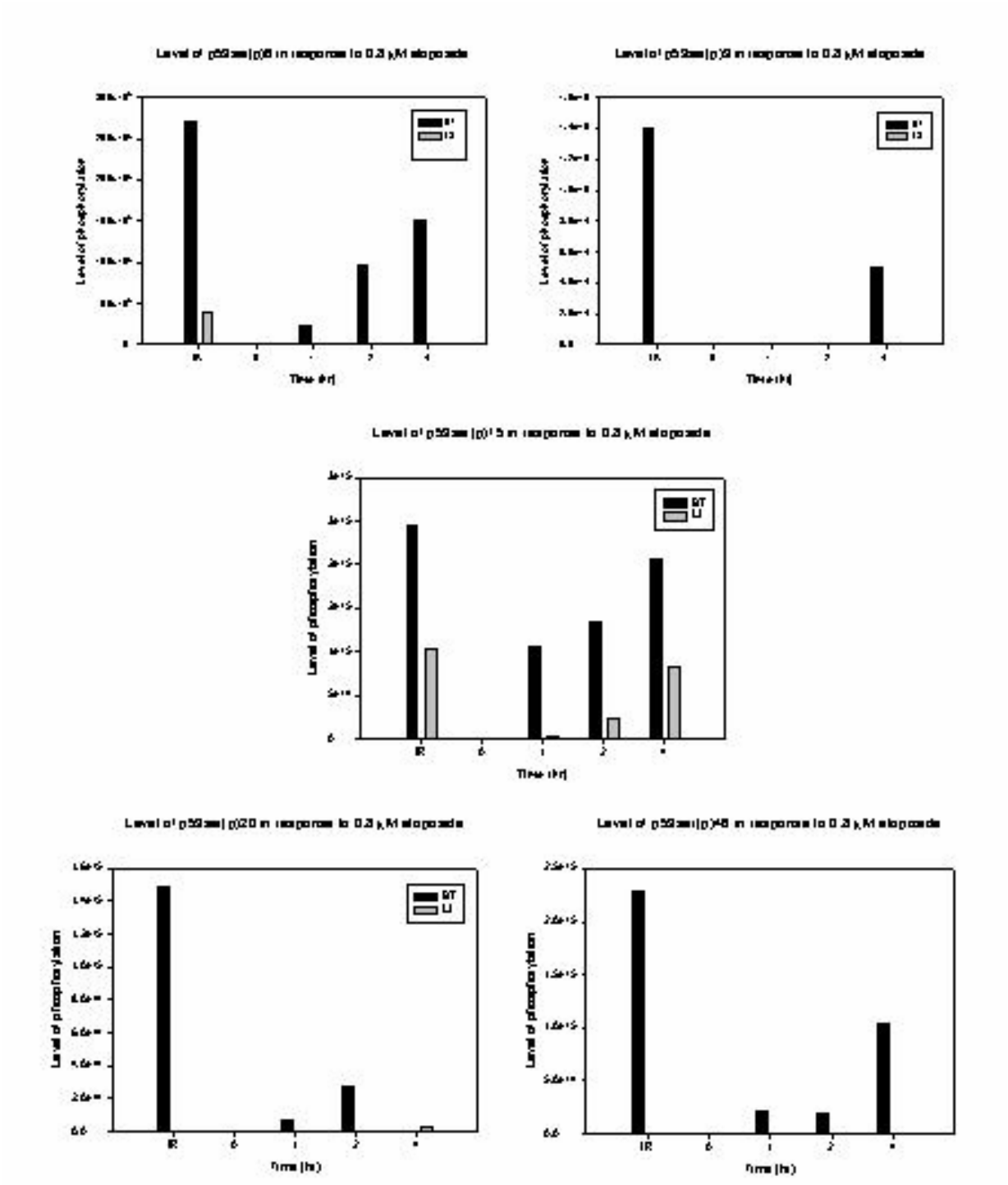

FIGURE 3.18: Quantified time course of phosphorylation of the ATM downstream effector p53 at other serine residues in response to etoposide. The panels indicate the quantified results presented in figure 3.17.

15 immunoblot confirmed the results obtain in the previous set of experiments (see figure 3.16). The serine 20 immunoblot suggests that this site is not phosphorylated in response to 0.8 μM etoposide. Lanes 2 and 7 show that serine 46 is unphosphorylated in untreated BT and L3 cells, respectively. BT cells show an increase in phosphorylation at this site in response to a low dose of etoposide. Lanes 6 through 10 show that ATM is required for phosphorylation of p53 at this site in response to both IR and etoposide. Figure 3.18 represents the increase in the phosphorylation at individual p53 sites based on the quantified data.

3.4 Activation of p53 binding ability in response to etoposide

The transcriptional activation of p53 can be analysed by examining its ability to bind to a synthetic oligonucleotide containing its specific DNA binding concensus, this has been demonstrated following treatment with IR (described in Woo *et al*, 1998). Briefly, nuclear extracts of drug treated cells were incubated with approximately 10 fmoles of 5' ^{32}P labelled oligonucleotide. Samples were incubated and loaded on a prerun, nondenaturing polyacrylamide gel as described previously (Ye et al, 2001). The gel was exposed to X-ray film with intensifying screens overnight at –80^{o}C.

In figure 3.19, BT and L3 cells were treated with 0, 0.5, 1 or 50 μM etoposide. The nuclear fractions of cell extracts were assayed for p53 binding ability to its consensus sequence. This figure shows a dose dependent increase of p53 binding in response to etoposide. Lane 1 shows the position of free probe. Lane 2 shows low p53 binding in the absence of etoposide in BT cells, while lanes 3 through 5 show increased binding in response to etoposide concentration. Lane 6 shows low p53 binding in the absence of

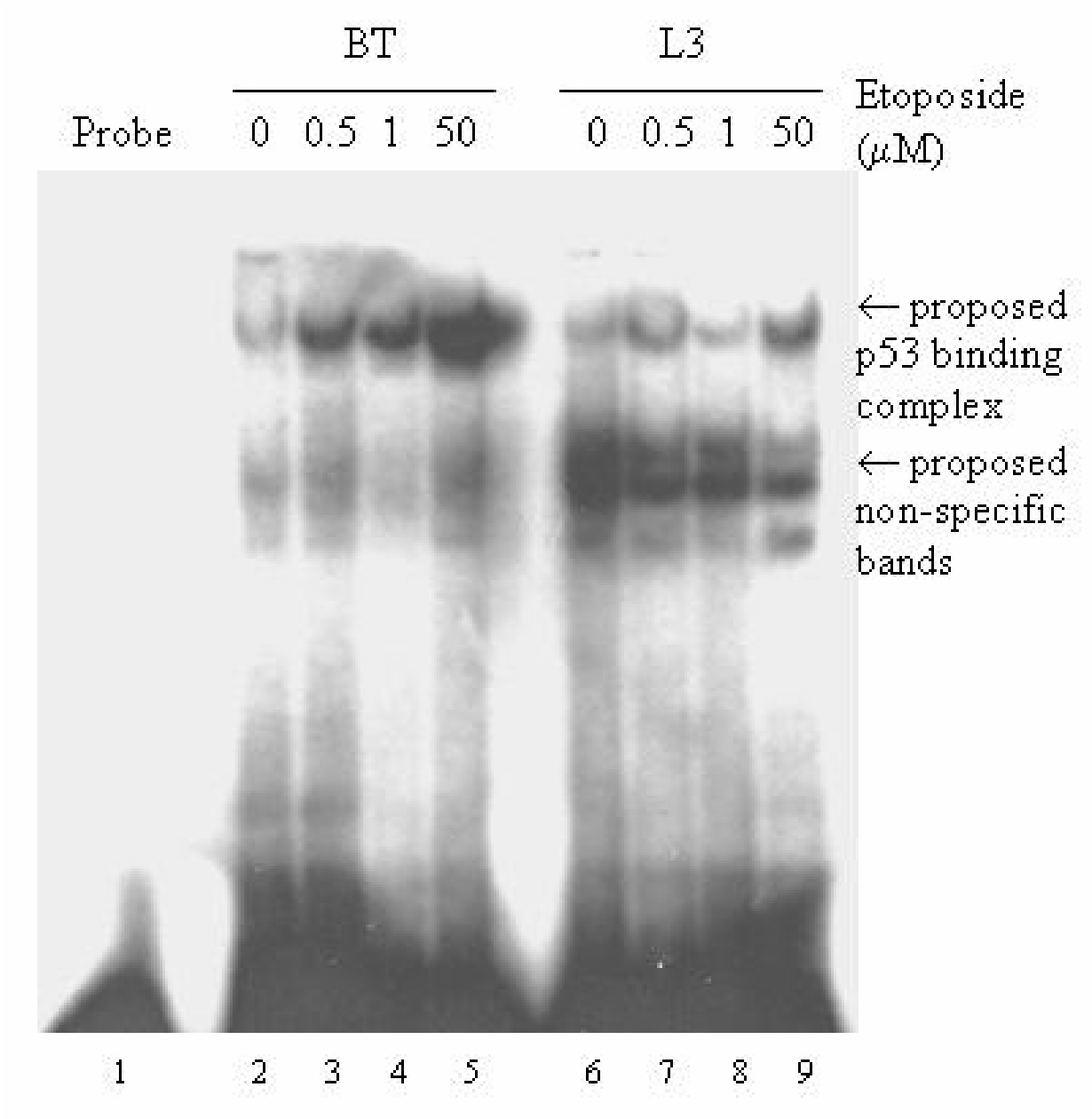

FIGURE 3.19: Enhanced binding of p53 to its cognate DNA binding sequence in etoposide-treated cells. BT and L3 cells were treated with 0, 1, 5, 50 μM etoposide or with 0.8μM etoposide in a 2 hr time course. The nuclear fractions of cell extracts were assayed for p53 binding ability to its consensus sequence. This experiment shows a dose dependent increase of p53 binding in response to etoposide. Lane 1 shows the position of free probe. Lane 2 shows a low level of p53 binding in the absence of etoposide in BT cells, while lanes 3 through 5 show increased binding in response to etoposide concentration. Lane 6 shows no p53 binding in the absence of etoposide in L3 cells, while lanes 7 through 9 show increased binding in response to etoposide concentration which is lower than that observed in BT cells.

etoposide in L3 cells, while lanes 7 through 9 show increased binding in response to etoposide concentration which is less pronounced than that observed in BT cells.

3.5 Investigating the role of other PIKKs

ATM, ATR, hSMG-1/ATX and DNA-PKcs have all been shown to phosphorylate p53 on serine 15 either *in vivo* or *in vitro*. Since our experiments determined that ATM does not exclusively phosphorylate p53 at this site in response to etoposide, we speculated that other PIKK family members may be involved in this event. Therefore, two approaches were used to investigate the role of other family members. In the first, the PIKK inhibitors caffeine and wortmannin were used to see if the phosphorylation at serine 15 could be reduced after pretreatment with these compounds before exposure to etoposide. In the second, DNA-PKcs positive and negative cell lines were used to investigate the levels of phosphorylation at this site following exposure to etoposide.

3.5.1 Effect of PIKK Inhibitors on phosphorylation of p53 at serine 15

In figure 3.20, BT, L3, C3ABR and AT1ABR cells were pretreated for 30 mins with 0, 1, 2, 4, 5 mM of caffeine. The cells were then exposed to 0.8 μM etoposide for 2 hours. In panel A, lanes 1 and 7 shows that p53 showed a basal level of phosphorylation in untreated BT and L3 cells, respectively. Lanes 2 and 8 show the levels of serine 15 phosphorylation after exposure to 0.8 μM etoposide in BT and L3 cells, respectively. In both cases, this level was decreased with increasing concentrations of caffeine. This is represented in lanes 3 through 6 in BT cells and lanes 9 through 12 in L3 cells. C3ABR and AT1ABR cells showed a lower level of basal phosphorylation on serine 15. Otherwise, Panel B shows similar results in these two cell lines

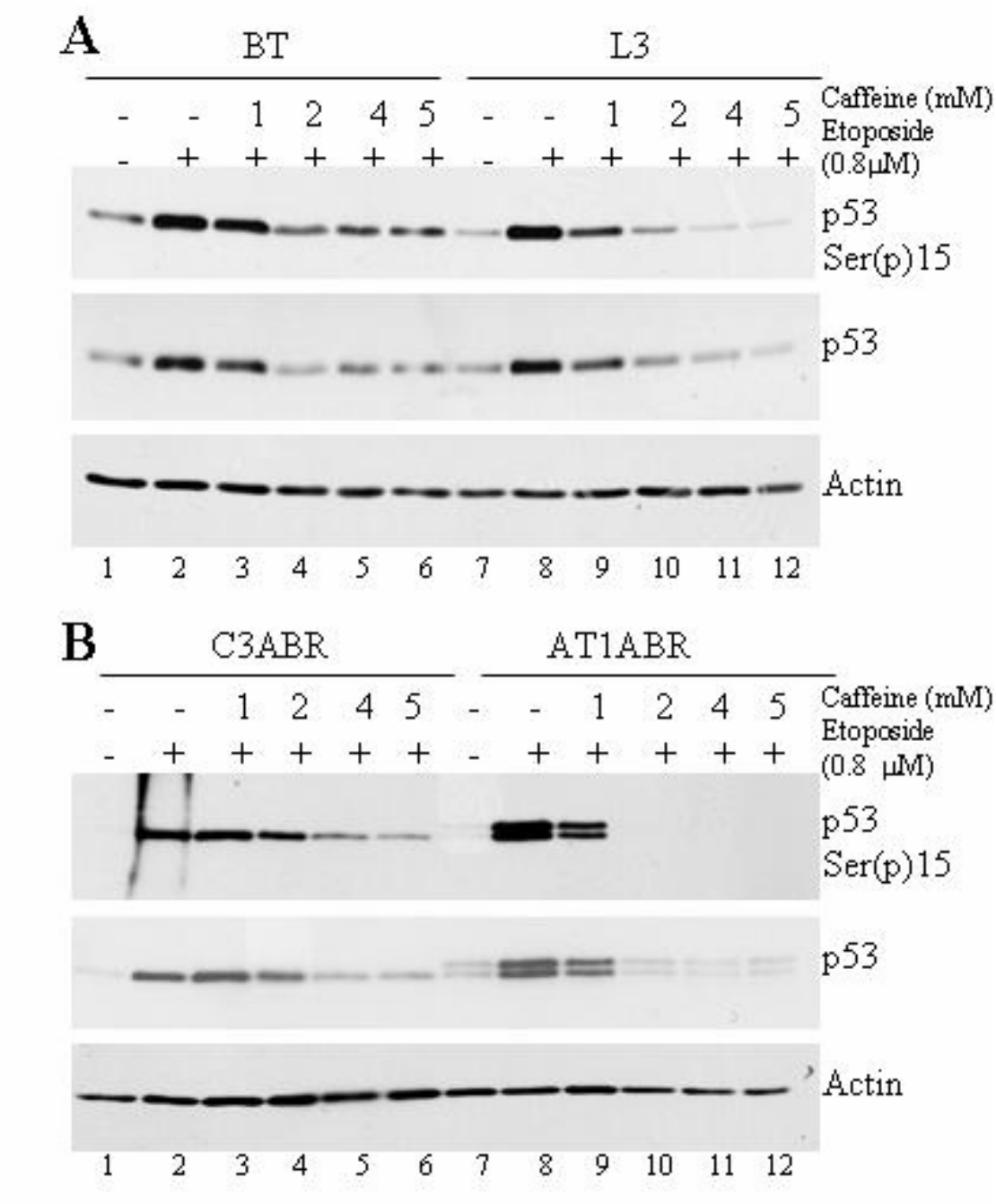

FIGURE 3.20: Inhibition by caffeine. BT, L3, C3ABR and AT1ABR cells were pretreated for 30 mins with 0,1, 2, 4, 5 mM caffeine. The cells were then exposed to 0.8 μM of etoposide for 2 hours. In panel A, Lanes 1 and 7 represent untreated cells. Lanes 2 and 8 represent cells treated with etoposide only. Lanes 3 through 6 represent BT cells treated with increasing concentrations of caffeine. Lanes 9 through 12 represent the same conditions in L3 cells. Panel B shows similar results in the C3ABR and AT1ABR cell lines.

In figure 3.21, BT, L3, C3ABR and AT1ABR cells were pretreated for 30 mins with 0, 5, 10, 20, 40 μM of wortmannin, followed by a 2 hour exposure to 0.8 μM etoposide. Similar results were obtained by inhibiting the etoposide induced phosphorylation of serine 15 by wortmannin as were obtained with caffeine. An increasing concentration of wortmannin resulted in a decrease in this phosphorylation at this site. Panel A demonstrates this in BT and L3 cells while panel B shows similar results in the C3ABR and AT1ABR cell lines.

3.5.2 *Investigating the role of DNA-PK in phosphorylation of p53 at serine 15*

Since both caffeine and wortmannin inhibited the phosphorylation at this site, it is likely to be the result of another PIKK family member. To determine the contribution of DNA-PKcs in this phosphorylation event, M059K and M059J cells were used to investigate the effect of treatment with increasing doses of etoposide and a time course of a low dose treatment (0.8 μM). In short, M059K and M059J cells were treated with 0, 1, 5, 10 μM of etoposide for 2 hours or, with 0.8 μM of etoposide over a two hour time course. WCEs were prepared in NET-N buffer. Immunoblots from 30 μg of WCE were probed for p53 serine 15, stripped/reprobed for total p53 and stripped/reprobed for actin. Results are presented in Figure 3.22. Panel A shows a dose-dependent increase in phosphorylation at this site in response to etoposide (lanes 1 though 4). Lanes 5 through 8 show that the level of phosphorylation was comparable in a DNA-PKcs negative background, indicating this protein is not required for this response. Panel B shows that in response to a low dose of etoposide, DNA-PKcs is not required for phosphorylation of p53 on serine 15. The DNA-PKcs positive cells (lanes 1 through 4) and the DNA-PKcs negative cells (lanes 5 through

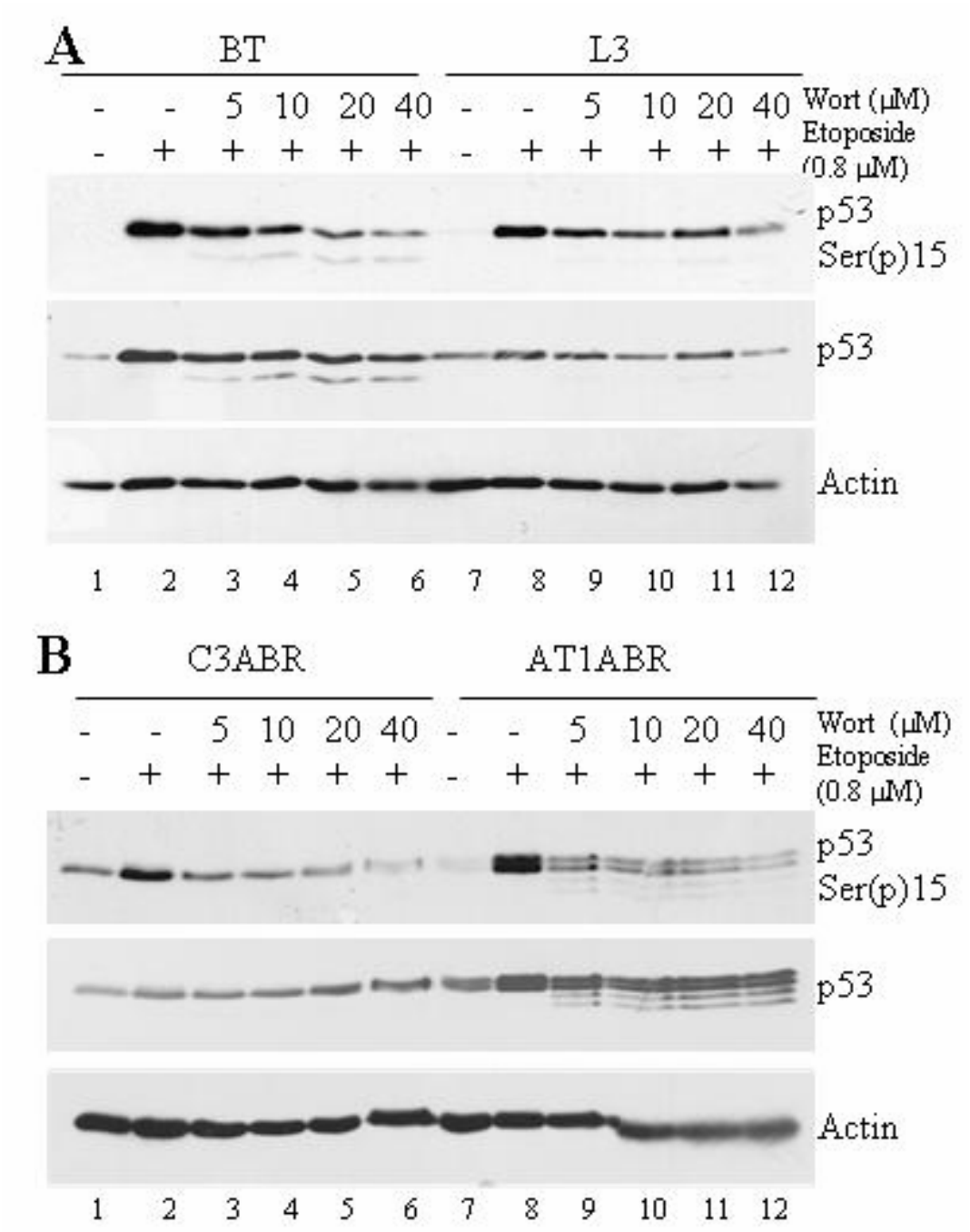

FIGURE 3.21: Inhibition by wortmannin. BT, L3, C3ABR and AT1ABR cells were pretreated for 30 mins with 0, 10, 20 μM wortmannin. The cells were then exposed to 0.8 μM etoposide for 2 hours. In panel A, Lanes 1 and 7 represent untreated cells. Lanes 2 and 8 represent cells treated with etoposide only. Lanes 3 through 6 represent BT cells treated with increasing concentrations of caffeine. Lanes 9 through 12 represent the same conditions in L3 cells. Panel B shows similar results in the C3ABR and AT1ABR cell lines.

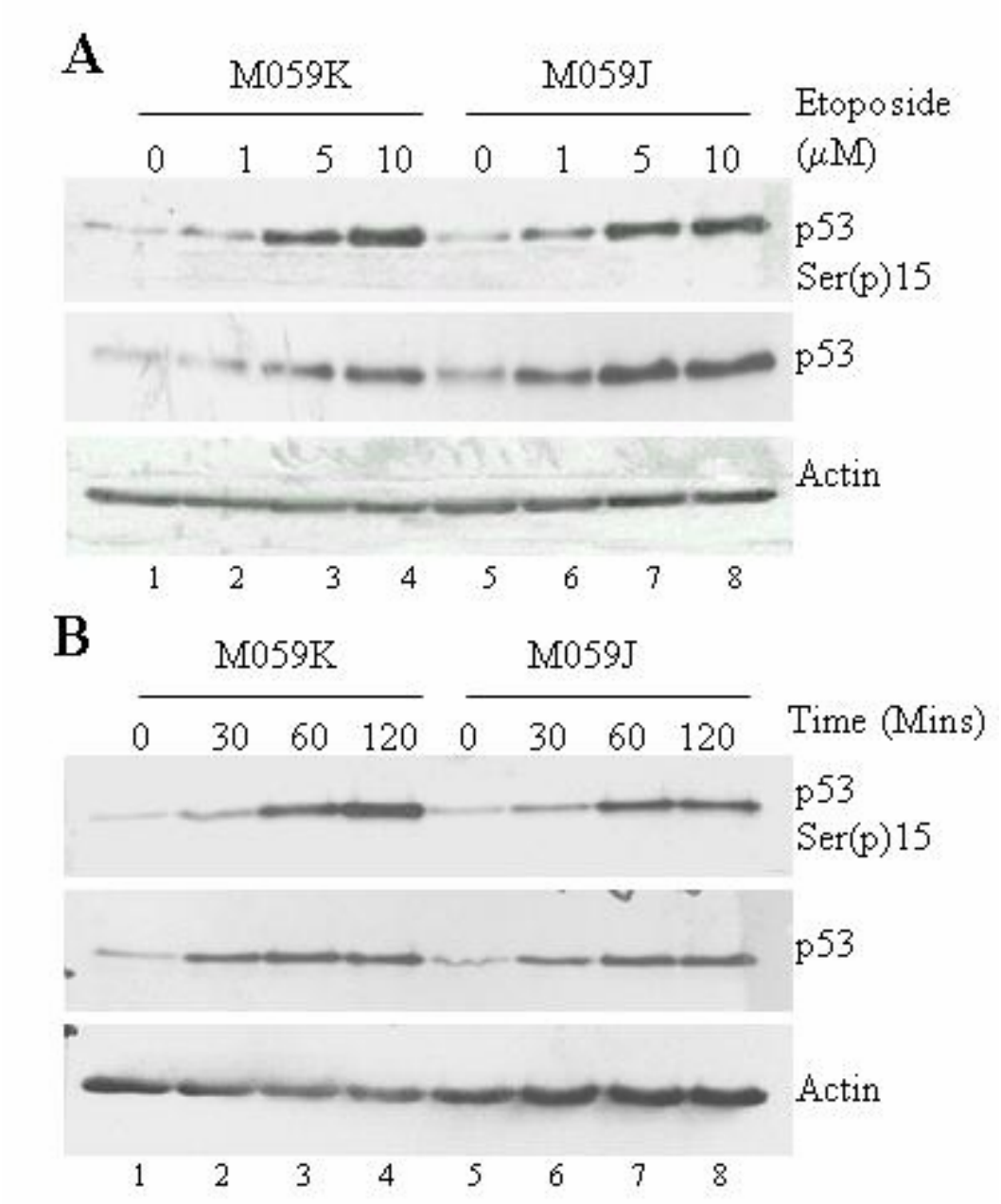

FIGURE 3.22: Phosphorylation of p53 serine 15 in DNA-PKcs deficient cells. In panel A, M059K and M059J cells were were exposed to 0, 1, 5, 10 μM etoposide for 2 hours. Each lane represents 60 μg of a NET-N WCE. In panel A, lanes 1 through 5 represent M058K extracts of cells treated with increasing concentrations of etoposide. Lanes 5 through 10 represent M059J cell extracts treated with increasing concentrations of etoposide. Panel B shows cells which were exposed to 0.8 μM etoposide over a time course of 2 hours. Lanes 1 through 4 represents M059K cell extracts treated with etoposide for an increasing period of time. Lanes 5 through 8 represent M059J cell extracts treated with etoposide for an increasing period of time.

8) showed a comparable increase in the phosphorylation at this site over a 2 hour time course.

SECTION IV : DISCUSSION

4.1 Summary of findings

The results presented in the previous section served to show the effects of etoposide on the activation of different components of the DNA damage response. The experiments performed demonstrated that ATM was phosphorylated at serine 1981 in responses to doses as low as 0.8 μM within 30 minutes (Figure 3.3). Furthermore, treatment of cells with 0.8 μM etoposide was shown to result in increased protein kinase activity of ATM towards the *in vitro* PHAS-I substrate.

Subsequent experiments showed that several of the components of the DNA DSB signaling pathway were phosphorylated in response to etoposide treatments. These phosphorylation events include: (1) p53 on serines 6, 9, 15 and 46, (2) Nbs1 on serine 343, (3) Chk1 on serine 345, (4) Chk2 on threonine 68 and, (5) SMC1 on serine 957. The role of ATM in each of these phosphorylation events was also examined. ATM was found to be required for the phosphorylation of: (1) p53 on serines 6, 9, and 46, (2) Chk2 on threonine 68 and, (3) SMC1 on serine 957. The phosphorylation of p53 on serines 15 and of Nbs1 on serine 343 both showed reduced levels of phosphorylation in ATM negative cell lines while the phosphorylation of Chk1 was unaffacted in the absence of ATM.

Further investigations indicated that the phophorylation of p53 on serine 15 in response to etoposide was sensitive to both caffeine and wortmannin treatments, however did not require the presence of DNA-PKcs. Furthermore, etoposide incressed p53's ability to bind to its concensus sequence *in vitro*.

4.2 Limitations of cell line models used in this study

The cell lines most often used for these experiments were lymphoblastoid transformed cell lines derived from A-T patients (L3 and AT1ABR) or normal controls (BT and C3ABR) (Figure 3.1). Since these cell lines are age and gender matched but originate from different individuals, they are not isogenic. Therefore, it is conceivable that the effect observed in ATM-deficient cells could be due to some other defect present in these cells. Consequently, to justify the results obtained in these experiments, two sets of cell lines are used. It is relatively unlikely that a "false" result would appear in both pairs of cell lines. However, these cell lines remain Epstein-Barr transformed cell lines and may potentially affect the results. In order to confirm that results obtained are not specific to Epstein-Barr transformation, the SV-40 transformed fibroblasts GM0637 (ATM+/+) and GM05849 (ATM-/-) (Hahn *et al*, 1987) cell lines could be used for experiments that do not involve p53, since SV-40 transformation inactivates p53 (Sarnow *et al*, 1982). However, under ideal conditions, the experiments should be performed in primary cell cultures from A-T patients. Alternatively, the GM05823 cell line, which is the untransformed parental fibroblast cell line of GM05849 (Nagasawa *et al*, 1987), is also available from the Coriell institute. Instead of using isogenic cell lines, levels of the ATM protein could be knocked-down using an RNA interference (RNAi) method. However, this must be used with caution since these experiments generally result only in a partial knock down in protein expression. Alternatively, kinase dead ATM could be ectopically expressed in A-T cells.

The M059J cell line was used in this study in part because it is the only known human DNA-PKcs negative cell line (Lees-Miller *et al*, 1995). It was used in conjunction with the M059K cell line (Figure 3.1), which although isolated from the same malignant glioma, was shown not to be isogenic, notably as to its ATM status (Tsuchida *et al*, 2002).

Due to the highly mutagenic nature of tumour tissue, it is likely that other loci are also affected. Results obtained in these cell lines must also be interpreted with caution because of the low levels of ATM they express. Effects observed should be confirmed to be DNA-PKcs-dependent and not ATM-dependent by using ATM deficient cells. Furthermore, this model also remains an Epstein-Barr transformed cell line model. These models are not ideal since the specific effects of transformation with oncogenic viruses in these cells, is unknown. Alternatively, DNA-PKcs could be expressed in a DNA-PKcs negative cell line. This has previously been done using the V3 hamster cell line (Ding *et al*, 2003).

4.3 ATM is activated by the topoisomerase II inhibitor etoposide

ATM has been reported to be maximally phosphorylated at serine 1981 quickly after very low dose exposure to IR. Half a Gy of IR causes maximal serine 1981 phosphorylation within 5 minutes (Bakkenist and Kastan, 2003). Furthermore, several other agents (both DNA-damaging and non DNA-damaging) have been shown to cause ATM phosphorylation at serine 1981 and to stimulate ATM kinase activity (reviewed in Kurz and Lees-Miller, 2004). Our laboratory has demonstrated that other topoisomerase inhibiting/antineoplastic compounds cause phosphorylation at serine 1981 of ATM. These include: (1) the topo II inhibitor, doxorubicin and, (2) the topo I inhibitor, camptothecin (Kurz and Less-Miller, 2004). For these reasons, we predicted that the topo II inhibitor etoposide would stimulate phosphorylation of ATM at this site. Therefore, we were interested in investigating whether or not etoposide caused ATM phosphorylation as well as, the dose and time-dependence of this event.

Customarily, studies with etoposide use a relatively high dose of this drug, 50 μM or higher (Burma *et al*, 2001; Ye *et al*, 2001). Since a study in our lab demonstrated that 68

μM of etoposide caused ATM-independent phosphorylation of p53 on serine 15 (Ye *et al*, 2001), we were interested in investigating lower/less cytotoxic doses of etoposide. We speculated that at higher doses cells were probably going through cell death pathways, while lower doses may initiate ATM-dependent cell cycle arrest to allow for DNA repair. This hypothesis should be tested by performing PARP-cleavage or TUNEL assays to assess for apoptosis in response to a concentration range of etoposide. Therefore, the first step was to look at a concentration range of etoposide to determine concentrations required to cause ATM phosphorylation at serine 1981. Concentrations were chosen between 1 and 50 μM etoposide. Cell treatments with the chosen concentrations were performed for 2 hours. This represents a time point which I found provides the detection of a good signal for phosphorylation of ATM substrates in ATM-dependent responses. Based on this experiment I was able to determine that ATM is phosphorylated on serine 1981 by cell treatments with concentrations as low as 1 μM etoposide for 2 hours (Figure 3.2). Furthermore, this response appears to be maximal at this low concentration.

Our next interest lay in the DNA damage response elicited by a low dose of etoposide. Therefore, a two hour time course of exposure to a low dose of etoposide (0.8 μM) was performed. The 2 hour time course was chosen for the same reasons as stated above. The immunoblot results indicated that most of the ATM phosphorylation on serine 1981 occurs within the first 30 minutes (Figure 3.3a and b). However, the quantified data indicates there may be a slight increase in phosphorylation up to 2 hours (Figure 3.3c). It would be of interest to investigate lower concentrations and a time course within 30 minutes to determine the minimal requirements for phosphorylation of ATM at serine 1981.

Bakkenist and Kastan showed that ATM with a serine to alanine mutation at serine 1981 failed to phosphorylate p53 at serine 15 *in vivo* or, to promote cell cycle arrest in

response to IR. This finding suggests that phosphorylation at serine 1981 is critical for ATM function. However, they also showed that the ATM protein containing a mutation at this site retains its kinase activity. Thus, no direct evidence was provided showing that ATM phosphorylation at this site corresponded directly to an increase in ATM kinase activity. For this reason, we chose to investigate the effect of etoposide on ATM *in vitro* kinase activity as described by Canman *et al*. Furthermore, this method and variations thereof have shown that ATM kinase activity is increased by treatment with several different compounds (reviewed in Kurz and Lees-Miller, 2004). Ionising radiation, radiomimetic compounds, alkylating agents, bioflavonoids, peroxide compounds and the DNA cross-linking agent chromium have all been shown to increase ATM kinase activity. On the other hand, the topoisomerase poisons have not been shown to do so. However, since we observed ATM phosphorylation at serine 1981 at a low dose of etoposide, we hypothesized that this same dose would stimulate ATM kinase activity in a similar time course as serine 1981 phosphorylation.

We tested this hypothesis by looking at the immunoprecipitated ATM kinase activity towards PHAS-I after treatment with the same low dose of etoposide. Based on the previous experiment, ATM phosphorylation at serine 1981 appears to be maximal at 60 minutes. For this reason, this experiment was performed over the course of 60 minutes. The results presented showed that the *in vitro* ATM kinase activity was stimulated by 0.8 μM of etoposide after a 30 minute exposure (Figure 3.4). However, the difference observed in this assay showed an increase in kinase activity between 30 and 60 minutes while ATM phosphorylation appeared almost maximal by 60 minutes. This suggests that the phosphorylation of ATM at serine 1981 may precede its kinase activation in response to etoposide. This should be addressed by performing the immunoprecipitation-kinase assay

on PHAS-I simultaneously with an immunoblot for ATM phosphorylation at serine 1981. This would also provide a control for the amount of ATM immunoprecipitated under the assay conditions used.

4.4 Chk2 and SMC1 are phosphorylated in an ATM-dependent manner in response to etoposide

Two IR-induced, ATM-dependent, phosphorylation sites have been identified in SMC1, serines 957 and 966. Cell treated with other agents such as UV or HU, showed phosphorylation at these sites in both ATM-positive and ATM-negative cell lines. This suggests that ATM is not required for phosphorylation at these sites in response to some types of DNA damage or replication blocks (Kim *et al*, 2002). Therefore, it was of interest to investigate whether or not serine 957 was phosphorylated in response to etoposide, as well as, determine if this occurred in an ATM-dependent manner. This provides an interesting model to help decipher how etoposide induced damage is recognised in the cell: (1) as a DSB (IR induced damage), (2) as a replication block (HU induced damage), or (3) as a bulky lesion (UV induced damage). Because of it mode of action, it is conceivable that etoposide may act as any of the three fore-mentioned types of damage. First, etoposide is known to cause DSBs in DNA. Alternatively, since etoposide stabilises the cleavage/religation complex of topo II, it can act as a replication block when DNA processing enzymes encounter it and thus, be recognized as such. Finally, the larger topo II molecule bound to DNA with altered kinetics may resemble a bulky adduct on the DNA molecule. For these reasons, we were interested in investigating whether or not etoposide induced SMC1 phosphorylation, the ATM-dependence of phosphorylation at this site, as well as the time and dose dependence of this event.

The experiments conducted to look at SMC1 phosphorylation (as well as other ATM substrates) used the same concentrations and time course presented for ATM phosphorylation at serine 1981. The concentration study (Figure 3.6), indicates that phosphorylation at serine 957 of SMC1 is severely impaired in responses to etoposide doses below 50 μM in ATM cells. This suggests that this phosphorylation event is dependent on ATM status. At the higher dose, a low level of phosphorylation suggests there exists a redundant pathway for phosphorylation at this site. The time course experiment demonstrates a similar result. Treated with 0.8 μM of etoposide, cells lacking ATM failed to phosphorylate SMC1 (Figure 3.7). These results provide the first line of evidence that DSB incurred as a result of etoposide treatment may be recognised by similar pathways as those produced by IR.

SMC1 phosphorylation by ATM has been shown to be involved in the intra-S-phase checkpoint (Kim *et* al, 2004). Furthermore, cells over-expressing SMC1 with a serine to alanine mutation at ATM phosphorylation sites act in a dominant negative manner (Kim *et al*, 2002). It would be interesting to see if these cells displayed intra-S-phase arrest defect in response to similar treatments with etoposide. It would also be of interest to investigate the kinetics of phosphorylation at serine 966, to determine if the two sites provide a distinction between different types of damage.

Similarly to SMC1, Chk2 phosphorylation on threonine 68 is ATM-dependent in response to IR but ATM-independent in response to UV radiation or HU-induced replication blocks (Matsuoka *et al*, 2000). Therefore, we were interested in investigating whether or not etoposide induces Chk2 phosphorylation, the ATM-dependence of phosphorylation at this site, as well as the time and dose dependence of this event. Furthermore, it also provides and interesting model to study the type of DNA damage

detection pathways required for etoposide induced damage. In our study, similar results were observed for Chk2 phosphorylation at threonine 68 and SMC1 phosphorylation at serine 957. We found Chk2 phosphorylation to be impaired in ATM negative cells at all concentrations tested (Figure 3.12a and b). Higher concentrations also appeared to have redundant pathways responsible for phosphorylating this site. Time course experiments also indicated that ATM was required for the phosphorylation of Chk2 threonine 68 (Figure 3.13). These results also lead to believe that the detection of DSBs produced by etoposide activates similar pathways as IR.

4.5 Redundant pathways likely exist for the phosphorylation of p53 and NBS1

p53 is well recognized as a nodal point in the DNA damage response. Furthermore, serine 15 is well established as a DNA damage induced phosphorylation site. As previously mentioned, this site has been shown to require ATM and ATR in response to IR and UV, respectively. Therefore, it was of interest to investigate whether or not this site required ATM for its phosphorylation. This would provide insight into the type of damage being recognised by the cell in response to etoposide. The results obtained in this study indicate that ATM is not absolutely required for p53 phosphorylation at this site (Figure 3.16). However, the response is delayed and phosphorylation occurs 2 hours after incubation with etoposide. This suggests that ATM could be responsible for the "early" response to etoposide-induced damage, while another protein kinase can phosphorylated this site at later times. This would suggest that there either exists a redundant pathway for phosphorylation at this site, or alternatively, that the damage induced by etoposide may be recognised by respective kinases as DSBs and "bulky" lesions.

A similar situation was observed for the phosphorylation of NBS1. As previously mentioned, the phosphorylation of NBS1 on serine 343 is important for intra-S-phase arrest in response to IR-induced DNA damage. Therefore, it was of interest to determine whether etoposide-induced damage also caused phosphorylation at this site. The results obtained indicate that the phosphorylation at this site is also delayed in the absence of ATM (Figure 3.7). Similarly to p53, this suggests that the type of damage may be recognised by several protein kinases or there exists a redundant pathway. It would be of interest to examine whether or not the lack of phosphorylation at this site impairs the ability of these cells to undergo intra-S-phase arrest.

4.6 Chk1 and H2AX are not phosphorylated in an ATM-dependent manner in response to etoposide

It was long believed that the ATM-Chk2 and ATR-Chk1 pathways existed in parallel. ATM-Chk2 was activated in response to IR-induced DNA damage while the ATR-Chk1 pathway was activated in response to UV radiation induced damage and replication blocks. However, as previously mentioned, this dogma was challenged in a set of studies showing that Chk1 was phosphorylated in an ATM-dependent manner at two serine residues, serine 317 and serine 345 (Gatei *et al*, 2003; Sapkota *et al*, 2002). More recently, an exclusive role has been attributed for the ATM-Chk1 pathway (but not ATM-Chk2). It is implicated in the phosphorylation of Tousled like kinases (Tlks) which are required for intra-S-phase arrest (Groth *et al*, 2003). We determined that the presence of etoposide was being signaled through an ATM-Chk2 pathway. Considering both pathways are, in some cases, not mutually exclusive, we wanted to determine if Chk1 was phosphorylated in response to etoposide and determine if this phosphorylation event

requires ATM. The results obtained in these experiments showed that Chk1 was phosphorylated on serine 345. However, Chk1 was equally phosphorylated in the presence and absence of ATM, indicating it is not the kinase responsible for phosphorylation at this site (Figure 3.15). We speculate that, phosphorylation of Chk1 at this site is ATR-dependent. In order to address this, cells expressing a kinase-dead ATR or an ATR directed siRNA will need to be treated with etoposide under similar conditions.

As previously mentioned, diverse sources of DSBs result in the phosphorylation of H2AX at serine 139. Furthermore, this event has been shown to be ATM-dependent in response to IR and the topo II inhibitor genistein (Ye *et al*, 2004). Therefore, we hypothesized that the DSBs induced by etoposide would cause the phosphorylation of H2AX. Our results indicate that phosphorylation at this site occurs only at high concentrations of etoposide (50 μM), in an ATM-independent manner (Figure 3.4). This is the first result presented which indicates that the signaling pathways activated in response to low doses of etoposide are different from those activated by IR. This may indicate that the DSBs induced by etoposide are somehow distinct from those produced by IR, or alternatively, that the DNA damage caused is more readily recognized as a bulky lesion or replication block. This result should be followed up by looking at H2AX foci formation in response to etoposide. This is a more powerful technique to look at this phosphorylation event.

4.7 Etoposide causes multisite phosphorylation of p53 and induces increased binding ability

In response to IR-induced DNA damage, the tumour suppressor p53 is phosphorylated on 7 serine residues in the first 50 a.a.s of its N-terminal end. It has been

suggested that particular phosphorylation events may contribute to specific downstream transcriptional activation or repression events (Saito *et al*, 2002; Dumaz *et al*, 2001; Jabbur *et al*, 2000). ATM has been shown to play a role in the phosphorylation of several of these sites. It is thought to phosphorylate serine 15 directly *in vivo* (Banin *et al*, 1998; Canman *et al*, 1998) and through Chk2 on serine 20 (Chehab *et al*, 1999; Hirao *et al*, 2000). In addition, ATM is absolutely required for the phosphorylation of p53 on serine 46 (Saito *et al*, 2002). In response to etoposide, p53 phosphorylation on serine 15 has been demonstrated by us and others (Ye *et al*, 2001; Karpinich *et al*, 2002; Ding *et al*, 2003). The time course and dose dependence of this event in response to etoposide were demonstrated in this study (as described in section 3.3.6). However, the phosphorylation of other N-terminal p53 sites in response to etoposide, as well as the potential role of ATM in these phosphorylation events still required further investigation. Therefore, we hypothesised that etoposide would cause multisite phosphorylation of p53 and that ATM likely plays a role in the phosphorylation of these sites.

Several of the phosphorylation sites examined in response to etoposide showed a lower level of phosphorylation than that observed in IR-treated cells. IR-treated cells showed phosphorylation at serine 6, 9, 15, 20 and 46, 2 hours after treatment with 10 Gy of IR. However, treatment with 0.8 μM of etoposide only resulted in 2 sites with comparable levels of phosphorylation after 2 hours (Figure 3.17). Serines 6 and 15 were both shown to be phosphorylated at 1 hour with an increase up to 4 hours. This may suggests these sites play an important role in the early signaling of etoposide-induced DNA damage. Meanwhile, serine 9 and 46 were phosphorylated to a much lesser extent, indicating they may not be required for early events following etoposide treatment. It could be suggested that phosphorylation on serine 6 and 15 are a prerequisite for the phosphorylation of other

sites. In order to test this hypothesis, serine to alanine mutations could be made at individual sites to determine if there is a "hierarchical" order of phosphorylation in response to etoposide. Of the sites phosphorylated in response to etoposide treatment, only serine 15 and 46 have suggested roles. Serine 15 has been shown to be implicated in transcription activation (Shieh *et al*, 1997) and, in its absence increased apoptosis is observed (Unger *et al*, 1999a), while serine 46 has been shown to be required for apoptosis (Oda *et al*, 2000). No roles have been elucidated for the phosphorylation at serines 6 and 9. The proposed mutation experiments would also be interesting to evaluate the function of these individual sites in cell cycle arrest and apoptosis after etoposide treatments. Interestingly, etoposide does not appear to cause phosphorylation on serine 20, a site associated with stabilisation in response to DNA damage (Chehab *et al*, 1999; Unger *at al*, 1999b). However, our experiments show an increase in p53 levels in response to etoposide suggesting it is being stabilised (Figure 3.15, 3.16, 3.17).

Since p53 was being stabilised, we speculated that its transcriptional activity was also stimulated by etoposide. Therefore, we hypothesised that etoposide would increase p53 ability to bind to its consensus sequence *in vitro* (described in section 2.7), a standard method to indicate that transcriptional activity may be activated *in vivo*. Furthermore, we wanted to investigate whether or not this was an ATM-dependent event. This hypothesis was supported by findings from our lab which suggest that the topo II inhibitors genistein and doxorubicin have the ability to increase p53 binding towards its consensus sequence and that ATM was required for this to occur (Ye *et al*, 2001; Kurz and *et al*, 2004). The results presented in this study suggest that etoposide does increase p53's ability to bind to its consensus sequence (Figure 3.18). Moreover, ATM appears to be involved but not

absolutely required for this response, suggesting that a redundant pathway exists for the activation of p53 binding ability.

The experiment presented above would largely benefit from additional controls. In order to confirm the identity of the p53 DNA binding complex, a p53 supershift using the pAb1801 (Santa Cruz, Cat # SC-98) could be used to visualise a larger complex. In addition, since these experiments are performed in the presence of pAb421, removal of this antibody should result in the disappearance of the p53 DNA binding complex. The figure presented here has additional complexes forming with greater mobility than the p53 complex. We speculate that these complexes represent Ku binding to free DNA ends. To confirm this suspicion, a supershift should be performed using a Ku antibody. Alternatively, experiments could be performed in Ku negative cell lines. Electromobility shift assays have additional limitations; they represent a very "artificial" *in vitro* situation. Therefore, ideally, this experiment should be performed using a transcriptional reporter assay.

Multisite phosphorylation of transcription factors is being established as a "fine tuning" mechanism for their activity (Holmberg *et al*, 2002). Mechanisms of cooperative and sequential phosphorylation have also been suggested for transcription factors without necessarily understanding the implications of these mechanisms. The experiments performed in this study can provide valuable information towards the role of multisite phosphorylation in transcription factors.

4.8 Other PIKK family members likely contribute to p53 phosphorylation on serine 15

Four members of the PIKK family of protein kinases have been shown to phosphorylated p53 on serine 15, ATM, ATR and ATX/hSMG-1 *in vivo* and DNA-PKcs *in vitro* (Nakagawa *et al*, 1999; Tibbetts *et al*, 1999; Brumbaugh *et al*, 2004; Lees-Miller *et al*, 1992). Experiments in this study showed that ATM was not absolutely required for phosphorylation at this site in response to etoposide, suggesting that redundant pathways likely exist for this phosphorylation event (see section 4.4). Therefore, we hypothesised that phosphorylation on serine 15 of p53 was likely being performed by another member of the PIKK family. We were able to rule out DNA-PKcs rapidly by observing no change in the phosphorylation status at this site in M059J cells (Figure 3.22). The inhibition observed by wortmannin and caffeine indicate that PIKK family members are in fact responsible for this phosphorylation event (Figures 3.20 and 3.21). However, this method does not allow the differentiation between ATM, ATX and ATX/hSMG-1. In addition, studies performed using kinase inhibitors must be interpreted by caution. Several kinase inhibitors have been shown to be less specific than proclaimed (Davies *et al*, 2000).

It would be useful to specifically determine the kinases (there likely exist redundant pathways) involved in this phosphorylation event. The simplest way to address this question would be to use ATR or ATX/hSMG-1 negative cell lines. Unfortunately, null mutations in ATR are embryonic lethal and therefore established ATR negative cell lines do not exist. However, Seckel syndrome cell are available in culture. They have residual but markedly reduced levels of ATR (O'Driscoll *et al*, 2003). Others have also used a conditional knockout allele or a dominant-negative kinase dead mutant to study this protein (Tibbetts *et al*, 1999). Alternatively, ATR phosphorylation at this site in response to etoposide could also be studied using small interference RNA (siRNA) technology. In which case, levels of ATR are reduced in cells transfected with a vector containing the

siRNA towards ATR. The *in vitro* affinity of ATX/hSMG-1, for the p53 serine 15 sequence, has been shown to be 3.5 fold higher than ATM in response to IR (Brumbaugh *et al*, 2004). It is therefore an important candidate for the phosphorylation of this site in response to etoposide. Unfortunately, no human disease is associated with mutations in the ATX/hSMG-1 gene. Therefore, an established cell line to study its function does not exist. Studies will have to be performed using a conditional knockout allele, a dominant-negative kinase-dead mutant or, siRNA.

4.9 Distinct pathways exist to signal DSBs induced by etoposide and IR

The DNA damage induced by etoposide is complex. It is difficult to speculate how this damage will be perceived by the cell. IR and etoposide are both known to cause DSBs. However, the mechanisms by which they do so are very different. Etoposide stabilizes the cleavage/religation equilibrium of topo II causing DSBs but also several other potential "species" of DNA damage which could be processed in another fashion by the cell. The blocked topo II molecule may act to stall replication forks or, be recognised as a bulky adduct.

The first line of evidence presented in this study, the phosphorylation of ATM on serine 1981, indicates that ATM pathways are activated in response to this type of damage. This is substantiated by the increase in ATM protein kinase activity in response to etoposide. These results initially suggest the recognition of DSBs. However, both Chk1 and Chk2 are phosphorylated, indicating that the two classically described pathways (ATM-Chk2 and ATR-Chk1) are likely activated. This assumption is substantiated by the fact that Chk2 is activated in an ATM-dependent manner while Chk1 activation occurs independently from ATM. Therefore, the recognition of etoposide-induced DNA damage

activates different pathways than those observed after IR induced DNA damage. However, the ATM-dependence of Chk2 and SMC1 phosphorylation in response to etoposide indicates that there exists overlapping pathways between the response to this drug and IR. Similarly, the activation of Chk1 suggests that there is overlap with the pathway responsible for the detection of UV or HU induced DNA damage.

DNA damaging agents were originally thought to activate one of the two ATR-Chk1 or ATM-Chk2 pathways. Some of these DNA damaging agents such as irofluven, a semi-synthetic derivative of the mushroom toxin illudin S, have been shown to exclusively activate the ATM-Chk2 pathway (Wang *et al*, 2004), while other activate the ATR-Chk1 pathway. However, the study of etoposide demonstrates that it appears to activate both of these pathways.

4.10 Conclusions

The DSB is a particularly damaging lesion in the cell. DNA damaging agents used to treat neoplastic disease take advantage of this characteristic. Although these chemotherapeutic agents are widely used, the molecular mechanisms by which they activate DNA repair or cause cell death remain relatively obscure. The purpose of the studies performed here was to determine which of the signal transduction pathways are activated by the epidophyllotoxin etoposide. A model of the findings is presented in Figure 4.1. This figure demonstrates that the pathways signaling IR induced DNA damage and those signaling etoposide induced DNA damage overlap but remain dinstinct in the components which are phophorylated, and likely activated, as a result of these two genotoxic stresses.

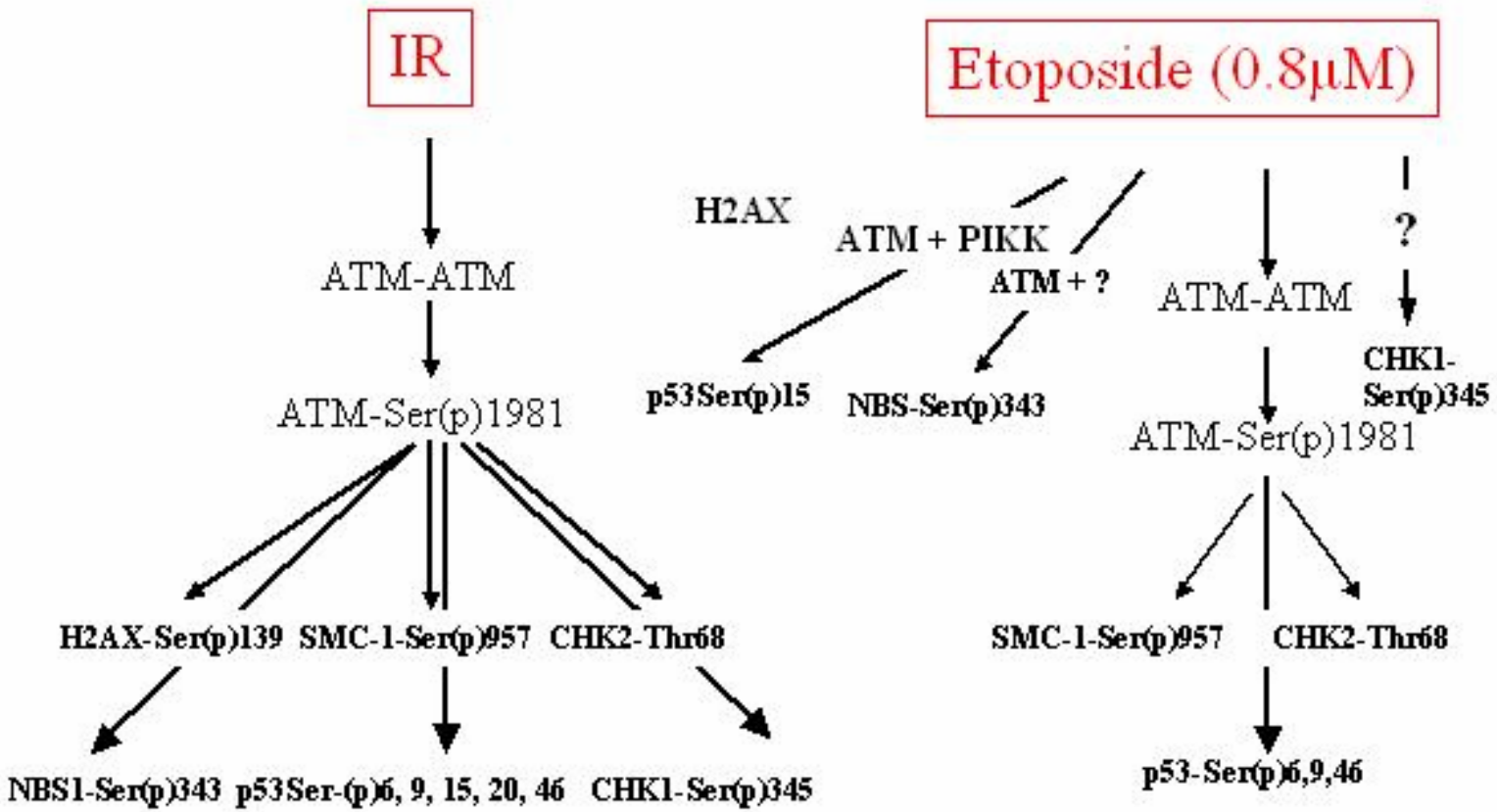

Figure 4.1: Model of DNA damage signaling in response to etoposide. Different signal transduction pathways are activated in response to etoposide and IR

4.11 Future directions

A complete understanding of the factors involved in the pathway from sensing the damage to complete repair or cell death caused by chemotherapeutics will help understand some of the questions which are still wide open in the field of DNA damage signaling. Although ATM has been extensively studied as a transducer of DNA damage, the types of damage which activate it and exactly how it does so, are unknown. The studies presented here provide insight into the types of damage which activate ATM.

Determining the precise pathways by which the cell signals the genotoxic stress induced by etoposide remains of primary importance. Therefore, it is imperative to identify the individual kinases responsible for phosphorylation of all sites which have been shown not to require ATM or have a partial requirement for ATM. Furthurmore, comparing the results obtained here to other compounds with different mechanisms and sites of action will also provide insight into how these types of damage are detected and repaired. The first step would be to see if the signal transduction pathways activated by teniposide, another compound in the epipodophyllotoxin class of drugs, are similar. Furthermore, since results indicate that, in some cases, the damage induced by the etoposide resembles the mechanisms activated in response to DNA adducts as in UV induced damage, other DNA adducting agents (alkalating agents, platinums, etc…) should be examined. Ultimately it would be interesting to classify antineoplastic agents according to the signal transduction pathways they activate.

SECTION V: REFERENCES

Abraham RT. (2001) Cell cycle checkpoint signaling through the ATM and ATR kinases. *Genes Dev.* **15(17):** 2177-96.

Abraham RT. (2004) PI 3-kinase related kinases: 'big' players in stress-induced signaling pathways. *DNA Repair (Amst).* **3(8-9):** 883-7.

Ahn JY, Schwarz JK, Piwnica-Worms H, Canman CE. (2000) Threonine 68 phosphorylation by ataxia telangiectasia mutated is required for efficient activation of Chk2 in response to ionizing radiation. *Cancer Res*. **60(21):** 5934-6.

Ahn J, Urist M, Prives C. (2004) The Chk2 protein kinase. *DNA Repair (Amst).* **3(8-9):** 1039-47.

Ali A, Zhang J, Bao S, Liu I, Otterness D, Dean NM, Abraham RT, Wang XF. (2004) Requirement of protein phosphatase 5 in DNA-damage-induced ATM activation. *Genes Dev*. **18(3):** 249-54.

Andegeko Y, Moyal L, Mittelman L, Tsarfaty I, Shiloh Y, Rotman G. (2001) Nuclear retention of ATM at sites of DNA double strand breaks. *J Biol Chem*. **276(41):** 38224-30.

Anderson L, Henderson C, Adachi Y. (2001) Phosphorylation and rapid relocalization of 53BP1 to nuclear foci upon DNA damage. *Mol Cell Biol.* **21(5):** 1719-29.

Andoh T, Ishida R. (1998) Catalytic inhibitors of DNA topoisomerase II. *Biochim Biophys Acta*. **400(1-3):** 155-71.

Appella E, Anderson CW. (2001) Post-translational modifications and activation of p53 by genotoxic stresses. *Eur J Biochem.* **268(10):** 2764-72.

Austin CA, Sng JH, Patel S, Fisher LM. (1993) Novel HeLa topoisomerase II is the II beta isoform: complete coding sequence and homology with other type II topoisomerases. *Biochim Biophys Acta*. **(3):** 283-91.

Bakkenist CJ, Kastan MB. (2003) DNA damage activates ATM through intermolecular autophosphorylation and dimer dissociation. *Nature*. **421(6922):** 499-506.

Banin S, Moyal L, Shieh S, Taya Y, Anderson CW, Chessa L, Smorodinsky NI, Prives C, Reiss Y, Shiloh Y, Ziv Y. (1998) Enhanced phosphorylation of p53 by ATM in response to DNA damage. *Science.* **281(5383):** 1674-7.

Bankert RB, Hess SD, Egilmez NK. (2002) SCID mouse models to study human cancer pathogenesis and approaches to therapy: potential, limitations, and future directions. *Front Biosci.* (**1)7:** c44-62.

Beamish H, Kedar P, Kaneko H, Chen P, Fukao T, Peng C, Beresten S, Gueven N, Purdie D, Lees-Miller S, Ellis N, Kondo N, Lavin MF. (2002) Functional link between BLM

defective in Bloom's syndrome and the ataxia-telangiectasia-mutated protein, ATM. *J Biol Chem*. **277(34):** 30515-23.

Bennett CB, Lewis AL, Baldwin KK, Resnick MA. (1993) Lethality induced by a single site-specific double-strand break in a dispensable yeast plasmid. *Proc Natl Acad Sci U S A.* **90(12):** 5613-7.

Berger JM. (1998a) Structure of DNA topoisomerases. *Biochim Biophys Acta.* **1400(1-3):** 3-18.

Berger JM. (1998b) Type II DNA topoisomerases. *Curr Opin Struct Biol.* **(1):** 26-32.
Block WD, Merkle D, Meek K, Lees-Miller SP. (2004) Selective inhibition of the DNA-dependent protein kinase (DNA-PK) by the radiosensitizing agent caffeine. *Nucleic Acids Res.* **32(6):** 1967-72.

Bradbury JM, Jackson SP. (2003) The complex matter of DNA double-strand break detection. *Biochem Soc Trans.* **31(Pt 1):** 40-4.

Brown AL, Lee CH, Schwarz JK, Mitiku N, Piwnica-Worms H, Chung JH. (1999) A human Cds1-related kinase that functions downstream of ATM protein in the cellular response to DNA damage. *Proc Natl Acad Sci U S A.* **96(7):** 3745-50.

Brumbaugh KM, Otterness DM, Geisen C, Oliveira V, Brognard J, Li X, Lejeune F, Tibbetts RS, Maquat LE, Abraham RT. (2004) The mRNA surveillance protein hSMG-1 functions in genotoxic stress response pathways in mammalian cells. *Mol Cell.* **14(5):** 585-98.

Bryans M, Valenzano MC, Stamato TD. (1999) Absence of DNA ligase IV protein in XR-1 cells: evidence for stabilization by XRCC4. *Mutat Res.* **433(1):** 53-8.

Burma S, Chen BP, Murphy M, Kurimasa A, Chen DJ. (2001) ATM phosphorylates histone H2AX in response to DNA double-strand breaks. *J Biol Chem*. **276(45):** 42462-7.

Buscemi G, Savio C, Zannini L, Micciche F, Masnada D, Nakanishi M, Tauchi H, Komatsu K, Mizutani S, Khanna K, Chen P, Concannon P, Chessa L, Delia D. (2001) Chk2 activation dependence on Nbs1 after DNA damage. *Mol Cell Biol.* **21(15):** 5214-22.

Burden DA, Kingma PS, Froelich-Ammon SJ, Bjornsti MA, Patchan MW, Thompson RB, Osheroff N. (1996) Topoisomerase II.etoposide interactions direct the formation of drug-induced enzyme-DNA cleavage complexes. *J Biol Chem.* **271(46):** 29238-44.

Burden DA and Osheroff N. (1998) Mechanism of action of eukaryotic topoisomerase II and drugs targeted to the enzyme. *Biochim Biophys Acta.* **1400(1-3):** 139-154.

Canman CE, Lim DS, Cimprich KA, Taya Y, Tamai K, Sakaguchi K, Appella E, Kastan MB, Siliciano JD. (1998) Activation of the ATM kinase by ionizing radiation and phosphorylation of p53. *Science.* **281(5383):** 1677-9.

Carson CT, Schwartz RA, Stracker TH, Lilley CE, Lee DV, Weitzman MD. (2003) The Mre11 complex is required for ATM activation and the G2/M checkpoint. *EMBO J* **22(24):** 6610-20.

Celeste A, Petersen S, Romanienko PJ, Fernandez-Capetillo O, Chen HT, Sedelnikova OA, Reina-San-Martin B, Coppola V, Meffre E, Difilippantonio MJ, Redon C, Pilch DR, Olaru A, Eckhaus M, Camerini-Otero RD, Tessarollo L, Livak F, Manova K, Bonner WM, Nussenzweig MC, Nussenzweig A. (2002) Genomic instability in mice lacking histone H2AX. *Science.* **296(5569):** 922-7.

Celeste A, Fernandez-Capetillo O, Kruhlak MJ, Pilch DR, Staudt DW, Lee A, Bonner RF, Bonner WM, Nussenzweig A. (2003) Histone H2AX phosphorylation is dispensable for the initial recognition of DNA breaks. *Nat Cell Biol*. **5(7):** 675-9.

Chahwan C, Nakamura TM, Sivakumar S, Russell P, Rhind N. (2003) The fission yeast Rad32 (Mre11)-Rad50-Nbs1 complex is required for the S-phase DNA damage checkpoint. *Mol Cell Biol.* **23(18):** 6564-73.

Chan DW, Chen BP, Prithivirajsingh S, Kurimasa A, Story MD, Qin J, Chen DJ. (2002) Autophosphorylation of the DNA-dependent protein kinase catalytic subunit is required for rejoining of DNA double-strand breaks. *Genes Dev*. **16(18):** 2333-8.

Chan DW, Ye R, Veillette CJ, Lees-Miller SP. (1999) DNA-dependent protein kinase phosphorylation sites in Ku 70/80 heterodimer. *Biochemistry*. **38(6):** 1819-28.

Chappell C, Hanakahi LA, Karimi-Busheri F, Weinfeld M, West SC. (2002) Involvement of human polynucleotide kinase in double-strand break repair by non-homologous end joining. *EMBO J.* **21(11):** 2827-32.

Chaturvedi P, Eng WK, Zhu Y, Mattern MR, Mishra R, Hurle MR, Zhang X, Annan RS, Lu Q, Faucette LF, Scott GF, Li X, Carr SA, Johnson RK, Winkler JD, Zhou BB. (1999) Mammalian Chk2 is a downstream effector of the ATM-dependent DNA damage checkpoint pathway. *Oncogene*. **18(28):** 4047-54.

Chehab NH, Malikzay A, Stavridi ES, Halazonetis TD. (1999) Phosphorylation of Ser-20 mediates stabilization of human p53 in response to DNA damage. *Proc Natl Acad Sci U S A.* **96(24):** 13777-82.

Chen Y, Sanchez Y. (2004) Chk1 in the DNA damage response: conserved roles from yeasts to mammals. *DNA Repair (Amst).* **3(8-9):** 1025-32.

Chikamori K, Grabowski DR, Kinter M, Willard BB, Yadav S, Aebersold RH, Bukowski RM, Hickson ID, Andersen AH, Ganapathi R, Ganapathi MK. (2003) Phosphorylation of serine 1106 in the catalytic domain of topoisomerase II alpha regulates enzymatic activity and drug sensitivity. *J Biol Chem*. **278(15):** 12696-702.

Constantinou A, Davies AA, West SC. (2001) Branch migration and Holliday junction resolution catalyzed by activities from mammalian cells. *Cell*. **104(2):** 259-68.

Corbett AH, DeVore RF, Osheroff N. (1992) Effect of casein kinase II-mediated phosphorylation on the catalytic cycle of topoisomerase II. Regulation of enzyme activity by enhancement of ATP hydrolysis. *J Biol Chem*. **267(28):** 20513-8.

Cortez D, Wang Y, Qin J, Elledge SJ (1999) Requirement of ATM-dependent phosphorylation of brca1 in the DNA damage response to double-strand breaks. *Science* **286(5442):** 1162-6.

Cortez D, Guntuku S, Qin J, Elledge SJ. (2001) ATR and ATRIP: partners in checkpoint signaling. *Science*. **294(5547):** 1713-6.

d'Adda di Fagagna F, Reaper PM, Clay-Farrace L, Fiegler H, Carr P, Von Zglinicki T, Saretzki G, Carter NP, Jackson SP. (2003) A DNA damage checkpoint response in telomere-initiated senescence. *Nature*. **426(6963):** 194-8.

D'Amours D, Jackson SP. (2002) The Mre11 complex: at the crossroads of dna repair and checkpoint signalling. *Nat Rev Mol Cell Biol.* **3(5):** 317-27.

Davies SP, Reddy H, Caivano M, Cohen P. (2000) Specificity and mechanism of action of some commonly used protein kinase inhibitors. *Biochem J.* **351(Pt 1):** 95-105.

DeFazio LG, Stansel RM, Griffith JD, Chu G. (2002) Synapsis of DNA ends by DNA-dependent protein kinase. *EMBO J*. **21(12):** 3192-200.

Douglas P, Sapkota GP, Morrice N, Yu Y, Goodarzi AA, Merkle D, Meek K, Alessi DR, Lees-Miller SP. (2002) Identification of in vitro and in vivo phosphorylation sites in the catalytic subunit of DNA-dependent protein kinase. *Biochem. J.* **368:** 243-251.

Drake FH, Zimmerman JP, McCabe FL, Bartus HF, Per SR, Sullivan DM, Ross WE, Mattern MR, Johnson RK, Crooke ST, *et al*. (1987) Purification of topoisomerase II from amsacrine-resistant P388 leukemia cells. Evidence for two forms of the enzyme. *J Biol Chem*. **262(34):** 16739-47.

Den Elzen NR, O'Connell MJ. (2004) Recovery from DNA damage checkpoint arrest by PP1-mediated inhibition of Chk1. *EMBO J.* **23(4):** 908-18.

Desai-Mehta A, Cerosaletti KM, Concannon P. (2001) Dinstinct functional domains of nibrin mediate Mre11 binding, focus formation, and nuclear localisation. *Mol Cell Biol.* **21(6):** 2184-91.

Ding H, Duan W, Zhu WG, Ju R, Srinivasan K, Otterson GA, Villalona-Calero MA. (2003a) P21 response to DNA damage induced by genistein and etoposide in human lung cancer cells. *Biochem Biophys Res Commun.* **305(4):** 950-6.

Ding Q, Reddy YV, Wang W, Woods T, Douglas P, Ramsden DA, Lees-Miller SP, Meek K. (2003b) Autophosphorylation of the catalytic subunit of the DNA-dependent protein kinase is required for efficient end processing during DNA double-strand break repair. *Mol Cell Biol.* **23(16):** 5836-48.

Dohoney KM, Guillerm C, Whiteford C, Elbi C, Lambert PF, Hager GL, Brady JN. (2004) Phosphorylation of p53 at serine 37 is important for transcriptional activity and regulation in response to DNA damage. *Oncogene*. **23(1):** 49-57.

Dumaz N, Milne DM, Jardine LJ, Meek DW. (2001) Critical roles for the serine 20, but not the serine 15, phosphorylation site and for the polyproline domain in regulating p53 turnover. *Biochem J*. **359(Pt 2):** 459-64.

Falck J, Petrini JH, Williams BR, Lukas J, Bartek J. (2002) The DNA damage-dependent intra-S phase checkpoint is regulated by parallel pathways. *Nat Genet.* **30(3):**290-4**.**

Fernandez-Capetillo O, Lee A, Nussenzweig M, Nussenzweig A. (2004) H2AX: the histone guardian of the genome. *DNA Repair (Amst).* **3(8-9):** 959-67.

Fernandez-Capetillo O, Celeste A, Nussenzweig A. (2003) Focussing on foci: H2AX and the recruitment of DNA-damage response factors. *Cell Cycle* **2(5):** 426-7

Fernandez-Capetillo O, Chen HT, Celeste A, Ward I, Romanienko PJ, Morales JC, Naka K, Xia Z, Camerini-Otero RD, Motoyama N, Carpenter PB, Bonner WM, Chen J, Nussenzweig A. (2002) DNA damage-induced G2-M checkpoint activation by histone H2AX and 53BP1. *Nat Cell Biol*. **4(12):** 993-7.

Foray N, Marot D, Gabriel A, Randrianarison V, Carr AM, Perricaudet M, Ashworth A, Jeggo P. (2003) A subset of ATM- and ATR-dependent phosphorylation events requires the BRCA1 protein. *EMBO J.* **22(11):** 2860-71.

Fortune JM, Lavrukhin OV, Gurnon JR, Van Etten JL, Lloyd RS, Osheroff N. (2001) Topoisomerase II from Chlorella virus PBCV-1 has an exceptionally high DNA cleavage activity. *J Biol Chem.* **276(26):** 24401-8.

Froelich-Ammon SJ, Patchan MW, Osheroff N, Thompson RB. (1995) Topoisomerase II binds to ellipticine in the absence or presence of DNA. Characterization of enzyme-drug interactions by fluorescence spectroscopy. *J Biol Chem.* **270(25):** 14998-5004.

Freedman DA, Levine AJ. (1998) Nuclear export is required for degradation of endogenous p53 by MDM2 and human papillomavirus E6. *Mol Cell Biol*. **18(12):** 7288-93.

Furuta T, Takemura H, Liao ZY, Aune GJ, Redon C, Sedelnikova OA, Pilch DR, Rogakou EP, Celeste A, Chen HT, Nussenzweig A, Aladjem MI, Bonner WM, Pommier Y. (2003) Phosphorylation of histone H2AX and activation of Mre11, Rad50, and Nbs1 in response to replication-dependent DNA double-strand breaks induced by mammalian DNA topoisomerase I cleavage complexes. *J Biol Chem*. **278(22):** 20303-12.

Gatei M, Sloper K, Sorensen C, Syljuasen R, Falck J, Hobson K, Savage K, Lukas J, Zhou BB, Bartek J, Khanna KK. (2003) Ataxia-telangiectasia-mutated (ATM) and NBS1-dependent phosphorylation of Chk1 on Ser-317 in response to ionizing radiation. *J Biol Chem*. **278(17):** 14806-11.

Gatei M, Young D, Cerosaletti KM, Desai-Mehta A, Spring K, Kozlov S, Lavin MF, Gatti RA, Concannon P, Khanna K. (2000) ATM-dependent phosphorylation of nibrin in response to radiation exposure. *Nat Genet* **25(1):** 115-9.

Goldberg M, Stucki M, Falck J, D'Amours D, Rahman D, Pappin D, Bartek J, Jackson SP. (2003) MDC1 is required for the intra-S-phase DNA damage checkpoint. *Nature.* **421(6926):** 952-6.

Gellert M. (2002) V(D)J recombination: RAG proteins, repair factors and regulation. *Annu Rev Biochem* **71:** 101-32.

Gingras AC, Raught B, Sonenberg N. (2001) Control of translation by the target of rapamycin proteins. *Prog Mol Subcell Biol*. **27:**143-74.

Goodarzi AA, Block WD, Less-Miller SP. (2003) The role of ATM and ATR in DNA damage-induced cell cycle control. *Progress in Cell Cycle Research.* Vol.5 393-411.

Grawunder U, Wilm M, Wu X, Kulesza P, Wilson TE, Mann M, Lieber MR. (1997) Activity of DNA ligase IV stimulated by complex formation with XRCC4 protein in mammalian cells. *Nature*. **388(6641):** 492-5.

Groth A, Lukas J, Nigg EA, Sillje HH, Wernstedt C, Bartek J, Hansen K. (2003) Human Tousled like kinases are targeted by an ATM- and Chk1-dependent DNA damage checkpoint. *EMBO J*. **22(7):** 1676-87.

Haber JE. (1995) *In vivo* biochemistry: physical monitoring of recombination induced by site-specific endonucleases. *Bioessays*. **17(7):** 609-20.

Haber JE. (2000) Partners and pathwaysrepairing a double-strand break. *Trends Genet.* **16(6):** 259-64.

Hahn P, Kapp LN, Painter RB. (1987) Establishment and characterization of two human cell lines with amplified dihydrofolate reductase genes. *Exp Cell Res.* **168:** 89-94.

Hanakahi LA, Bartlet-Jones M, Chappell C, Pappin D, West SC. (2000) Binding of inositol phosphate to DNA-PK and stimulation of double-strand break repair. *Cell*. **102(6):** 721-9.

Hanakahi LA, West SC. (2002) Specific interaction of IP6 with human Ku70/80, the DNA-binding subunit of DNA-PK. *EMBO J.* **21(8):** 2038-44.

Haneda M, Kojima E, Nishikimi A, Hasegawa T, Nakashima I, Isobe K. (2004) Protein phosphatase 1, but not protein phosphatase 2A, dephosphorylates DNA-damaging stress-induced phospho-serine 15 of p53. *FEBS Lett*. **567(2-3):** 171-4.

Hartley KO, Gell D, Smith GC, Zhang H, Divecha N, Connelly MA, Admon A, Lees-Miller SP, Anderson CW, Jackson SP. (1995) DNA-dependent protein kinase catalytic subunit: a relative of phosphatidylinositol 3-kinase and the ataxia telangiectasia gene product. *Cell.* **82(5):** 849-56.

Higashimoto Y, Saito S, Tong XH, Hong A, Sakaguchi K, Appella E, Anderson CW. (2000) Human p53 is phosphorylated on serines 6 and 9 in response to DNA damage-inducing agents. *J Biol Chem*. **275(30):** 23199-203

Hirao A, Kong YY, Matsuoka S, Wakeham A, Ruland J, Yoshida H, Liu D, Elledge SJ, Mak TW. (2000) DNA damage-induced activation of p53 by the checkpoint kinase Chk2. *Science.* **287(5459):** 1824-7.

Holmberg CI, Tran SE, Eriksson JE, Sistonen L. (2002) Multisite phosphorylation provides sophisticated regulation of transcription factors. *Trends Biochem Sci*. **27(12):** 619-27.

Huang J, Dynan WS. (2002) Reconstitution of the mammalian DNA double-strand break end-joining reaction reveals a requirement for an Mre11/Rad50/NBS1-containing fraction. *Nucleic Acids Res*. **30(3):** 667-74.

Izzard RA, Jackson SP, Smith GC. (1999) Competitive and noncompetitive inhibition of the DNA-dependent protein kinase. *Cancer Res.* **59(11):** 2581-6.

Jabbur JR, Huang P, Zhang W. (2000) DNA damage-induced phosphorylation of p53 at serine 20 correlates with p21 and Mdm-2 induction in vivo. *Oncogene.* **19(54):** 6203-8.

Karpinich NO, Tafani M, Rothman RJ, Russo MA, Farber JL. (2002) The course of etoposide-induced apoptosis from damage to DNA and p53 activation to mitochondrial release of cytochrome c. *J Biol Chem*. **277(19):** 16547-52.

Karmakar P, Piotrowski J, Brosh RM Jr, Sommers JA, Miller SP, Cheng WH, Snowden CM, Ramsden DA, Bohr VA. (2002a) Werner protein is a target of DNA-dependent protein kinase in vivo and in vitro, and its catalytic activities are regulated by phosphorylation. *J Biol Chem.* **277(21):** 18291-302.

Karmakar P, Snowden CM, Ramsden DA, Bohr VA. (2002b) Ku heterodimer binds to both ends of the Werner protein and functional interaction occurs at the Werner N-terminus. *Nucleic Acids Res.* **30(16):** 3583-91.

Kastan MB, Lim DS. (2000) The many substrates and functions of ATM. *Nat Rev Mol Cell Biol*. **1(3):** 179-86.

Kerr P, Ashworth A. (2001) New complexities for BRCA1 and BRCA2. *Curr Biol*. **11(16):** R668-76.

Kim ST, Xu B, Kastan MB. (2002) Involvement of the cohesin protein, Smc1, in Atm-dependent and independent responses to DNA damage. *Genes Dev*. **16(5):** 560-70.

Kim ST, Lim DS, Canman CE, Kastan MB. (1999) Substrate specificities and identification of putative substrates of ATM kinase family members. *J Biol Chem* **274(53):** 37538-43.

Ko LJ, Prives C. (1996) p53: puzzle and paradigm *Genes Dev.* **10(9):** 1054-72.

Kobayashi J, Antoccia A, Tauchi H, Matsuura S, Komatsu K. (2004) NBS1 and its functional role in the DNA damage response. *DNA Repair (Amst).* **3(8-9):** 855-61.

Kobayashi J, Tauchi H, Sakamoto S, Nakamura A, Morishima K, Matsuura S, Kobayashi T, Tamai K, Tanimoto K, Komatsu K. (2002) NBS1 localizes to gamma-H2AX foci through interaction with the FHA/BRCT domain. *Curr Biol.* **12(21):** 1846-51.

Kozlov S, Gueven N, Keating K, Ramsay J, Lavin MF. (2003) ATP activates ataxia-telangiectasia mutated (ATM) in vitro. Importance of autophosphorylation. *J Biol Chem* **278(11):** 9309-17.

Kurz EU, Douglas P, Lees-Miller SP. (2004) Doxorubicin activates ATM-dependent phosphorylation of multiple downstream targets in part through the generation of reactive oxygen species. *J Biol Chem*. **279(51):** 53272-81.

Kurz EU, Lees-Miller SP. (2004) DNA damage-induced activation of ATM and ATM-dependent signaling pathways. *DNA Repair (Amst*). **3(8-9):** 889-900.

Larsen AK, Escargueil AE, Skladanowski A. (2003) From DNA damage to G2 arrest: the many roles of topoisomerase II. *Prog Cell Cycle Res*. **5:** 295-300.

Lavin MF, Shiloh Y. (1997) The genetic defect in ataxia-telangiectasia. *Annu Rev Immunol*. **15:** 177-202.

Lee JH, Paull TT. (2004) Direct activation of the ATM protein kinase by the Mre11/Rad50/Nbs1 complex. *Science.* **304(5667):** 93-6.

Lees-Miller SP, Sakaguchi K, Ullrich SJ, Appella E, Anderson CW. (1992) Human DNA-activated protein kinase phosphorylates serines 15 and 37 in the amino-terminal transactivation domain of human p53. *Mol Cell Biol*. **12(11):** 5041-9.

Lees-Miller SP, Godbout R, Chan DW, Weinfeld M, Day RS 3rd, Barron GM, Allalunis-Turner J. (1995) Absence of p350 subunit of DNA-activated protein kinase from a radiosensitive human cell line. *Science*. **267(5201):** 1183-5.

Leuther KK, Hammarsten O, Kornberg RD, Chu G. (1999) Structure of DNA-dependent protein kinase: implications for its regulation by DNA. *EMBO J.* **18(5):** 1114-23.

Li, S. Banin, H. Ouyang, G.C. Li, G. Courtois, Y. Shiloh, M. Karin and G. Rotman. (2001) ATM is required for IkappaB kinase (IKKk) activation in response to DNA double strand breaks. *J. Biol. Chem.* **276**: 8898–8903.

Lieber MR, Ma Y, Pannicke U, Schwarz K. (2003) Mechanism and regulation of human non-homologous DNA end-joining. *Nat Rev Mol Cell Biol*. **4(9):** 712-20.

Lim DS, Kim ST, Xu B, Maser RS, Lin J, Petrini JH, Kastan MB. (2000) ATM phosphorylates p95/nbs1 in an S-phase checkpoint pathway. *Nature.* **404(6778):** 613-7.

Lima CD, Wang JC, Mondragon A. (1994) Three-dimensional structure of the 67K N-terminal fragment of E. coli DNA topoisomerase I. *Nature.* **367(6459):** 138-46.

Liu Q, Guntuku S, Cui XS, Matsuoka S, Cortez D, Tamai K, Luo G, Carattini-Rivera S, DeMayo F, Bradley A, Donehower LA, Elledge SJ. (2000) Chk1 is an essential kinase that is regulated by Atr and required for the G(2)/M DNA damage checkpoint. *Genes Dev***. 14(12):** 1448-59.

Liu Y, Virshup DM, White RL, Hsu LC. (2002) Regulation of BRCA1 phosphorylation by interaction with protein phosphatase 1alpha. *Cancer Res*. **62(22):** 6357-61.

Llorca O, Rivera-Calzada A, Grantham J, Willison KR. (2003) Electron microscopy and 3D reconstructions reveal that human ATM kinase uses an arm-like domain to clamp around double-stranded DNA. Oncogene **22(25):**3867-74.

Lopez-Girona A, Tanaka K, Chen XB, Baber BA, McGowan CH, Russell P. (2001) Serine-345 is required for Rad3-dependent phosphorylation and function of checkpoint kinase Chk1 in fission yeast. *Proc Natl Acad Sci U S A.* **98(20):** 11289-94.

Lopez-Girona A, Furnari B, Mondesert O, Russell P. (1999) Nuclear localization of Cdc25 is regulated by DNA damage and a 14-3-3 protein. *Nature.* **397(6715):** 172-5.

Luger K, Mader AW, Richmond RK, Sargent DF, Richmond TJ. (1997) Crystal structure of the nucleosome core particle at 2.8 A resolution. *Nature*. **389(6648):** 251-60.

Lukas C, Falck J, Bartkova J, Bartek J, Lukas J. (2003) Distinct spatiotemporal dynamics of mammalian checkpoint regulators induced by DNA damage. *Nat Cell Biol.* **5(3):** 255-60.

Ma Y, Lieber MR. (2002) Binding of inositol hexakisphosphate (IP6) to Ku but not to DNA-PKcs. *J Biol Chem*. **277(13):** 10756-9

Ma Y, Pannicke U, Schwarz K, Lieber MR. (2002) Hairpin opening and overhang processing by an Artemis/DNA-dependent protein kinase complex in nonhomologous end joining and V(D)J recombination. *Cell.* **108(6):** 781-94.

Mahajan KN, Nick McElhinny SA, Mitchell BS, Ramsden DA. (2002) Association of DNA polymerase mu (pol mu) with Ku and ligase IV: role for pol mu in end-joining double-strand break repair. *Mol Cell Biol*. **22(14):** 5194-202.

Maser RS, Monsen KJ, Nelms BE, Petrini JH. (1997) hMre11 and hRad50 nuclear foci are induced during the normal cellular response to DNA double-strand breaks. *Mol Cell Biol*. **17(10):** 6087-96.

Matsuoka S, Rotman G, Ogawa A, Shiloh Y, Tamai K, Elledge SJ. (2000) Ataxia telangiectasia-mutated phosphorylates Chk2 in vivo and in vitro. *Proc Natl Acad Sci U S A*. **97(19):** 10389-94.

Maya R, Balass M, Kim ST, Shkedy D, Leal JF, Shifman O, Moas M, Buschmann T, Ronai Z, Shiloh Y, Kastan MB, Katzir E, Oren M. (2001) ATM-dependent phosphorylation of Mdm2 on serine 395: role in p53 activation by DNA damage. *Genes Dev*. **15(9):** 1067-77.

McGowan CH. (2002) Checking in on Cds1 (Chk2): A checkpoint kinase and tumor suppressor. *Bioessays*. **24(6):** 502-11.

Melchionna R, Chen XB, Blasina A, McGowan CH. (2000) Threonine 68 is required for radiation-induced phosphorylation and activation of Cds1. *Nat Cell Biol*. **2(10):** 762-5.

Mirzoeva OK, Petrini JH. (2003) DNA replication-dependent nuclear dynamics of the Mre11 complex. *Mol Cancer Res*. **1(3):** 207-18.

Mochan TA, Venere M, DiTullio RA Jr, Halazonetis TD. (2003) 53BP1 and NFBD1/MDC1-Nbs1 function in parallel interacting pathways activating ataxia-telangiectasia mutated (ATM) in response to DNA damage. *Cancer Res*. **63(24):** 8586-91.

Melo JA, Cohen J, Toczyski DP. (2001) Two checkpoint complexes are independently recruited to sites of DNA damage in vivo *Genes Dev*. **15(21):** 2809-21.

Mortensen UH, Bendixen C, Sunjevaric I, Rothstein R. (1996) DNA strand annealing is promoted by the yeast Rad52 protein. *Proc Natl Acad Sci U S A*. **93(20):** 10729-34.

Moshous D, Callebaut I, de Chasseval R, Corneo B, Cavazzana-Calvo M, Le Deist F, Tezcan I, Sanal O, Bertrand Y, Philippe N, Fischer A, de Villartay JP. (2001) Artemis, a novel DNA double-strand break repair/V(D)J recombination protein, is mutated in human severe combined immune deficiency. *Cell*. **105(2):** 177-86.

Muscarella DE, Rachlinski MK, Sotiriadis J, Bloom SE. (1998) Contribution of gene-specific lesions, DNA-replication-associated damage, and subsequent transcriptional inhibition in topoisomerase inhibitor-mediated apoptosis in lymphoma cells. *Exp Cell Res*. **238(1):** 155-67.

Nagasawa H, Kraemer KH, Shiloh Y, Little JB. (1987) Detection of ataxia telangiectasia heterozygous cell lines by postirradiation cumulative labeling index: measurements with coded samples. *Cancer Res.* **47(2):** 398-402.

Nakanishi K, Taniguchi T, Ranganathan V, New HV, Moreau LA, Stotsky M, Mathew CG, Kastan MB, Weaver DT, D'Andrea AD. (2002) Interaction of FANCD2 and NBS1 in the DNA damage response. *Nat Cell Biol*. **4(12):** 913-20.

Nakagawa K, Taya Y, Tamai K, Yamaizumi M. (1999) Requirement of ATM in phosphorylation of the human p53 protein ar serine 15 following DNA double-stranded breaks. *Mol Cell Biol.* **19(4):** 2828-34.

Nick McElhinny SA, Snowden CM, McCarville J, Ramsden DA. (2000) Ku recruits the XRCC4-ligase IV complex to DNA ends. *Mol Cell Biol*. **20(9):** 2996-3003.

Nitiss JL. (1998) Investigating the biological functions of DNA topoisomerases in eukaryotic cells. *Biochim, Biophys. Acta.* **1400**: 63-81.

O'Driscoll M, Ruiz-Perez VL, Woods CG, Jeggo PA, Goodship JA. (2003) A splicing mutation affecting expression of ataxia-telangiectasia and Rad3-related protein (ATR) results in Seckel syndrome. *Nat Genet*. **33(4):**497-501.

O'Neill T, Dwyer AJ, Ziv Y, Chan DW, Lees-Miller SP, Abraham RH, Lai JH, Hill D Shiloh Y, Cantley LC, Rathbun GA. (2000) Utilization of oriented peptide libraries to identify substrate motifs selected by ATM. *Biol Chem.* **275(30):** 22719-27.

Oda K, Arakawa H, Tanaka T, Matsuda K, Tanikawa C, Mori T, Nishimori H, Tamai K, Tokino T, Nakamura Y, Taya Y. (2000) p53AIP1, a potential mediator of p53-dependent apoptosis, and its regulation by Ser-46-phosphorylated p53. *Cell.* **102(6):** 849-62.

Osheroff N. (1989) Effect of antineoplastic agents on the DNA cleavage/religation reaction of eukaryotic topoisomerase II: inhibition of DNA religation by etoposide. *Biochemistry*. **28(15):** 6157-60.

Osheroff N, Zechiedrich EL, Gale KC. (1991) Catalytic function of DNA topoisomerase II. *Bioassays.* **13:** 269-273.

Park MS, Ludwig DL, Stigger E, Lee SH. (1996) Physical interaction between human RAD52 and RPA is required for homologous recombination in mammalian cells. *J Biol Chem*. **271(31):** 18996-9000.

Park J, Kunjibettu S, McMahon SB, Cole MD. (2001) The ATM-related domain of TRRAP is required for histone acetyltransferase recruitment and Myc-dependent oncogenesis. *Genes Dev.* **15(13):** 1619-24.

Parrilla-Castellar ER, Arlander SJ, Karnitz L. (2004) Dial 9-1-1 for DNA damage: the Rad9-Hus1-Rad1 (9-1-1) clamp complex. *DNA Repair (Amst).* **3(8-9):** 1009-14.

Paull TT, Rogakou EP, Yamazaki V, Kirchgessner CU, Gellert M, Bonner WM (2000) A critical role for histone H2AX in recruitment of repair factors to nuclear foci after DNA damage. *Curr Biol.* **10(15):** 886-95.

Petrini JH, Stracker TH. (2003) The cellular response to DNA double-strand breaks: defining the sensors and mediators. *Trends Cell Biol*. **13(9):** 458-62.

Perry J, Kleckner N. (2003) The ATRs, ATMs, and TORs are giant HEAT repeat proteins. *Cell*. **112(2):** 151-5.

Petukhova G, Stratton S, Sung P. (1998) Catalysis of homologous DNA pairing by yeast Rad51 and Rad54 proteins. *Nature.* **393(6680):** 91-4.

Prives, C. (1998) Signalling to p53: Breaking the MDM2-p53 circuit. *Cell.* **95:** 5-8.

Prives C, Manley JL. (2001) Why is p53 acetylated? *Cell.* **107(7):** 815-8.

Redon C, Pilch D, Rogakou E, Sedelnikova O, Newrock K, Bonner W. (2002) Histone H2A variants H2AX and H2AZ. *Curr Opin Genet Dev*. **12(2):** 162-9.

Rogakou EP, Nieves-Neira W, Boon C, Pommier Y, Bonner WM. (2000) Initiation of DNA fragmentation during apoptosis induces phosphorylation of H2AX histone at serine 139. *J Biol Chem*. **275(13):**9 390-5.

Rogakou EP, Boon C, Redon C, Bonner WM. (1999) Megabase chromatin domains involved in DNA double-strand breaks in vivo. *J Cell Biol*. **146(5):** 905-16.

Rogakou EP, Pilch DR, Orr AH, Ivanova VS, Bonner WM. (1998) DNA double-stranded breaks induce histone H2AX phosphorylation on serine 139. *J Biol Chem*. **273(10):** 5858-68.

Saito S, Goodarzi AA, Higashimoto Y, Noda Y, Lees-Miller SP, Appella E, Anderson CW. (2002) ATM mediates phosphorylation at multiple p53 sites, including Ser(46), in response to ionizing radiation. *J Biol Chem*. **277(15):** 12491-4.

Sanchez Y, Bachant J, Wang H, Hu F, Liu D, Tetzlaff M, Elledge SJ. (1999) Control of the DNA damage checkpoint by chk1 and rad53 protein kinases through distinct mechanisms. *Science*. **286(5442):** 1166-71.

Sapkota GP, Deak M, Kieloch A, Morrice N, Goodarzi AA, Smythe C, Shiloh Y, Lees-Miller SP, Alessi DR. (2002) Ionizing radiation induces ataxia telangiectasia mutated kinase (ATM)-mediated phosphorylation of LKB1/STK11 at Thr-366. *Biochem J*. **368(Pt 2):** 507-16.

Sarkaria JN, Eshleman JS (2001) ATM as a target for novel radiosensitizers. *Semin Radiat Oncol* **11(4):** 316-27.

Sarkaria JN, Busby EC, Tibbetts RS, Roos P, Taya Y, Karnitz LM, Abraham RT. (1999) Inhibition of ATM and ATR kinase activities by the radiosensitizing agent, caffeine. *Cancer Res.* **59(17):** 4375-82.

Sarkaria JN, Tibbetts RS, Busby EC, Kennedy AP, Hill DE, Abraham RT. (1998) Inhibition of phosphoinositide 3-kinase related kinases by the radiosensitizing agent wortmannin. *Cancer Res.* **58(19):** 4375-82

Sarnow P, Ho YS, Williams J, Levine AJ. (1982) Adenovirus E1b-58kd tumor antigen and SV40 large tumor antigen are physically associated with the same 54 kd cellular protein in transformed cells. *Cell*. **28(2):** 387-94.

Scully R, Chen J, Ochs RL, Keegan K, Hoekstra M, Feunteun J, Livingston DM. (1997) Dynamic changes of BRCA1 subnuclear location and phosphorylation state are initiated by DNA damage. *Cell.* **90(3):** 425-35.

Shaulsky G, Goldfinger N, Ben-Ze'ev A, Rotter V. (1990) Nuclear accumulation of p53 protein is mediated by several nuclear localization signals plays a role in tumorigenesis. *Mol Cell Biol*. **10(12):** 6565-77.

Shechter D, Costanzo V, Gautier J. (2004) Regulation of DNA replication by ATR: signaling in response to DNA intermediates. *DNA Repair (Amst).* **3(8-9):** 901-8.
Shen Z, Cloud KG, Chen DJ, Park MS. (1996) Specific interactions between the human RAD51 and RAD52 proteins. *J Biol Chem*. **271(1)**: 148-52.

Shieh SY, Ikeda M, Taya Y, Prives C. (1997) DNA damage-induced phosphorylation of p53 alleviates inhibition by MDM2. *Cell.* **91(3):** 325-34.

Shiloh Y. (2003) ATM and related protein kinases; safeguarding genome integrity. *Nat Rev Cancer*. **3(3):** 155-68.

Shiloh Y. (2001) ATM (ataxia telangiectasia mutated): expanding roles in the DNA damage response and cellular homeostasis. *Biochem Soc Trans* ;**29(Pt 6):**661-6.

Sjogren C, Nasmyth K. (2001) Sister chromatid cohesion is required for postreplicative double-strand break repair in Saccharomyces cerevisiae. *Curr Biol*. **11(12):**991-5.

Skulachev VP. (1997) Aging is a specific biological function rather than the result of a disorder in complex living systems: biochemical evidence in support of Weismann's hypothesis. *Biochemistry (Mosc).* **62(11):**1191-5.

Smith GC, Jackson SP. (1999) The DNA-dependent protein kinase. *Genes Dev*. **13(8)**:916-34.

Smith GC, d'Adda di Fagagna F, Lakin ND, Jackson SP. (1999) Cleavage and inactivation of ATM during apoptosis. *Mol Cell Biol*. **19(9):** 6076-84.

Stewart GS, Maser RS, Stankovic T, Bressan DA, Kaplan MI, Jaspers NG, Raams A, Byrd PJ, Petrini JH, Taylor AM. (1999) The DNA double-strand break repair gene hMRE11 is mutated in individuals with an ataxia-telangiectasia-like disorder. *Cell***. 99(6):** 577-87.

Stewart GS, Wang B, Bignell CR, Taylor AM, Elledge SJ. (2003) MDC1 is a mediator of the mammalian DNA damage checkpoint. *Nature.* **421(6926):** 961-6.

Stiff T, O'DriscollM, Rief N, Iwabuchi K, Lobrich M, Jeggo P (2004) ATM and DNA-PK function redundantly to phosphorylate H2AX after exposure to ionising radiation. *Cancer Res.* **64(7):** 2390-6.

Strunnikov AV, Jessberger R. (1999) Structural maintenance of chromosomes (SMC) proteins: conserved molecular properties for multiple biological functions. *Eur J Biochem.* **263(1):** 6-13.

Takata M, Sasaki MS, Sonoda E, Morrison C, Hashimoto M, Utsumi H, Yamaguchi-Iwai Y, Shinohara A, Takeda S. (1998) Homologous recombination and non-homologous end-joining pathways of DNA double-strand break repair have overlapping roles in the maintenance of chromosomal integrity in vertebrate cells. *EMBO J.* **17(18):** 5497-508.

Taniguchi T, Garcia-Higuera I, Andreassen PR, Gregory RC, Grompe M, D'Andrea AD. (2002) S-phase-specific interaction of the Fanconi anemia protein, FANCD2, with BRCA1 and RAD51. *Blood*. **100(7):** 2414-20.

Tauchi H, Kobayashi J, Morishima K, van Gent DC, Shiraishi T, Verkaik NS, vanHeems D, Ito E, Nakamura A, Sonoda E, Takata M, Takeda S, Matsuura S, Komatsu K. (2002) Nbs1 is essential for DNA repair by homologous recombination in higher vertebrate cells. *Nature.* **420(6911):** 93-8.

Tibbetts RS, Brumbaugh KM, Williams JM, Sarkaria JN, Cliby WA, Shieh SY, Taya Y, Prives C, Abraham RT. (1999) A role for ATR in the DNA damage-induced phosphorylation of p53. *Genes Dev* **13(2):** 152-7.

Tibbetts RS, Cortez D, Brumbaugh KM, Scully R, Livingston D, Elledge SJ, Abraham RT (2000) Functional interactions between BRCA1 and the checkpoint kinase ATR during genotoxic stress. *Genes Dev*. **14(23):** 2989-3002.

Ting NS, Lee WH. (2004) The DNA double-strand break response pathway: becoming more BRCAish than ever. *DNA Repair (Amst).* **3(8-9):** 935-44.

Tsuchida R, Yamada T, Takagi M, Shimada A, Ishioka C, Katsuki Y, Igarashi T, Chessa L, Delia D, Teraoka H, Mizutani S. (2002) Detection of ATM gene mutation in human glioma

cell line M059J by a rapid frameshift/stop codon assay in yeast. *Radiat Res.* **158(2):** 195-201.

Tsutakawa SE, Muto T, Kawate T, Jingami H, Kunishima N, Ariyoshi M, Kohda D, Nakagawa M, Morikawa K. (1999) Crystallographic and functional studies of very short patch repair endonuclease. *Mol Cell*. **3(5):** 621-8.

Unger T, Sionov RV, Moallem E, Yee CL, Howley PM, Oren M, Haupt Y (1999a) Mutations in serines 15 and 20 of human p53 impair its apoptotic activity. *Oncogene* **18(21):** 3205-12.

Unger T, Juven-Gershon T, Moallem E, Berger M, Vogt Sionov R, Lozano G, Oren M, Haupt Y. (1999b) Critical role for Ser20 of human p53 in the negative regulation of p53 by Mdm2. *EMBO J.* **18(7):** 1805-14.

Uziel T, Lerenthal Y, Moyal L, Andegeko Y, Mittelman L, Shiloh Y. (2003) Requirement of the MRN complex for ATM activation by DNA damage. *EMBO J.* **22(20):** 5612-21.

Van Dyck E, Stasiak AZ, Stasiak A, West SC (1999) Binding of double-strand breaks in DNA by human Rad52 protein. *Nature* **398(6729):** 728-31.

Varon R, Vissinga C, Platzer M, Cerosaletti KM, Chrzanowska KH, Saar K, Beckmann G, Seemanova E, Cooper PR, Nowak NJ, Stumm M, Weemaes CM, Gatti RA, Wilson RK, Digweed M, Rosenthal A, Sperling K, Concannon P, Reis A. (1998) Nibrin, a novel DNA double-strand break repair protein, is mutated in Nijmegen breakage syndrome. *Cell.* **93(3):** 467-76.

Venkitaraman AR. (1999) Breast cancer genes and DNA repair. *Science.* **286(5442):** 1100-2.

Walker EH, Pacold ME, Perisic O, Stephens L, Hawkins PT, Wymann MP, Williams RL. (2000) Structural determinants of phosphoinositide 3-kinase inhibition by wortmannin, LY294002, quercetin, myricetin, and staurosporine. *Mol Cell.* **6(4):** 909-19.

Walker JR, Corpina RA, Goldberg J. (2001) Structure of the Ku heterodimer bound to DNA and its implications for double-strand break repair. *Nature*. **412(6847):** 607-14.

Walworth N, Davey S, Beach D. (1993) Fission yeast chk1 protein kinase links the rad checkpoint pathway to cdc2. *Nature.* **363(6427):** 368-71.

Wang, J. (1971) Interaction between DNA and an Escherichia coli protein omega. *J. Mol. Bio.* **55:** 523-33.

Wang Y, Cortez D, Yazdi P, Neff N, Elledge SJ, Qin J (2000) BASC, a super complex of BRCA1-associated proteins involved in the recognition and repair of aberrant DNA structures. *Genes Dev*.**14(8):** 927-39.

Wang J, Wiltshire T, Wang Y, Mikell C, Burks J, Cunningham C, Van Laar ES, Waters SJ, Reed E, Wang W. (2004) ATM-dependent CHK2 activation induced by anticancer agent, irofulven. *J Biol Chem.* **279(38):** 39584-92.

Ward IM, Chen J. (2001) Histone H2AX is phosphorylated in an ATR-dependent manner in response to replicational stress. *J Biol Chem*. **276(51):** 47759-62.

Ward IM, Wu X, Chen J. (2001) Threonine 68 of Chk2 is phosphorylated at sites of DNA strand breaks. *J Biol Chem.* **276(51):** 47755-8.

Watters D, Khanna KK, Beamish H, Birrell G, Spring K, Kedar P, Gatei M, Stenzel D, Hobson K, Kozlov S, Zhang N, Farrell A, Ramsay J, Gatti R, Lavin M. (1997) Cellular localisation of the ataxia-telangiectasia (ATM) gene product and discrimination between mutated and normal forms. *Oncogene.* **14(16):** 1911-21.

Wechsler T, Chen BP, Harper R, Morotomi-Yano K, Huang BC, Meek K, Cleaver JE, Chen DJ, Wabl M. (2004) DNA-PKcs function regulated specifically by protein phosphatase 5. *Proc Natl Acad Sci U S A.* **101(5):** 1247-52.

West SC. (2003) Molecular views of recombination proteins and their control. *Nat Rev Mol Cell Biol.* **4(6):** 435-45.

Wilstermann AM and Osheroff N. (2003) Stabilization of Eukaryotic Topoisomerase II-DNA Cleavge Complexes. *Curr Top Med Chem* **3:** 321-338.

Wong AK, Pero R, Ormonde PA, Tavtigian SV, Bartel PL. (1997) RAD51 interacts with the evolutionarily conserved BRC motifs in the human breast cancer susceptibility gene brca2. *J Biol Chem*. **272(51):** 31941-4.

Woo RA, McLure KG, Lees-Miller SP, Rancourt DE, Lee PW. (1998) DNA-dependent protein kinase acts upstream of p53 in response to DNA damage. *Nature.* **394(6694):** 700-4.

Xu B, O'Donnell AH, Kim ST, Kastan MB. (2002) Phosphorylation of serine 1387 in Brca1 is specifically required for the Atm-mediated S-phase checkpoint after ionizing irradiation. *Cancer Res*. **62(16):**4588-91.

Xu B, Kim St, Kastan MB. (2001) Involvement of Brca1 in S-phase and G(2)-phase checkpoints after ionizing irradiation. *Mol Cell Biol*. **21(10):** 3445-50.

Yamashita A, Ohnishi T, Kashima I, Taya Y, Ohno S (2001) Human SMG-1, a novel phosphatidylinositol 3-kinase-related protein kinase, associates with components of the mRNA surveillance complex and is involved in the regulation of nonsense-mediated mRNA decay. *Genes Dev.* **15(17):**2215-28.

Yaneva M, Kowalewski T, Lieber MR. (1997) Interaction of DNA-dependent protein kinase with DNA and with Ku: biochemical and atomic-force microscopy studies. *EMBO J*. **16(16):** 5098-112.

Yarden RI, Brody LC. (2001) Identification of proteins that interact with BRCA1 by Far-Western library screening. *J Cell Biochem*. **83(4):** 521-31.

Yazdi PT, Wang Y, Zhao S, Patel N, Lee EY, Qin J. (2002) SMC1 is a downstream effector in the ATM/NBS1 branch of the human S-phase checkpoint. *Genes Dev.* **16(5):** 571-82.

Ye R, Bodero A, Zhou BB, Khanna KK, Lavin MF, Lees-Miller SP. (2001) The plant isoflavenoid genistein activates p53 and Chk2 in an ATM-dependent manner. *J Biol Chem.* **276(7):**4828-33.

Ye R, Goodarzi AA, Kurz EU, Saito S, Higashimoto Y, Lavin MF, Appella E, Anderson CW, Lees-Miller SP. (2004) The isoflavonoids genistein and quercetin activate different stress signaling pathways as shown by analysis of site-specific phosphorylation of ATM, p53 and histone H2AX. *DNA Repair (Amst).* **3(3):** 235-44.

Zhao S, Weng YC, Yuan SS, Lin YT, Hsu HC, Lin SC, Gerbino E, Song MH, Zdzienicka MZ, Gatti RA, Shay JW, Ziv Y, Shiloh Y, Lee EY. (2000) Functional link between ataxia-telangiectasia and Nijmegen breakage syndrome gene products. *Nature*. **405(6785):** 473-7.

Zechiedrich EL, Christiansen K, Andersen AH, Westergaard O, Osheroff, N. (1989) Double-stranded DNA cleavage/religation reaction of eukaryotic topoisomerase II: evidence for a nicked intermediate. *Biochemistry*. **28:** 6229-6236.

Zou L, Elledge SJ. (2003) Sensing DNA damage through ATRIP recognition of RPA-ssDNA complexes. *Science*. **300(5625):** 1542-8.

Zou L, Liu D, Elledge SJ. (2003) Replication protein A-mediated recruitment and activation of Rad17 complexes. *Proc Natl Acad Sci U S A.* **100(24):** 13827-32.